This project has received funding from the European Union's Horizon 2020 research and innovation programme under grant agreement No 723583

RE^4 Project

REuse and REcycling of CDW materials and structures in energy efficient pREfabricated elements for building REfurbishment and construction

D4.2

Geometrical, physical and chemical characterisation of CDW-derived materials

Author(s)[1]:	CBI
Date:	31/07/2017
Work package:	WP4 - Technical characterisation of CDW-derived materials for the production of building elements
Distribution[2]	PU
Status[3]:	Final
Abstract:	The Deliverable D4.2 summarises the results obtained by the RE^4 team involved in Task 4.2 – *Characterisation of CDW-derived materials*. The work in this task focused on geometrical, chemical and physical characterization of different sorted CDW fractions, delivered by CDE from recycling centres in Southern and Northern Europe.
File Name	Deliverable D4.2_Geometrical physical and chemical characterization of CDW-derived materials_Final_V2.0

Version	Date	Description	Written By	Approved by
1.0	18/07/2017	Complete draft	CBI et al.	
1.1	25/07/2017	Quality checked document	CBI et al.	QUB
1.2	28/07/2017	Revised by Project Coordinator	CBI et al.	
2.0	31/07/2017	Final version	CBI et al.	CETMA (PC)

[1] *Just mention the partner(s) responsible for the Deliverable*

[2] *PU: Public, RE: restricted to a group specified by the consortium, CO: Confidential, only for members of the consortium; Commission services always included.*

[3] *Draft, Revised, Final*

TABLE OF CONTENTS

1. EXECUTIVE SUMMARY 11

2. INTRODUCTION 13

2.1 RELEVANT WORK PACKAGE INPUT 13

3. DESCRIPTION OF WORK UNDERTAKEN 14

3.1 WP OBJECTIVES AND LIMITATIONS 14

3.2 METHODS FOR MINERAL MATERIALS 15

3.2.1 PETROGRAPHIC DESCRIPTION – FOLLOWING EN 932-3 18

3.2.2 CONSTITUENT CLASSIFICATION OF COARSE AGGREGATE – FOLLOWING EN 933-11:2009 19

3.2.3 WATER-SOLUBLE CHLORIDE SALT CONTENT – FOLLOWING EN 1744-1 21

3.2.4 WATER-SOLUBLE SULPHATE CONTENT – FOLLOWING EN 1744-1:2009+A1:2012 23

3.2.5 CARBONATE CONTENT OF FINE AGGREGATES – USING XRD AND TGA 25

3.2.6 ORGANIC MATTER – FOLLOWING EN 1744-1:2009+A1:2012 28

3.2.7 WATER-SOLUBLE COMPONENTS FROM RECYCLED AGGREGATE – FOLLOWING EN 1744-6:2006 29

3.2.8 TOTAL/BULK CHEMISTRY OF THE MATERIAL – USING XRF 30

3.2.9 RESISTANCE TO FREEZING AND THAWING – FOLLOWING EN 1367-1:2007 32

3.2.10 RESISTANCE TO WEATHERING (MAGNESIUM SULPHATE TEST) – FOLLOWING EN 1367-2:2009 34

3.2.11 VOLUME STABILITY-DRYING SHRINKAGE – FOLLOWING EN 1367-4:2008 37

3.2.12 ALKALI-SILICA REACTIVITY 40

3.2.13 GRADING – FOLLOWING EN 933-1:2012 41

3.2.14 FLAKINESS INDEX – FOLLOWING EN 933-3:2012 42

3.2.15 FLOW COEFFICIENT OF FINE AGGREGATES – FOLLOWING EN 933-6:2014 42

3.2.16 RESISTANCE TO FRAGMENTATION – FOLLOWING EN 1097-2:2011 43

3.2.17 RESISTANCE TO WEAR – FOLLOWING EN 1097-1:2011 44

3.2.18 PARTICLE DENSITY AND WATER ABSORPTION – FOLLOWING EN 1097-6:2013 44

3.3 METHODS FOR FINE MATERIALS 45
3.3.1 LIQUID LIMIT (W_L) – FOLLOWING BS 1377-2:1990 46
3.3.2 PLASTIC LIMIT (W_P) – FOLLOWING BS 1377-2:1990 47
3.3.3 PLASTICITY – FOLLOWING BS 1377-2:1990 47
3.3.4 XRF ANALYSIS 48
3.3.5 XRD ANALYSIS 48
3.3.6 FTIR SPECTROSCOPY 48
3.3.7 DTA-TGA 48
3.3.8 SOLUBLE COMPONENTS – FOLLOWING EN 1744-1:2009+A1:2012 AND ICP-MS 48
3.3.9 ACTIVITY INDEX 49
3.3.10 REACTIVITY/ISOTHERMAL CALORIMETRY 49
3.4 METHODS FOR LIGHTWEIGHT MATERIALS 51
3.4.1 MATERIALS OVERVIEW 51
3.4.2 CHARACTERIZATION METHODS 53
3.5 METHODS FOR TIMBER MATERIALS 56
3.5.1 IN SITU STRENGTH ASSESSMENT 56
3.5.2 VISUAL ON-SITE INSPECTION 57
3.5.3 ASSESSMENT ON CHEMICAL CONTAMINATION 57
3.5.4 ON-SITE SEPARATION 57
3.5.5 REPROCESSING AND STRENGTH GRADING 57
4. RESULTS AND COMMENTS ON THE RESULTS 58
4.1 MINERAL MATERIALS 58
4.1.1 PETROGRAPHIC DESCRIPTION 58
4.1.2 CONSTITUENT CLASSIFICATION OF COARSE AGGREGATE 65
4.1.3 WATER-SOLUBLE CHLORIDE SALT CONTENT 69
4.1.4 WATER-SOLUBLE SULPHATE CONTENT 69
4.1.5 CARBONATE CONTENT OF FINE AGGREGATES 70

4.1.6 ORGANIC MATTER (HUMUS AND FULVO ACID CONTENT) 74
4.1.7 WATER-SOLUBLE COMPONENTS FROM RECYCLED AGGREGATE 76
4.1.8 TOTAL/BULK CHEMISTRY OF THE MATERIAL 77
4.1.9 RESISTANCE TO WEATHERING 78
4.1.10 RESISTANCE TO FREEZING AND THAWING 78
4.1.11 VOLUME STABILITY-DRYING SHRINKAGE 81
4.1.12 ALKALI-SILICA REACTIVITY 82
4.1.13 GRADING 83
4.1.14 FLAKINESS INDEX 90
4.1.15 FLOW COEFFICIENT OF FINE AGGREGATES 90
4.1.16 MECHANICAL PROPERTIES (RESISTANCE TO FRAGMENTATION AND RESISTANCE TO WEAR) 90
4.1.17 PARTICLE DENSITY AND WATER ABSORPTION 90
4.2 FINE MATERIALS 93
4.2.1 LIQUID LIMIT 93
4.2.2 PLASTIC LIMIT (W_P) 94
4.2.3 PLASTICITY 94
4.2.4 XRF ANALYSIS 95
4.2.5 XRD ANALYSIS 96
4.2.6 FTIR SPECTROSCOPY 97
4.2.7 DTA-TGA 99
4.2.8 SOLUBLE COMPONENTS (HUMUS, FULVO ACID, SULPHATES, CHLORIDES & ALKALIS) 100
4.2.9 ACTIVITY INDEX 102
4.2.10 REACTIVITY/ISOTHERMAL CALORIMETRY 103
4.3 LIGHTWEIGHT MATERIALS 105
4.3.1 GRAIN SIZE 105
4.3.2 DENSITY, WATER ABSORPTION AND MOISTURE CONTENT 113

4.3.3 CONSIDERATIONS ON VARIABILITY OF PHYSICAL PROPERTIES OF LW FRACTIONS 116

4.4 TIMBER MATERIALS 116

4.4.1 IN SITU STRENGTH ASSESSMENT 116

4.4.2 VISUAL ON-SITE INSPECTION 116

4.4.3 ASSESSMENT ON CHEMICAL CONTAMINATION 117

4.4.4 ON-SITE SEPARATION 119

4.4.5 REPROCESSING AND STRENGTH GRADING 121

5. CONCLUSION AND RECOMMENDATIONS 130

6. REFERENCES 133

DISCLAIMER 140

INDEX OF FIGURES

Figure 1 Reduction of large amounts of 8/16 S.E.S. mineral fraction, using four rigid plastic containers on a pallet. 16
Figure 2. Constituent classification of N.E.S. samples taken from M_2. 20
Figure 3. Constituent classification of S.E.S. samples taken from M_2. 21
Figure 4 RETSCH PM 400 centrifuge grinding machine. 27
Figure 5 PHILIPS X'Pert Pro multi-purpose diffractometer. 27
Figure 6 NETZSCH TG209 F1 Libra thermal gravimetry analyser. 28
Figure 7 Schematic diagram of XRF analysis adopted from Thermo Fisher Scientific [28]. 31
Figure 8 Freeze-thaw test sample of S.E.S. aggregate (8/16 mm). 33
Figure 9 TAS MTCL 1000 Series 3 environmental chamber. 33
Figure 10 Freeze-thaw test temperature profiles. 34
Figure 11 Coarse N.E.S. aggregate sample placed inside mesh baskets for performing the $MgSO_4$ test. 36
Figure 12 Coarse N.E.I.S. aggregate sample placed inside mesh baskets for performing the $MgSO_4$ test. 36
Figure 13 Coarse S.E.S. aggregate sample placed inside mesh baskets for performing the $MgSO_4$ test. 36
Figure 14 Coarse S.E.I.S. aggregate sample placed inside mesh baskets for performing the $MgSO_4$ test. 36
Figure 15 CDW concrete prisms for drying shrinkage testing. 39
Figure 16 Concrete prisms for drying shrinkage testing (control specimens). 39
Figure 17 Comparator for measuring drying shrinkage of concrete samples. 39
Figure 18 Mortar prisms for ASR testing, immersed in 1 M NaOH solution. Prisms made using CDW sand (0/2 mm). 41
Figure 19 Mortar prisms for ASR testing, immersed in 1 M NaOH solution. Prisms made using virgin sand (0/2 mm). 41
Figure 20 Penetrometer and sample holder. 46
Figure 21 TAM-air 8 channel calorimeter. 50
Figure 22 Wood and Plastic fractions rejected from CDW processing plants and relevant magnification (on the right) showing polystyrene particles and cortex pieces. 51
Figure 23 Rigid Plastic fractions from S-EU source as received, grinder and after the grinding process (coarse fraction). 52
Figure 24 Rigid Plastic fractions from N-EU source as received, grinding process and resulting material (fine fraction). 52
Figure 25 Wood fractions from S-EU source as received, grinder, 20 mm circular mesh sieve and wood after grinding process (size <20 mm). 52
Figure 26 Wood fractions from N-EU source (as received). 53
Figure 27 N.E.I.S. aggregate Type 1. 59
Figure 28 N.E.I.S. aggregate Type 2. 59
Figure 29 N.E.I.S. aggregate Type 3. 59
Figure 30 N.E.I.S. aggregate Type 4. 59
Figure 31 N.E.I.S. aggregate Type 5. 60
Figure 32 S.E.I.S. aggregate Type 1. 62
Figure 33 S.E.I.S. aggregate Type 2. 62
Figure 34 S.E.I.S. aggregate Type 3. 62
Figure 35 S.E.I.S. aggregate Type 4. 62
Figure 36 S.E.I.S. aggregate Type 5. 63

Figure 37 S.E.I.S. aggregate Type 6. 63
Figure 38 Typical cross-section of N.E.S. (0/2 mm) under polarized light. 64
Figure 39 Typical cross-section of N.E.S. (0/2 mm) under cross-polarized light. 64
Figure 40 Typical cross-section of S.E.S. (0/2 mm) under polarized light. 64
Figure 41 Typical cross-section of S.E.S. (0/2 mm) under cross-polarized light. 64
Figure 42 Quartz particle coated with thin layer of carbonated cement paste. 65
Figure 43 Coarse recycled aggregate composition of N.E.S. mineral fraction. 67
Figure 44 Coarse recycled aggregate composition of S.E.S. mineral fraction. 68
Figure 45 XRD results for N.E.S. fine mineral fractions. 70
Figure 46 XRD results for S.E.S. fine mineral fractions. 71
Figure 47 N.E.S. sample weight (%) versus heating temperature (°C). 72
Figure 48 N.E.S. rate of change of sample weight (%/°C) versus heating temperature (°C). 72
Figure 49 S.E.S. sample weight (%) versus heating temperature (°C). 73
Figure 50 S.E.S. Rate of change of sample weight (%/°C) versus heating temperature (°C). 73
Figure 51 Colorimetric identification of the presence of humus in all 0/2 mm mineral fractions & fine fraction. 75
Figure 52 Colorimetric identification of the presence of fulvo acid in all 0/2 mm mineral fractions & fine fraction. 75
Figure 53 Penetration depth of Vicat apparatus needle versus time. Height of cement paste sample is 40 mm. 76
Figure 54 Percentage mass loss of different mineral fractions exposed to 5 cycles of $MgSO_4$ solution. 78
Figure 55 Percentage mass loss of different mineral fractions subjected to 10 freeze-thaw cycles. 79
Figure 56 State of N.E.S mineral fractions after 10 freeze-thaw cycles. 80
Figure 57 State of N.E.I.S. mineral fractions after 10 freeze-thaw cycles. 80
Figure 58 State of S.E.S. mineral fractions after 10 freeze-thaw cycles. 80
Figure 59 State of S.E.I.S. mineral fractions after 10 freeze-thaw cycles. 80
Figure 60 N.E.S. fine particles (< 4 mm) collected after the end of 10 freeze-thaw cycles. 81
Figure 61 N.E.I.S. fine particles (< 4 mm) collected after the end of 10 freeze-thaw cycles. 81
Figure 62 S.E.S. fine particles (< 4 mm) collected after the end of 10 freeze-thaw cycles. 81
Figure 63 S.E.I.S. fine particles (< 4 mm) collected after the end of 10 freeze-thaw cycles. 81
Figure 64 Expansion of mortar prisms versus time in ASR test. 82
Figure 65 Particle size distribution of N.E.S. mineral-fraction 8/16. 84
Figure 66 Particle size distribution of N.E.S. mineral-fraction 2/8 85
Figure 67 Particle-size distribution of N.E.S. mineral-fraction 0/2 mm 86
Figure 68 Particle-size distribution of S.E.S. mineral-fraction 8/16 mm. 87
Figure 69 Particle-size distribution of S.E.S. mineral-fraction 2/8 mm. 88
Figure 70 Particle-size distribution of S.E.S. mineral-fraction 0/2 mm. 89
Figure 71 Penetration depth of cone penetrometer as a function of paste moisture content. 94
Figure 72 Plasticity chart adopted from BS 5930:2015 [56]. 95
Figure 73 XRD analysis of uncalcined fine material oven dried at 40 °C. 96
Figure 74 XRD analysis of fine material calcined at 700 °C. 97
Figure 75 FTIR spectra of uncalcined and calcined fine material. 98
Figure 76 Sample weight (%) and rate of change of sample weight (%/°C) versus temperature (°C). 100
Figure 77 Ion current of H_2O and CO_2. 100

Figure 78 Particle size distribution of the particles < 0.063 mm determined by laser diffractometer (left). Cumulative particle size distribution of the fine material (right). 103
Figure 79 Heat release during hydration of uncalcined fine material versus time. 104
Figure 80 Heat release during hydration of calcined fine material versus time. 104
Figure 81 Visual observation of the uncalcined (bottom) and calcined (top) fine material. 105
Figure 82 Grading size distribution of Wood and Plastic fine fractions (S.E.S.) according to UNI EN 933-1. 106
Figure 83 Grading size distribution of Wood and Plastic fine fractions (N.E.S.) according to UNI EN 933-1.107
Figure 84 Grading size distribution of Rigid Plastic fine fractions (S.E.S) according to UNI EN 933-1. 109
Figure 85 Grading size distribution of Rigid Plastic fine fractions (N.E.S.) according to UNI EN 933-1..... 110
Figure 86 Grading size distribution of W (S.E.S. and N.E.S.) according to UNI EN 933-1. 112
Figure 87 Length distribution of W fractions (S.E.S. and N.E.S.). 113
Figure 88 Length distribution result of W, from S-EU and N-EU. 113
Figure 89 Equipment used for testing Wood and Plastic and Rigid Plastic materials. 115
Figure 90 On-site Inspection of a roof structure. 117
Figure 91 Production process of glue laminated timber. © Glued Laminated Timber Research Association [83]..... 124
Figure 92 Example from national grading rule DIN 4074: Measurement of knots and knot content in square shaped timber. 125
Figure 93 Exemplary reprocessing of salvaged timbers. 129

INDEX OF TABLES

Table 1 Waste and size fraction of sorted CDW. 14
Table 2 Test methods for CDW mineral fraction. 15
Table 3 Maximum replacement levels of coarse aggregates according to EN 206. 17
Table 4 Recommendations for coarse recycled aggregates according to EN 12620. 17
Table 5 Requirements for coarse Crushed Concrete (CCA) Aggregate according to BS 8500-2. 18
Table 6 Amount of aggregate and water required for the Volhard method. 22
Table 7 Classification of organic compounds in terms of effect on concrete setting time. 28
Table 8 Required vs adopted grading of aggregate used for making drying shrinkage test concrete prisms. 38
Table 9 Aggregate grading requirements adopted from RILEM TC106-2. 41
Table 10 Flakiness Index – sub-fractions and bar sieve widths. 42
Table 11 Test methods for CDW fine materials fraction. 45
Table 12 Physical and geometrical test methods for CDW LW fractions. 53
Table 13 Test methods for CDW timber elements. 56
Table 14 Physical classification of N.E.I.S. (8/16 mm) aggregates. 60
Table 15 Mineralogical classification of N.E.I.S (8/16 mm) aggregates. 60
Table 16 Physical classification of S.E.I.S. (8/16 mm) aggregates. 61
Table 17 Mineralogical classification of S.E.I.S. (8/16 mm) aggregates. 61
Table 18 Quantification of N.E.S. and S.E.S. 0/2 mm mineral fractions observed under microscope. 65
Table 19 Coarse recycled aggregate composition of N.E.S. mineral fraction. 66
Table 20 Coarse recycled aggregate composition of S.E.S. mineral fraction. 66
Table 21 Comparison of N.E.S. and S.E.S. compositions against requirements set by EN 206 and BS 8500-2. 68
Table 22 Water-soluble chloride content of 0/2 mm mineral fractions. 69

Table 23 Water-soluble chloride content of 8/16 mm mineral fractions. 69
Table 24 Water-soluble sulphate content of fine and coarse mineral fractions at room temperature. 69
Table 25 Water-soluble sulphate content of fine mineral fractions at 60 °C. 70
Table 26 Mineral composition of N.E.S. and S.E.S. fine mineral fractions based on XRD. 71
Table 27 Actual and estimated CO_2 mass loss using TGA and XRD. 74
Table 28 Initial and final setting times of cement pastes. 76
Table 29 Chemical composition of N.E.S. and N.E.I.S. mineral fractions. 77
Table 30 Chemical composition of S.E.S. and S.E.I.S. mineral fractions. 77
Table 31 Average drying shrinkage of prisms versus time. 82
Table 32 Particle-size distribution of N.E.S. mineral-fraction 8/16 mm. 84
Table 33 Particle-size distribution of N.E.S. mineral-fraction 2/8 mm. 85
Table 34 Particle-size distribution of N.E.S. mineral-fraction 0/2 mm. 86
Table 35 Particle-size distribution of S.E.S. mineral-fraction 8/16 mm. 87
Table 36 Particle-size distribution of S.E.S. mineral-fraction 2/8 mm. 88
Table 37 Particle-size distribution of S.E.S. mineral-fraction 0/2 mm. 89
Table 38 Results on flakiness index. 90
Table 39 Results on flow coefficient on fine aggregates. 90
Table 40 Results on resistance to fragmentation and wear. 90
Table 41 Mineral fraction particle densities and 24 h water absorption. 91
Table 42 Mineral fraction particle densities and long-time water absorption. 92
Table 43 Compilation of results on density and water absorption obtained from several laboratories. 93
Table 44 Determination of the plastic limit. 94
Table 45 XRF analysis of the fine material. 95
Table 46 Quantification of major phases identified by XRD 97
Table 47 FTIR bands of the uncalcined fine material spectrum. 98
Table 48 Amount of water-soluble SO_3. 101
Table 49 Amount of water-soluble alkalis present in the fine material. 102
Table 50 Particle size distribution of the fine material from mechanical sieving. 102
Table 51 Grading size distribution of Wood and Plastic fine fractions (S.E.S.) according to UNI EN 933-1. 106
Table 52 Grading size distribution of Wood and Plastic fine fractions (N.E.S.) according to UNI EN 933-1. 107
Table 53 Grading size distribution of Rigid Plastic fine fractions (S.E.S.) according to UNI EN 933-1. 109
Table 54 Grading size distribution of Rigid Plastic fine fractions (N.E.S.) according to UNI EN 933-1. 110
Table 55 Results of CDW lightweight fractions: density and water absorption. 114
Table 56 Results of CDW lightweight W fractions: density and moisture content. 115
Table 57 Limits of chemicals in recycled wood used for wood based panels. 118
Table 58 Possible sorting categories according to future reprocessing steps. 120
Table 59 Mechanical properties of aged timber – summary of comparative study. 122

ACRONYMS & ABBREVIATIONS

CDW	Construction and Demolition Waste
FTIR	Fourier Transform Infra-Red spectroscopy
GGBS	Ground Granulated Furnace Slag
LW	Lightweight
MF	Mineral Fraction from CDW
N.E.S.	North Europe Sorted CDW
N.E.I.S.	Northern Europe Improved Sorted CDW
NW	Normal-weight
OPC	Ordinary Portland Concrete
PFA	Pulverised Fuel Ash
RP	Mixed Rigid Plastic from CDW
SCC	Self-Compacting Concrete
SCM	Supplementary Cementious Materials
S.E.S.	Southern Europe Sorted CDW
S.E.I.S.	Southern Europe Improved Sorted CDW
W	Wood from CDW
w/c	Water to cement ratio
WP	Mixed Wood and Plastic from CDW
XRD	X-ray diffraction
XRF	X-ray fluorescence

1. EXECUTIVE SUMMARY

Several different sorted CDW fractions have been investigated and characterized thoroughly – mineral fraction, fine mineral fraction (silt and clay), rigid plastics, wood chips and fibres as well as structural timber. The different sorted CDW fractions came from two different regional sources: Northern and Southern Europe. This report contains results on the chemical, mineralogical, physical, visual and geometrical characterization and assessment of these fractions.

All the different **mineral size-fractions** (0-2, 2-8 and 8-16 mm) were deemed suitable for use in different types of concrete, with the exception of S.E.S. (Southern Europe Sorted CDW) 0/2 mm fraction. Although passing other tests, the concentration of water soluble sulphates was right on the *present* limit of 0.2 wt.%. However, it was shown that the material could be improved by more careful sorting, removing (e.g. bituminous material and bricks). This was shown to improve the composition of the fractions (including water soluble salts), the high water absorption and susceptibility to freeze-thaw damage and successful sorting might even make the material suitable for even harsher exposure classes (improved sorting might shift the material from Type B to Type A, **Table 3**).

The **fine material** was characterised as silt with presence of clay, and with high plasticity and high organic content, although no or little fulvo acid. Isothermal calorimetry results showed that the material was of low reactivity when mixed with either water or water plus hydroxide activating solutions, but when calcined the fine material showed to be far more reactive and exhibited setting behaviour. However, if to be used as a precursor for geopolymer concrete, either on its own or blended with PFA/GGBS, further testing is required to assess strength gain and the effect of the higher chloride and sulphate contents.

The **Lightweight (LW) fractions** (mixed wood and plastic, mixed rigid plastic and wood scraps) have been physically tested to assess their use as aggregates for LW concretes and as components materials for LW panels. Mixed wood and plastic and rigid plastic (after size reduction) have the physical requirements to be considered lightweight aggregates , according to UNI EN 206-1 and UNI EN 13055-1 standards (even if specific for mineral aggregates). The typical quality and average composition of LW fractions are comparable, regardless to the source (S-EU or N-EU), with an intrinsic heterogeneity of each fraction (wood/plastic relative percentage, different typologies of plastics, different nature of wood).

Based on the physical assessment performed, **timber elements** from dismantled buildings can be reused as structural components. Possible defects, decay, and contamination have to be assessed carefully to receive a safe building material. In situ testing methods to assess chemical contamination of timber structures prior to dismantling would help to separate material streams at an early stage and result in a higher reuse fraction of timber from CDW. The standardization of limit values of contamination could help to break down constraints in the reuse of timber elements. The investigated reprocessing of salvaged timbers into lamellas for glued laminated timber is a good opportunity to cut out impurities and defects. The technical opportunity to create endless lamellas

increases the amount of timber that can being reused. By reprocessing, the strength class of the end product can be upgraded compared to the entry material.

2. INTRODUCTION

The Deliverable D4.2 summarises the results obtained by the RE^4 team involved in Task 4.2 (QUB, CBI, CETMA, ROS, ACCIONA) – *Characterisation of CDW-derived materials*. The work in this task focused on geometrical, chemical and physical characterization of different sorted CDW fractions, delivered by CDE from recycling centres in Southern and Northern Europe.

Mineral aggregate fractions were tested for the assessment of their use in vibrated, self-compacting (SCC) and semi-dry mix concretes. The tests included chemical and mineralogical composition, durability (resistance to weathering, freeze – thaw resistance, volume stability - drying shrinkage, and alkali-silica reactivity) and physical properties, according to relevant standards and specifications available at National and European level. Three different size-fractions were characterized – 0/2, 2/8 and 8/16 – and the usability of these as aggregates in concretes assessed, by comparing the results with levels and requirements in concrete and aggregate standards.

LW fractions such as mixed wood and plastic, mixed rigid plastic and wood scraps were tested in terms of physical performance (e.g. grain size, density, water absorption and moisture content). Tests on mixed wood and plastic (as received) and mixed rigid plastic (after a further mechanical process to allow size reduction) aimed to assess their use as aggregates for LW insulating concretes; mixed rigid plastic and wood (both after a further mechanical process to allow size reduction) were tested in the view of their use as component materials for LW insulating panels.

The **fine fraction** (output from the thickening of particle washing water) was characterised, to enable an assessment of its potential utilisation as filler, fine fraction for extruded products, plaster/adhesive, supplementary cementitious materials (SCM) or precursor for geopolymer reaction after calcination. Physical and chemical tests included liquid and plastic limits definition, X-ray fluorescence, X-ray diffraction and Fourier Transform Infrared Spectroscopy.

Finally, timber waste recovered from dismantled buildings, according to strategies defined in Task 2.2, has been characterised. Timber waste is currently mainly burned or shred, therefore relevant testing methods for classification for its reuse have to be developed. A visual inspection has been performed to identify different sorts of impurities such as fissures, means of connections (nails, screws, glue etc.) and paint.

2.1 Relevant Work Package input

This deliverable is to some degree a continuation of *D4.1 – Composition of materials from demolition and available volumes of sorted fractions*, since it deals with ***sorted CDW***, refined from ***unsorted CDW*** at CDE recycling centres in a process described in D4.1. The nature and composition of the unsorted CDW is also described in D4.1. However, both reports are independent. To some extent, the assessment on the use of sorted CDW in concrete relies on the literature study on concrete and aggregate standards in *D2.1 – CDW specifications and material requirements for prefabricated structures*.

3. DESCRIPTION OF WORK UNDERTAKEN

3.1 WP objectives and limitations

Task 4.2 aims at the procurement, analysis, characterisation and quality evaluation of sorted CDW materials, in relation to their value and use in building materials (e.g. concrete, insulating panels, timber or earthen materials used for building components and elements). The work in Task 4.2 builds on the characterization and evaluation of unsorted CDW performed in Task 4.1 and presented in Deliverable 4.1. However, the work there was conducted on unsorted CDW from the two different geographic sources (Northern and Southern Europe). The unsorted CDW came from mixed sources (i.e. mixed residential and commercial building typology) to the CDE recycling centre of each geographic region and was sorted there. The work in Task 4.2 thus focuses on characterization and analysis on ***sorted CDW*** from these two centres, in Northern (N.E.S.) and Southern (S.E.S.) Europe, respectively. Before sending the CDW fractions to the laboratory and industrial partners, CDE sieved them into different size-fractions, according to **Table 1**.

The material for characterisation of larger sized timber elements from CDW was dismantled from roof structures in Berlin, Germany.

Table 1 Waste and size fraction of sorted CDW.

Waste fraction	Size fraction(s) (mm)	Intended use
Mineral fraction – sorted CDW	8/16, 2/8, 0/2, silt and clay	Vibrated concrete, SCC, LW concrete, semi-dry mix concrete, supplementary cementitious materials (SCM)
Lightweight fraction – mixed wood and plastic	Fine fraction	LW concrete
Lightweight fraction – rigid plastic	< 100	LW concrete, insulating panels
Lightweight fraction – wood	< 100	Insulating panels
Larger sized timber elements	Beams with different cross sections	

Mineral fractions of sorted CDW from Northern and Southern Europe, respectively, were labelled as follows:

- Northern Europe Sorted (0/2 mm) – N.E.S. (0/2 mm)
- Northern Europe Sorted (2/8 mm) – N.E.S. (2/8 mm)
- Northern Europe Sorted (8/16 mm) – N.E.S. (8/16 mm)
- Southern Europe Sorted (0/2 mm) – S.E.S. (0/2 mm)
- Southern Europe Sorted (2/8 mm) – S.E.S. (2/8 mm)
- Southern Europe Sorted (8/16 mm) – S.E.S. (8/16 mm)

The effect of defective material (i.e. ceramics, bitumen and glass particles) removal on the chemical and durability performance of the above mineral fractions was also investigated. Improved quality material was obtained by first manually (i.e. by hand-picking) removing all defective particles from

the N.E.S. (8/16 mm) and S.E.S. (8/16 mm) mineral fractions. Thus, creating two new mineral fractions:

- Northern Europe Improved Sorted (8/16 mm) – N.E.I.S. (8/16 mm)
- Southern Europe Improved Sorted (8/16 mm) – S.E.I.S. (8/16 mm)

Smaller size-fractions (0/2 mm and 2/8 mm) of improved materials were then obtained by crushing and sieving the above two mineral fractions. These were labelled as follows:

- Northern Europe Improved Sorted (0/2 mm) – N.E.I.S. (0/2 mm)
- Northern Europe Improved Sorted (2/8 mm) – N.E.I.S. (2/8 mm)
- Southern Europe Improved Sorted (0/2 mm) – S.E.I.S. (0/2 mm)
- Southern Europe Improved Sorted (2/8 mm) – S.E.I.S. (2/8 mm).

3.2 Methods for Mineral materials

The relevant methods for the mineralogical, chemical and physical characterization of the CDW mineral fraction are summarized in **Table 2**. These are preferentially according to EN standards and are generally developed and designed for natural aggregates (sand, gravel and crushed rocks). Only few of them were originally developed to include alternative materials, such as recycled aggregates. One example of a method that is actually developed also for recycled aggregates is the test of resistance to fragmentation [1]. Nevertheless, the EN standards for concrete [2] and aggregate [3] states that these methods should be used also for characterization of coarse recycled aggregates.

Table 2 Test methods for CDW mineral fraction.

Property	Standard	Laboratories
Mineralogical and chemical testing		
Petrographic Description	EN 932-3:1997	QUB
Constituent Classification of coarse aggregate	EN 933-11:2009	QUB
Water-Soluble Chloride Salt Content	EN 1744-1: 2009+A1:2012	QUB
Water-Soluble Sulphate Content	EN 1744-1:2009+A1:2012	QUB
Carbonate Content of Fine Aggregates	XRD and TGA	QUB
Organic Matter (Humus and Fulvo Acid Content)	EN 1744-1:2009+A1:2012	QUB
Water Soluble Components from Recycled Aggregate	EN 1744-6:2006	QUB
Total/bulk chemistry of the material	XRF	QUB
Durability testing		
Resistance to Freezing and Thawing	EN 1367-1:2007	QUB
Resistance to weathering ($MgSO_4$-test)	EN 1367-2:2009	QUB
Volume Stability-Drying Shrinkage	EN 1367-4:2008	QUB
Alkali-Silica Reactivity	RILEM AAR 2	QUB
Geometric and physical Testing		

Grading	EN 933-1:2012	CBI
Flakiness Index	EN 933-3:2012	CBI
Flow Coefficient of Fine Aggregates	EN 933-6:2014	CBI
Resistance to Fragmentation	EN 1097-2:2010	CBI
Resistance to Wear	EN 1097-1:2011	CBI
Particle Density and Water Absorption	EN 1097-6:2013	CBI, QUB, CETMA, ACC

The used methods are briefly described below, with emphasis on special procedures and deviations used for the CDW. Reduction of all specimens was performed in accordance with [4], using standard laboratory equipment. Handling of the larger batches of aggregate (big-bags with up to 1 metric ton material in each), special reduction measures were taken. At CBI, these measures consisted in tying four large rigid plastic containers to each other using duct tape (**Figure 1**). A crane was used to position the big-bag directly above the point where all four containers met. Next, a hole was cut at the bottom of the bag, which allowed the aggregate to pour down and randomly fill all four containers.

Figure 1 Reduction of large amounts of 8/16 S.E.S. mineral fraction, using four rigid plastic containers on a pallet.

It should be noted that a number of national and European standards, specifications and recommendations exist ([5], [6], [7], [8], [9], [10], [11], [12], [2], [3] and [13]), which set the

requirements for the use of recycled aggregates in non-structural and structural concrete. When it comes to [2], [3] and [13], they only allow partial replacement of coarse virgin aggregates by recycled ones (coarse aggregates have minimum grain-size ≥ 2 mm and maximum grain-size ≥ 4 mm). A complete list of requirements set by the above three standards is given in **Table 3**, **Table 4** and **Table 5** (see also [14] for more details). In this study, the requirements of the above three standards are used as a baseline for assessing the performance of coarse mineral fractions.

Table 3 Maximum replacement levels of coarse aggregates according to EN 206.

Recycled aggregate type (A or B)	**Exposure classes**			
	X0	XC1, XC2	XC3, XC4, XF1, XA1, XD1	All other exposure classes
Type A Rc ≥ 90% Rc + Ru ≥ 95% Rb ≤ 10% Ra ≤ 1%, X + Rg ≤ 1% FL ≤ 2 cm^3/kg	50%	30%	30%	0%
Type B Rc ≥ 50% Rc + Ru ≥ 70% Rb ≤ 30% Ra ≤ 5% X + Rg ≤ 2% FL ≤ 2 cm^3/kg	50%	20%	0%	0%
Where: Rc is content of concrete, concrete products, mortar & concrete masonry units Ru is content of unbound aggregate, natural stone and hydraulically bound aggregate Rb is content of clay masonry units (i.e. bricks & tiles), calcium silicate masonry units & aerated non-floating concrete Ra is content of bituminous materials Rg is content of glass X is content of clay & soil, ferrous and non-ferrous metals, non-floating wood, plastic, rubber and gypsum FL is content of floating particles				
Notes: Type A recycled aggregates from a known source may be used in exposure classes to which the original concrete was designed with a maximum percentage of replacement of 30%. Type B recycled aggregates should not be used in concrete with compressive strength classes > C30/37.				

Table 4 Recommendations for coarse recycled aggregates according to EN 12620.

Recycled aggregate type (as defined in [3])	**Property**	**Requirement**
A & B	Fines content	Category or value to be declared
A & B	Shape	FI ≤ 50, or SI ≤ 55
A & B	Resistance to fragmentation	LA Coefficient ≤ 50, or SZ ≤ 32

A	Oven dried particle density ρ_{rd}	≥ 2100 kg/m^3
B		≥ 1700 kg/m^3
A & B	Water absorption	Value to be declared
A & B	Water soluble sulphate content	≤ 0.2% by mass of aggregate
A & B	Acid-soluble chloride ion content	Value to be declared
A & B	Influence on the initial setting time	Change in initial setting time ≤ 40 min

In addition, [3] states: "The use of recycled aggregates can influence the suitability of the above precautions. In the case of recycled concrete aggregates, it will be necessary to ascertain that the original concrete does not contain reactive (or reacting) aggregate and, where the alkali content of the new concrete (or the cement therein) is being limited, the alkali content of the recycled concrete aggregates will need to be determined and taken into account. In the case of general recycled aggregates, it will be appropriate to regard the material as being a potentially reactive aggregate, unless it has been specifically established to be non-reactive. In both cases, the possibility of unpredictable compositional variability should be considered. Further: "For special applications requiring high quality surface finish … FL should be limited to ≤ 0.2 cm^3/kg".

Table 5 Requirements for coarse Crushed Concrete (CCA) Aggregate according to BS 8500-2.

Property	Requirement	Maximum strength class	Exposure classes
Aggregate size	d ≥ 4 mm D ≥ 10 mm	C40/50	X0, XC1, XC2, XC3, XC4, XF1 & DC-1
Maximum fines content	≤ 4% by mass of particles passing 0.063 mm sieve		
Maximum acid-soluble sulphate (SO_3) content	≤ 0.8% by mass of aggregate		
Rc	≥ 90%		
Rc + Ru	≥ 90%		
Rb	≤ 10%		
Ra	≤ 5%		
X + Rg	≤1%		
FL	≤ 2 cm^3/kg		

Notes: Where the material to be used is obtained by crushing hardened concrete of known composition that has not been in use, e.g. surplus precast units or returned fresh concrete, and not contaminated by storage or processing, the only requirements are for aggregate size, fines content, drying shrinkage and resistance to fragmentation.
The designation accepts the presence of some particles which are retained on the upper sieve (oversize) and some which pass the lower sieve (undersize). For single size coarse aggregate with a specified maximum aggregate size of 40 mm, 20 mm 14 mm and 10 mm, the EN 12620 aggregate sizes are 20/40, 10/20, 6.3/14 and 4/10.
Material obtained by crushing hardened concrete of known composition that has not been in use and not contaminated during storage and processing may be used in any strength class.
CCA may be used in other exposure classes provided it has been demonstrated that the resulting concrete is suitable for the intended environment, e.g. freeze-thaw resisting, sulphate-resisting.

3.2.1 Petrographic Description – following EN 932-3

Petrographic examination was performed in accordance with [15] to determine the constituent rock types of the following mineral fractions:

a) N.E.I.S. (8/16 mm)
b) S.E.I.S. (8/16 mm)

c) N.E.S. (0/2 mm)
d) S.E.S. (0/2 mm)

The examination of N.E.I.S. and S.E.I.S. (8/16 mm) was performed using a magnifying glass, whereas the examination of N.E.S. and S.E.S. (0/2 mm) mineral fractions was performed using a Carl Zeiss Axioskop 40 routine microscope.

3.2.2 Constituent Classification of coarse aggregate – following EN 933-11:2009

Background Information

High levels of masonry (bricks and tiles), bitumen, glass and LW particles in recycled aggregate can adversely affect the mechanical and physical properties of concrete (drying shrinkage, compressive and tensile strength, modulus of elasticity and water permeability). Due to this reason, [2] and [13] set maximum allowable limits for the above constituents of recycled aggregate to be used in structural concrete.

Experimental Procedure

Test method [16] was employed in order to identify and estimate the constituent materials of the following coarse mineral fractions:

a) N.E.S. (8/16 mm)
b) S.E.S. (8/16 mm)

Initially, a test portion was oven dried at 40 ± 5 °C to constant mass. The oven dried mass of the test portion was then recorded as M_1 (M_1 minimum mass to be analysed is 20 kg). The test portion was immersed in a filled watertight tank in order to wash the particles and release the floating ones. The floating particles were collected and their volume V_{FL} was determined by placing them inside a graduated cylinder filled with a known volume of water. The non-floating particles were collected and oven dried at 40 °C to constant mass. Next, they were spread on a flat disc and all clay and soil, ferrous and non-ferrous metals, non-floating wood, plastic, rubber and gypsum particles were removed by hand. The above removed particles were weighed and their mass was recorded as M_x. The remaining non-floating particles were weighed and their mass was recorded as M_2. Next, a sample was taken from M_2 and manually sorted into Rc (concrete, concrete products, mortar and concrete masonry units), Ru (unbound aggregate, natural stone and hydraulically bound aggregate), Rb (clay masonry units, calcium silicate units and aerated non-floating concrete), Ra (bituminous materials) and Rg (glass) as shown in **Figure 2** and **Figure 3**. The mass of the sample taken from M_2 was recorded as M_3 (M_3 minimum mass to be manually sorted is 2 kg [16]). Next, the masses of the above constituents of M_3 sample were recorded as M_{Rc}, M_{Ru}, M_{Rb}, M_{Ra} and M_{Rg}, respectively. Finally, the proportion of each constituent of M_1 test portion was determined by the following expressions:

$$\mathbf{FL}\left(\frac{\mathbf{cm^3}}{\mathbf{kg}}\right) = (\mathbf{1000})\left(\frac{\mathbf{V_{FL}}}{\mathbf{M_1}}\right) \qquad (1)$$

$$\mathbf{X}(\%) = (\mathbf{100})\left(\frac{\mathbf{M_X}}{\mathbf{M_1}}\right) \quad (2)$$

$$\mathbf{Rc}(\%) = (\mathbf{100})\left(\frac{\mathbf{M_2}}{\mathbf{M_1}}\right)\left(\frac{\mathbf{M_{Rc}}}{\mathbf{M_3}}\right) \quad (3)$$

$$\mathbf{Ru}(\%) = (\mathbf{100})\left(\frac{\mathbf{M_2}}{\mathbf{M_1}}\right)\left(\frac{\mathbf{M_{Ru}}}{\mathbf{M_3}}\right) \quad (4)$$

$$\mathbf{Rb}(\%) = (\mathbf{100})\left(\frac{\mathbf{M_2}}{\mathbf{M_1}}\right)\left(\frac{\mathbf{M_{Rb}}}{\mathbf{M_3}}\right) \quad (5)$$

$$\mathbf{Ra}(\%) = (\mathbf{100})\left(\frac{\mathbf{M_2}}{\mathbf{M_1}}\right)\left(\frac{\mathbf{M_{Ra}}}{\mathbf{M_3}}\right) \quad (6)$$

$$\mathbf{Rg}(\%) = (\mathbf{100})\left(\frac{\mathbf{M_2}}{\mathbf{M_1}}\right)\left(\frac{\mathbf{M_{Rg}}}{\mathbf{M_3}}\right) \quad (7)$$

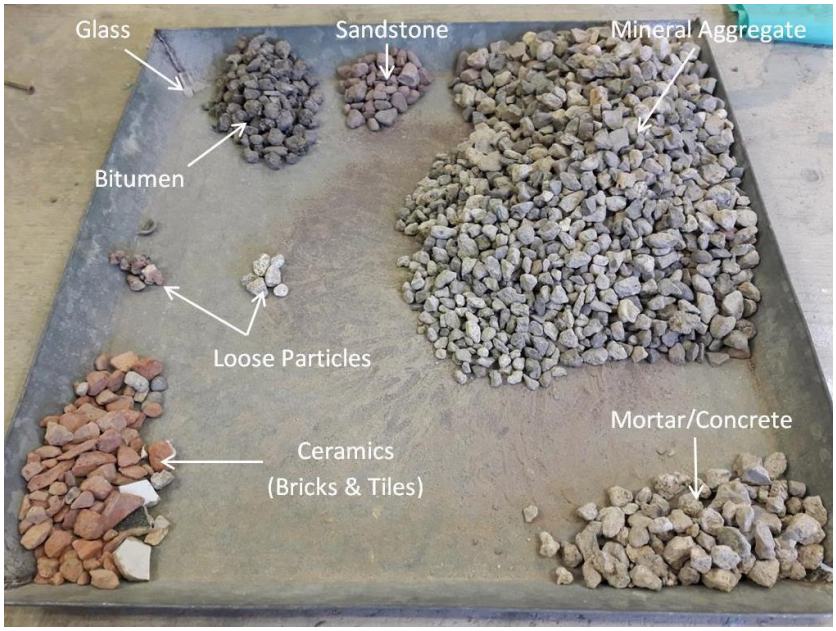

Figure 2. Constituent classification of N.E.S. samples taken from M_2.

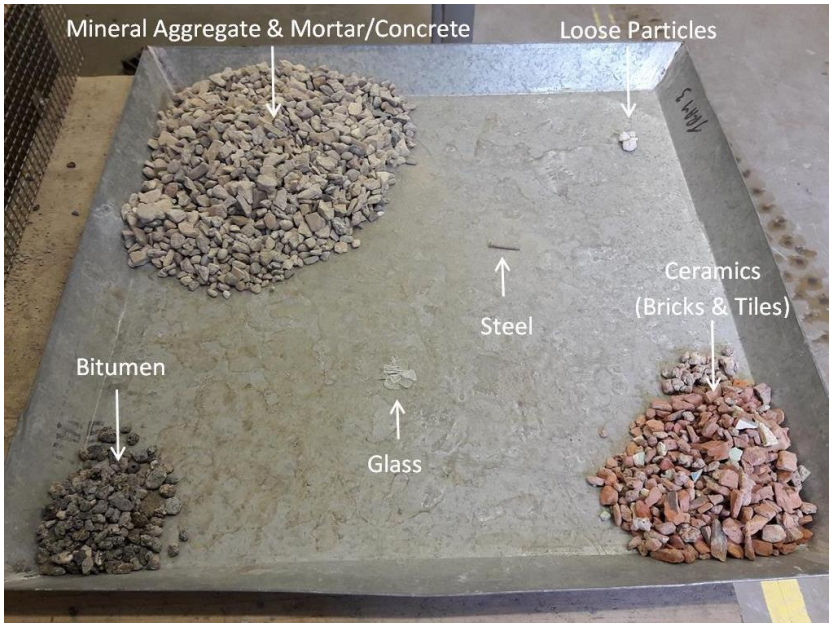

Figure 3. Constituent classification of S.E.S. samples taken from M_2.

3.2.3 Water-Soluble Chloride Salt Content – following EN 1744-1

Background Information

Portland cement concrete is highly alkaline (pH > 13) due to its chemical composition. Under these conditions, a thin passive oxide film that resists corrosion is formed on the surface of embedded steel reinforcement. However, when the concentration of chloride ions in contact with the steel reinforcement exceeds a threshold value it destroys the passivity of the oxide film [17]. Once the steel reinforcement is depassivated, corrosion will take place in the presence of moisture and oxygen in accordance with the following chemical reactions:

$$\mathbf{Fe^{2+} + 2Cl^{-} \rightarrow FeCl_2} \quad (8)$$

$$\mathbf{FeCl_2 + 2H_2O \rightarrow Fe(OH)_2 + 2HCl} \quad (9)$$

Since the volume of the products of corrosion is considerably greater than the volume of the original steel, tensile forces are generated causing the concrete to crack and delaminate. When cracking and delamination occur, the rate of corrosion is accelerated because of the easy access of chloride ions, moisture and oxygen into the concrete.

Chlorides can be introduced into reinforced concrete from direct contact with de-icing salts or seawater. Alternatively, chlorides can be introduced deliberately during casting in the form of accelerating admixtures such as $CaCl_2$, or through the use of inadequately washed sea dredged aggregates containing NaCl (historically the use of $CaCl_2$ as an accelerating admixture in the UK was banned in 1978). [2] sets limits for acceptable chloride levels in structural concrete. For reinforced concrete, the limit of chloride ion content is either 0.2% or 0.4% by mass of cement.

Experimental Procedure

Volhard and potentiometry test methods described in [18] were employed in order to estimate the amount of water-soluble chlorides present in the following mineral fractions:

a) N.E.S. (0/2 mm)
b) N.E.S. (8/16 mm)
c) S.E.S. (0/2 mm)
d) S.E.S. (8/16 mm)
e) N.E.I.S. (0/2 mm)
f) N.E.I.S. (8/16 mm)
g) S.E.I.S. (0/2 mm)
h) S.E.I.S. (8/16 mm)

Volhard Method

The method is based on back titrating excess silver nitrate ($AgNO_3$) added to water in which the aggregates were soaked with ammonium thiocyanate (NH_4SCN), in the presence of ammonium iron (III) sulphate ($NH_4Fe(SO_4)_2 \cdot 12H2O$). Before the titration, $AgNO_3$ reacted with water-soluble chlorides from the aggregates to form silver chloride AgCl (eq. 10). The remaining silver was then titrated with thiocyanate (SCN^-) to form silver thiocyanate (AgSCN) precipitate (eq. 11). Upon complete consumption of silver, any excess thiocyanate reacted with Fe^{3+} ions to form a dark red complex $[FeSCN]^{2+}$ (eq. 12). The titration was considered complete when the solution turned pale brown in colour and the volume of NH_4SCN was recorded. The amount of chloride was then determined from the difference of the known silver added and the silver remaining.

$$\mathbf{Ag^+_{(aq)} + Cl^-_{(aq)} \rightarrow AgCl_{(s)}} \quad (10)$$

$$\mathbf{Ag^+_{(aq)} + SCN^-_{(aq)} \rightarrow AgSCN_{(s)}} \quad (11)$$

$$\mathbf{Fe^{3+}_{(aq)} + SCN^-_{(aq)} \rightarrow [FeSCN]^{2+}_{(s)}} \quad (12)$$

The required amount of coarse aggregates specified in [18] was reduced from 2 to 1 kg to limit the aggregate quantity that had to be manually sorted (**Table 6**). The coarse and fine fractions were placed in 2 and 1 litre PTFE bottles, respectively, along with the specified amount of water. The bottles were put on a rotating table and shaken for 1 hour to extract the chlorides present in the aggregates. Thereafter, the water was extracted by filtering through a medium grade filter paper.

Table 6 Amount of aggregate and water required for the Volhard method.

Required quantities	Size fraction	
	0/2 mm	8/16 mm
Mass of aggregate (g)	500	1000
Mass of deionised water (g)	500	1000

Next, 100 ml of the extracted water was placed in a 250 ml flask. To the extract water were added in the following order, while stirring continuously:

- 5 ml of HNO_3 solution (6 M)

- 15 ml of $AgNO_3$ solution (0.1 M)
- 2 ml of 3,5,5-trimethylhexan-1-ol
- 5 ml of ($NH_4Fe(SO_4)_2 \cdot 12\ H_2O$) solution (prepared by adding 60 g H_2O to 50 g of $NH_4Fe(SO_4)_2$)

The excess silver remaining was titrated with NH_4SCN (0.1004 M) until the solution turned light brown. The amount of chlorides present in the aggregates was determined by the formula:

$$\mathbf{C = 0.003546\ W\left[V_{AgNO_3} - \left(10\ C_t V_{NH_4SCN}\right)\right]}\ \ (\%) \qquad (13)$$

Where:

C	is expressed as a % by mass of the aggregate
V_{AgNO3}	is the volume of $AgNO_3$ (ml)
V_{NH4SCN}	is the volume of NH_4SCN (ml)
W	is the water/aggregate ratio (g/g)
C_t	is the concentration of standardized thiocyanate solution (M)

Potentiometry

Using a pipette, 50 ml of the filtered extract prepared for the Volhard method was transferred to a 250 ml PTFE bottle. The content of the beaker was acidified using HNO_3 to a pH value of 2-3. Next, 5 ml NaCl solution (0.01 M) was added. The content of the bottle was titrated with $AgNO_3$ solution (0.01 M) by using a potentiometric titrator. Finally, the amount of chlorides present in the aggregate sample was determined by the expression:

$$\mathbf{C\ =\ 0.000709\ V_{AgNO_3}\ W}\ \ (\%) \qquad (14)$$

Where:

C	is expressed as a % by mass of the aggregate
V_{AgNO3}	is the consumption of $AgNO_3$ solution (ml), subtracting 10 ml for the added chloride solution
W	is the water/aggregate ratio (g/g)

3.2.4 Water-Soluble Sulphate Content – following EN 1744-1:2009+A1:2012

Background Information

Soluble sulphates such as Na_2SO_4, $CaSO_4$ and $MgSO_4$ present in soils and groundwater can react with hydrated $3CaO \cdot Al_2O_3$ and $Ca(OH)_2$ of the cement paste, of hardened concrete used for foundations. Na_2SO_4 and $CaSO_4$ are more common, whereas $MgSO_4$ is less common but more destructive. The reactions result in the formation of gypsum ($CaSO_4 \cdot 2H_2O$) and ettringite ($Ca_6Al_2(SO_4)_3(OH)_{12} \cdot 26H_2O$), with volume greater than that of the reactants. Gypsum and ettringite expand, pressurise and disrupt the hydrated cement paste leading to cracking, spalling and mass deterioration. Sulphate attack occurs only when the concentration of soluble sulphate ions exceeds a certain threshold.

Other factors influencing the rate of sulphate attack are the presence of water, the cement composition and the permeability of concrete [19].

During a period of 15 years (1987 to 2002), 80 cases involving the thaumasite form of sulphate attack (TSA) were reported to building and motorway bridge foundations in UK. TSA is different from the conventional form of sulphate attack because it is the calcium silicate hydrates and not the calcium aluminate hydrates, which are targeted for reaction. The result of the reaction is the formation of the rare mineral thaumasite ($Ca_3Si(OH)_6(CO_3)(SO_4)\cdot 12H_2O$). The formation of thaumasite is accompanied by a reduction in the binding ability of the affected cement paste in the hardened concrete, resulting in a loss of strength and transformation into a soft, incohesive mass. TSA depends upon large quantities of water and the rate of deterioration is significantly increased at cold temperatures (< 15 °C) [20].

Excessive amounts of sulphates present in the raw constituents of concrete (i.e. cement, aggregates and/or mixing water) can also lead to expansion and disruption of the cement paste. [13] imposes a maximum acid-soluble sulphate content (SO_3) of 0.8% by mass of coarse Crushed Concrete Aggregate (CCA) to be used in the production of structural concrete (maximum replacement level of virgin aggregate by CCA is set at 20%).

Experimental Procedure

The test method in [18] was employed In order to determine the amount of water-soluble sulphates present in the following mineral fractions:

a) N.E.S. (0/2 mm)
b) N.E.S. (8/16 mm)
c) S.E.S. (0/2 mm)
d) S.E.S. (8/16 mm)
e) N.E.I.S. (0/2 mm)
f) N.E.I.S. (8/16 mm)
g) S.E.I.S. (0/2 mm)
h) S.E.I.S. (8/16 mm)

The method is based on extracting the amount of water-soluble sulphates (SO_3) present in the aggregates by mixing them with deionized water. The water is filtered and the amount of sulphate leached into the water is determined by barium sulphate ($BaSO_4$) gravimetry. A barium chloride ($BaCl_2$) solution is added in excess to the sulphate-laden water to precipitate barium sulphate. The amount of sulphate present is determined from the amount of barium sulphate having formed, according to the equation:

$$\mathbf{Ba^{2+} + SO_4{}^{2-} \rightarrow BaSO_4} \qquad (15)$$

For the fine (0/2 mm) fraction, 500 g of aggregates were mixed with 1000 g of deionised water, whereas for the coarse (8/16 mm) fraction, 1000 g of aggregate were mixed with 2000 g of deionised

water. The test portions were continuously mixed on a rotating table for 24 hours, after which the sulphate-laden water was filtered.

In addition, [18] specifies a second method for recycled aggregates containing active sulphates. This involves mixing 25 g of aggregates < 4 mm in 1000 g of deionised water at 60 °C for 15 minutes only. Although the aggregates were thoroughly washed and did not appear to contain active gypsum (plasterboard), S.E.S. and N.E.S. were also investigated using this method.

Next, 50 ml of the sulphate rich filtered extract was transferred to a 500 ml beaker and the test portion was diluted with additional 250 ml of water. Following this, 10 ml of HCl solution (prepared by adding 200 ml concentrated HCl to 800 ml of H_2O) was added to the test portion. The solution was heated to boiling point after which 5 ml of $BaCl_2$ solution (prepared by dissolving 100 g $BaCl_2 \cdot 2H_2O$ in 1 l of H_2O and filtered through a medium grade filter paper before use) was added drop by drop using a burette. As $BaSO_4$ precipitate formed, the solution turned white opalescent. The solution was maintained at a temperature just below boiling point for 15 minutes after which it was allowed to cool to room temperature.

The $BaSO_4$ precipitate was collected by filtering the solution through an ashless fine filter paper. The filter paper containing the barium sulphate was placed in a ceramic crucible and ignited in a furnace initially set at 110 °C. Next, the temperature of the furnace was gradually increased to 925 °C during a period of 60 minutes. The amount of barium sulphate was then weighed and the amount of sulphate present in the aggregates was determined by the expression:

$$\mathbf{SO_3} = (\mathbf{2W})\left(\mathbf{0.343 m_{BaSO_4}}\right) \ (\%) \qquad (16)$$

Where:

m_{BaSO4} is the mass of the precipitate $BaSO_4$ (g)
W is the water aggregate ratio (g/g)

It should be noted, that no active gypsum (e.g. gypsum plaster) was detected in the recycled aggregates. Consequently, the testing procedures of [18] referring to virgin aggregates were used.

3.2.5 Carbonate Content of Fine Aggregates – using XRD and TGA

Background Information

Concrete made using aggregates with high calcium carbonate ($CaCO_3$) content may be more susceptible to damage caused by the action of repeated free-thaw cycles [21] (see also relevant section on the adverse effects of repeated free-thaw cycles on concrete durability).

Experimental Procedure for XRD

X-Ray Diffraction (XRD) is a rapid analytical technique used for determining the atomic and molecular structure of a crystalline material. XRD instruments use a cathode tube to create X-rays,

which are filtered to produce monochromatic radiation, collimated to concentrate and then directed towards the sample (powder). Since X-rays are essentially waves of electromagnetic radiation, their interaction with the sample creates destructive interference (i.e. waves cancelling each other) in most directions. However, in few directions constructive interference (i.e. superposition of waves) takes place leading to wave diffraction in accordance with Bragg's law:

$$\mathbf{2dsin\theta = n\lambda} \qquad (17)$$

Where:

d is the spacing between diffracting planes (nm)

θ is the incident angle (°)

λ is the wavelength of the X-ray beam (nm)

n is any integer

The X-ray diffraction pattern generated during XRD analysis provides a unique "fingerprint" of the crystals present in the sample. When properly interpreted, by comparing it with standard reference measurements and patterns, this allows identification of the crystalline phases [22].

XRD analysis was performed in the following mineral fractions in order to determine their $CaCO_3$ content:

- N.E.S. (0/2 mm)
- N.E.S. (50/50 blend of 0/2 mm & 2/4 mm)
- N.E.S. (2/4 mm)
- S.E.S. (0/2 mm)
- S.E.S. (50/50 blend of 0/2 mm & 2/4 mm)
- S.E.S. (2/4 mm).

For this reason, 100 g test portion from each of the above mineral fractions were grounded using a RETSCH PM 400 centrifuge grinding machine (**Figure 4**). A small sample of each test portion (less than 1 g) was placed in a PHILIPS X'Pert Pro multi-purpose diffractometer (**Figure 5**) and analysed.

Figure 4 RETSCH PM 400 centrifuge grinding machine.

Figure 5 PHILIPS X'Pert Pro multi-purpose diffractometer.

Experimental Procedure for TGA

Thermal Gravimetric Analysis (TGA) is used to monitor the mass of a sample as a function of increasing temperature (at a constant heating rate) or as a function of time (at a constant temperature and/or mass loss). More specifically, when carbonates (e.g. $CaCO_3$) are heated at high temperatures they undergo thermal decomposition. For example, $CaCO_3$ decomposes to calcium oxide (CaO) and carbon dioxide (CO_2) in accordance with the following reaction:

$$\mathbf{CaCO_3 \rightarrow CaO_{(s)} + CO_{2(g)}} \qquad (18)$$

TGA was performed in the following mineral fractions in order to determine their $CaCO_3$ content:

- N.E.S. (0/2 mm)
- N.E.S. (50/50 blend of 0/2 mm & 2/4 mm)
- N.E.S. (2/4 mm)
- S.E.S. (0/2 mm)
- S.E.S. (50/50 blend of 0/2 mm & 2/4 mm)
- S.E.S. (2/4 mm).

A small sample (approximately 0.135 g) from each of the test portions prepared for XRD was used. The samples were placed in a NETZSCH TG209 F1 Libra thermal gravimetry analyser (**Figure 6**) and heated up to 1000 °C at a heating rate of 20 °C/min.

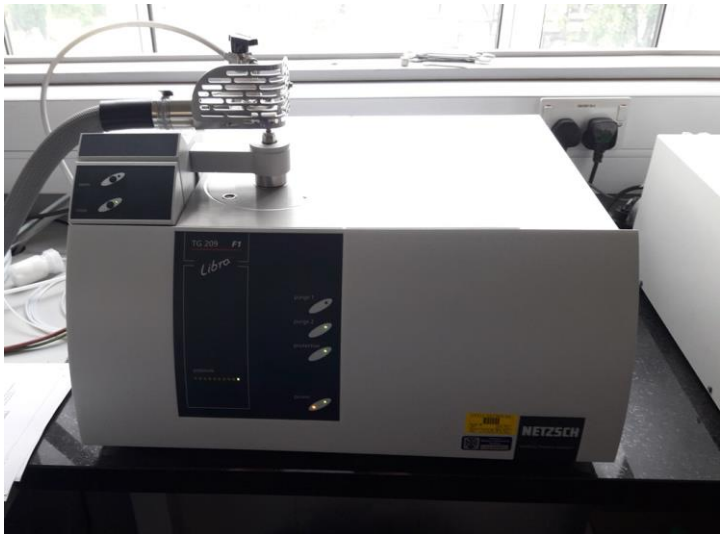

Figure 6 NETZSCH TG209 F1 Libra thermal gravimetry analyser.

3.2.6 Organic Matter – following EN 1744-1:2009+A1:2012

Background Information

The presence of organic matter (e.g. derived from the decomposition of carbon based organisms) in aggregates can prolong or even suspend setting of concrete [23], [24]. Clare and Sherwood [25] studied a range of organic compounds and classified them into three groups (**Table 7**), based on their potential to reduce the 7 day strength of mortar mixes.

Table 7 Classification of organic compounds in terms of effect on concrete setting time.

Effect on setting time of concrete	Organic substance
Inactive/slightly active	Cellulose, Wheat starch, Alginic acid, Wood, Straw, Esparto glass lignin, Gelatine
Active	Carboxylmethylcellulose, Pectin, Casein
Very active	Glucose, Nucleic acid

Experimental Procedure (Presence of Humus)

The test method in [18] was employed in order to determine the amount of humus present in the following mineral fractions:

- N.E.S. (0/2 mm)
- S.E.S. (0/2 mm)
- N.E.I.S. (0/2 mm)
- S.E.I.S. (0/2 mm).

When humus leaches in a basic aqueous environment (e.g. in the presence of NaOH), the leaching solution turns orange. The colour intensity of a solution is compared to a standard solution. If the leaching solution is darker than the standard solution, the test is deemed positive.

The standard solution was prepared by dissolving 45 g iron chloride ($FeCl_3 \cdot 6H_2O$) and 5.5 g $CoCl \cdot 6H_2O$ in 279.5 g water with 1 ml concentrated HCl, resulting in a brown/orange solution, comparable to Gardner Colour Standard Number°11 or Organic Plate Number°3. Enough aggregates (oven dried at 40 °C) from each mineral fraction were transferred to four glass bottles (one per mineral fraction). A 3% NaOH solution was carefully poured into each bottle until the solution reached a height of 120 mm. The bottles were sealed and shaken vigorously for 1 minute. The bottles were left to stand for 24 hours, where after approximately 50 ml NaOH solution from each bottle, now stained by the humus, were collected and compared to the standard solution.

Experimental Procedure (Presence of Fulvo Acid)
The method in [18] was employed in order to determine presence of fulvo acid in the fractions:

- N.E.S. (0/2 mm)
- S.E.S. (0/2 mm)
- N.E.I.S. (0/2 mm)
- S.E.I.S. (0/2 mm)

When fulvo acid is dissolved in HCl, it produces a yellow solution; the stronger the colour, the more fulvo acid is present. A quantity of 100 g aggregates (oven dried at 40 °C) from each of the mineral fractions was transferred into glass bottles to which 100 ml HCl solution (obtained by diluting 1 part of HCl to 23 parts of water by weight) was added. The bottles were sealed and vigorously shaken for 1 minute at 1 hour intervals for a period of 4 hours. Next, 75 ml of the solution was filtered off, to which 10 ml of stannous chloride was added. The stannous chloride was added to reduce any Fe^{3+} to Fe^{2+}, as the presence of Fe^{3+} ions produce a dark brown colour in the presence of HCl (Fe^{2+} is colourless).

3.2.7 Water Soluble Components from Recycled Aggregate – following EN 1744-6:2006

Background Information
Water soluble components from recycled aggregate can adversely affect the setting time of mortar and concrete.

Experimental Procedure
The test method in [26] was employed In order to determine the effect of soluble components on the initial setting time of cement. The following mineral fractions were tested:

- N.E.S. (Blend of 0/2 mm, 2/8 mm & 8/16 mm)
- S.E.S. (Blend of 0/2 mm, 2/8 mm & 8/16 mm).

The test relies on measuring setting time on cement pastes using the Vicat apparatus, in accordance with [27], prepared with water that has been soaking recycled aggregates for 3 hours.

20 kg of aggregates were placed in a 50 litre heavy duty plastic container. Since the standard does not specify a grading, aggregates were taken from all size fractions available in the following amounts: 6.7 kg of 0/2 mm, 4.4 kg of 2/8 mm and 8.9 kg of 8/16 mm. These amounts were chosen in order to approximately mimic the aggregate grading in real concrete. Enough water was added to fully cover the aggregates. Tap water was used due to the limited access to deionized water. The aggregates were allowed to stand in water for 3 hours during which they were shaken every 30 minutes. After 3 hours, the water was collected and filtered to remove any fine particles. The water was used to prepare pastes of standard consistency, achieved when the appropriate needle of the Vicat apparatus reached a distance of 6 ± 2 mm from the baseplate. This was fulfilled for mix of 500 g CEM I 52.5N with 148 g water.

3.2.8 Total/bulk chemistry of the material – using XRF

Background Information

Knowledge of the chemical composition of recycled aggregates is of paramount importance in order to detect any harmful substances that can affect the fresh, hardened and durability properties of concrete made using such aggregates.

Experimental Procedure

X-Ray Fluorescence (XRF) is a non-destructive analytical technique used to determine the elemental composition of materials. XRF devices measures the fluorescent (secondary) X-rays emitted from a sample when it is excited by bombardment with high-energy X-rays or gamma rays. When an atom in the sample is struck with an X-ray of sufficient energy, an electron from one of the atom's inner orbital shell is dislodged. Next, the atom regains stability by filling the vacancy left in the inner (lower energy) orbital shell with an electron from one of its higher energy orbital shells. The electron drops to this lower energy state by releasing an X-ray which energy is equal to the difference between the two quantum states of the electron. The measurement of this energy is the basis of XRF analysis (**Figure 7**). Each of the elements present in a sample produces a set of these characteristic fluorescent X-rays, that is unique for that specific element [28].

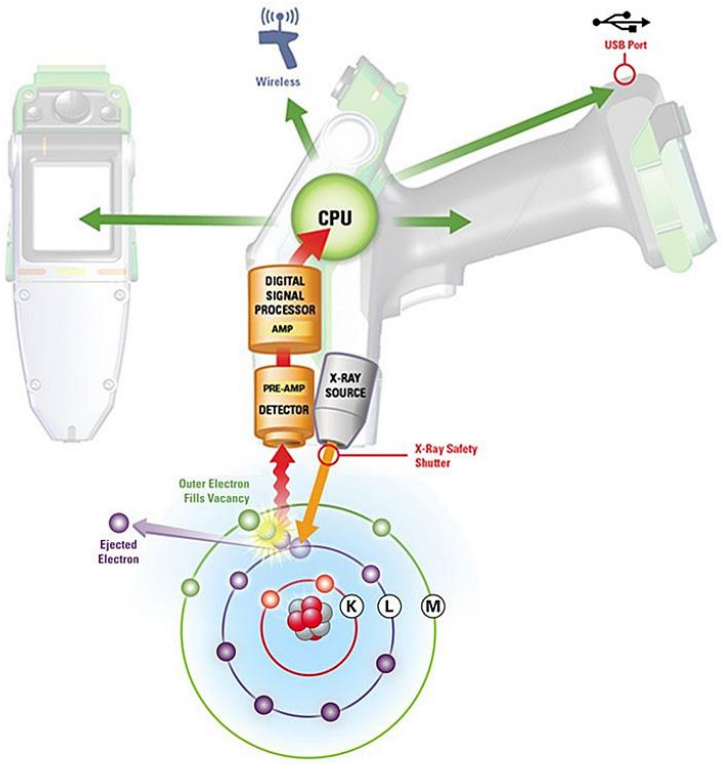

Figure 7 Schematic diagram of XRF analysis adopted from Thermo Fisher Scientific [28].

A 100 g test portion from each of the tested mineral fractions was grounded using a RETSCH PM 400 centrifuge grinding machine (**Figure 4**). Next, approximately 5 g samples from that test portions were sent to the Department of Geology, Leicester University (UK) and analysed using a PAN ANALYTICAL AXIOS Advanced XRF spectrometer.

XRF analysis was performed on the following mineral fractions:

- N.E.S. (0/2 mm)
- N.E.S. (2/8 mm)
- N.E.S. (8/16 mm)
- S.E.S. (0/2 mm)
- S.E.S. (2/8 mm)
- S.E.S. (8/16 mm)
- N.E.I.S. (8/16 mm)
- S.E.I.S. (8/16 mm).

3.2.9 Resistance to freezing and thawing – following EN 1367-1:2007

Background Information

When the temperature of saturated hardened concrete is lowered to 0 °C, the water held in the capillary pores of the cement paste matrix freezes in a manner similar to the freezing in the pores of a rock. The freezing water expands as it is converted into ice and the expansion causes localised tensile forces that fracture the surrounding cement paste matrix. The fracturing occurs in small areas, working from the outer surfaces inward. If subsequent thawing is followed by re-freezing, further expansion takes place. Hence, repeated cycles of freezing and thawing have a cumulative effect. Although the resistance of hardened concrete to repeated freeze-thaw cycles depends on its mechanical and physical properties (i.e. strength of the hardened cement paste, extensibility, creep and amount of entrained air), the main factors are the percentage of saturation and the pore system of the hardened cement paste. A closed container with >91.7% of its volume filled with water will, on freezing, become filled with ice and subjected to bursting pressure. Hence, 91.7% can be considered the critical saturation in a closed vessel. However, this is not always the case in a porous material, where the critical saturation is influenced by the size of the material, its homogeneity and the rate of freezing [19].

The concept of critical saturation also applies to individual coarse aggregate particles in concrete. Such particles can be considered as closed containers since the low permeability of the surrounding hardened cement paste will not allow water to move relatively quickly into air voids. Hence, a coarse aggregate particle saturated >91.7% will, on freezing, damage the surrounding hardened cement paste [19].

Experimental Procedure

The method in [29] was employed in order to assess the resistance to freeze-thaw cycles:

- Control – N Ireland Virgin Basalt (8/16 mm)
- N.E.S. (8/16 mm)
- S.E.S. (8/16 mm)
- N.E.I.S. (8/16 mm)
- S.E.I.S. (8/16 mm).

A sample of 2000 g coarse aggregate (8-16 mm) from each of the fractions was obtained by using a set of two sieves (aperture sizes of 8 and 16 mm). The aggregates were oven dried at 40 °C for 72 hours. The aggregates were placed in a heavy duty plastic cylindrical container, 150 mm in diameter and 160 mm high (**Figure 8**). Following this, 1000 g of deionized water were poured over the aggregates to cover them to a depth of at least 10 mm. The samples were placed in an environmental chamber set at 20 °C for 24 hours, as to fully saturate the aggregates prior to testing. The samples were then subjected to 10 freezing and thawing cycles using a TAS MTCL 1000 Series 3 environmental chamber (**Figure 9**), with temperature inside the test samples ranging from +20 °C to -17.5 °C in accordance with the temperature profile shown in **Figure 10**.

During testing, the samples were frequently inspected to maintain the water level constant. After completing the 10 cycles, all water was removed by filtering and the aggregates were oven dried at

40 °C to constant mass (since the material contains bitumen this temperature was used instead of the prescribed 110 ± 5 °C). The dried aggregates were sieved using a 4 mm sieve and the retained portion was weighed. The percentage loss in mass (%F) was given by the expression:

$$\%\mathbf{F} = \frac{\mathbf{M_1} - \mathbf{M_2}}{\mathbf{M_1}}(\mathbf{100}) \qquad (19)$$

Where:

M_1 is the initial mass of the aggregate test portion (g)

M_2 is the final mass of the aggregate test portion retained on the 4 mm sieve (g)

Figure 8 Freeze-thaw test sample of S.E.S. aggregate (8/16 mm).

Figure 9 TAS MTCL 1000 Series 3 environmental chamber.

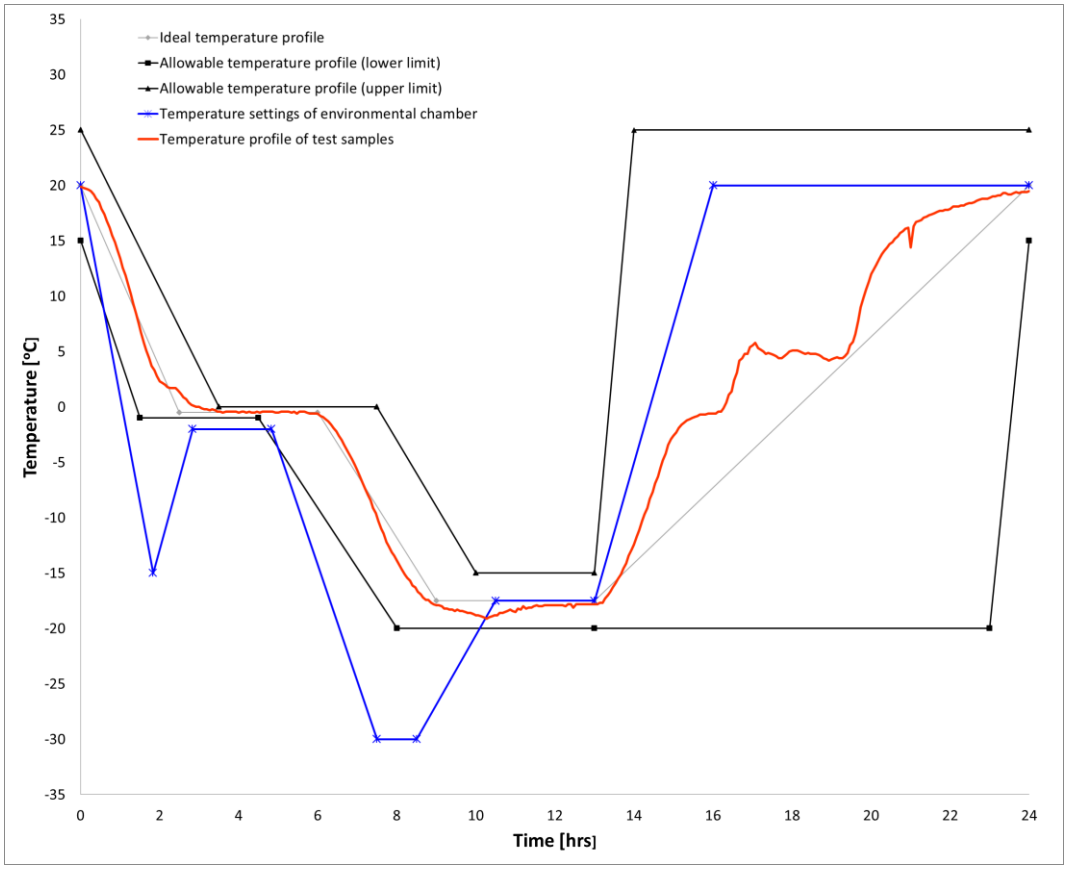

Figure 10 Freeze-thaw test temperature profiles.

3.2.10 Resistance to weathering (Magnesium Sulphate Test) – following EN 1367-2:2009

Background Information

This test subjects aggregate samples to five cycles of immersion in a saturated solution of magnesium sulphate followed by oven drying at 110 ± 5 °C (for the purpose of testing recycled aggregates which contain bitumen a temperature of 40 °C was used instead). The repeated crystallization and rehydration of magnesium sulphate within the pores of the aggregate is intended to mimic the disruptive effect of freezing and thawing (see above).

Experimental Procedure

The test method in [30] was employed in order to assess the resistance of the following coarse mineral fractions to repeated freeze-thaw cycles:

- N.E.S. (10/14 mm)
- S.E.S. (10/14 mm)
- N.E.I.S. (10/14 mm)
- S.E.I.S. (10/14 mm).

A sample of 500 g of oven dried (40 °C for 72 hours) coarse aggregate of 10-14 mm from each of the four fractions was obtained by using a set of two sieves (aperture sizes of 10 and 14 mm). The aggregates were then placed in a mesh basket 16 cm in diameter and 16 cm high (mesh opening of 4 mm), as shown in **Figure 11**, **Figure 12**, **Figure 13** and **Figure 14**. Next, 9 litres of saturated magnesium sulphate ($MgSO_4$) solution were prepared by dissolving 1500 g of salt for every 1 litre of deionized water. The solution was kept at 20 °C for the duration of testing. The test samples were then lowered in the salt solution for 17 hours. Following the above period, the test samples were removed from the solution, allowed to drain for 2 hours, and dried at 40 °C for 24 hours. This cycle was repeated 5 times. The test samples were then thoroughly washed and dried at 40 °C (instead of 110 °C) to constant mass. Finally, the aggregates were sieved using a 10 mm sieve and the weight of the retained portion was recorded.

The percentage mass loss ($\%\mathrm{MS}$), was determined according to the formula:

$$\%\mathbf{MS} = \frac{\mathbf{M_1} - \mathbf{M_2}}{\mathbf{M_2}}(\mathbf{100}) \qquad (20)$$

Where:

M_1 is the initial mass of the aggregate test portion (g)

M_2 is the final mass of the aggregate test portion retained on the 10 mm sieve (g)

Figure 11 Coarse N.E.S. aggregate sample placed inside mesh baskets for performing the $MgSO_4$ test.

Figure 12 Coarse N.E.I.S. aggregate sample placed inside mesh baskets for performing the $MgSO_4$ test.

Figure 13 Coarse S.E.S. aggregate sample placed inside mesh baskets for performing the $MgSO_4$ test.

Figure 14 Coarse S.E.I.S. aggregate sample placed inside mesh baskets for performing the $MgSO_4$ test.

3.2.11 Volume Stability-Drying Shrinkage – following EN 1367-4:2008

Background Information

Hardened Portland cement concrete tends to contract due to the loss of free water stored in the capillary pores when exposed to unsaturated air. This phenomenon is known as drying shrinkage. The amount of drying shrinkage is mainly influenced by the water content, i.e. the free water/cement ratio (w/c) of the fresh concrete mix as well as the amount and type of aggregate used. Higher w/c leads to higher levels of drying shrinkage of the hydrated cement paste. Aggregate on the other hand, restrains the amount of drying shrinkage that can be achieved by the hydrated cement paste. Consequently, the elastic properties of aggregate determine the level of restraint offered. Most types of virgin aggregate are not subject to shrinkage. However, some basalt, dolerite, greywacke and mudstone will be subjected to shrinkage. Concrete made using shrinking aggregate will exhibit high levels of shrinkage, which in turn may lead to excessive warping, deflection and cracking affecting its durability [19]. On the other hand, use of Recycled Aggregate (RA) in new concrete tends to increase its shrinkage levels. It is generally accepted that for low replacement levels (up to 30%) of coarse virgin aggregate by RA, very small or negligible increase in shrinkage is observed. However, in cases where 100% replacement level is used, an increase in shrinkage by 10-100% has been reported in literature [31].

Experimental Procedure

The [32] test method was employed in order to assess the effect of the following mineral fractions on the drying shrinkage of concrete:

- N.E.S. (Blend of 0/2 mm, 2/8 mm & 8/16 mm)
- S.E.S. (Blend of 0/2 mm, 2/8 mm & 8/16 mm)
- N.E.I.S. (Blend of 0/2 mm, 2/8 mm & 8/16 mm)
- S.E.I.S. (Blend of 0/2 mm, 2/8 mm & 8/16 mm).

Three concrete prism specimens (200 x 50 x 50 mm) were cast using saturated surface dry (SSD) recycled aggregate from each of the four fractions, CEM I 52.5 N Portland cement and w/c 0.55. The recycled aggregate used (0.125 μm to 16 mm) was graded as shown in **Table 8** (right hand side column). In addition to the four different types of recycled aggregate prisms (12 prisms in total, as shown in **Figure 15**), three control prisms using virgin aggregate (Lough Neagh Sand and basalt coarse aggregate) were cast (**Figure 16**). The prisms were cast in timber moulds (with 8 mm diameter stainless steel balls securely fixed to the centre of the inside faces of the 50 x 50 mm ends of the mould) and compacted using a vibrating table. Special care was taken to keep the trowelled face of the prisms smooth and level. The compacted prisms were covered with plastic sheets and kept in a laboratory environment (20 °C at 60% RH) for 24 hours after mixing. The prisms were then de-moulded, marked, covered with a damp hessian onto which a polyethylene sheet was placed and kept in a laboratory environment (20 °C at 60% RH) for a further 24 hours. Next, the prisms were placed in water at 20 °C for 120 hours. Following the above period, the prisms were removed from water and their length was measured using a digital length comparator (**Figure 17**). The prisms were

then placed in an oven at 40 °C (instead of 110 ± 5 °C, due to presence of bitumen in the aggregates) for 72 ± 2 hours. Next, the prisms were taken from the oven and allowed to cool in a desiccator for 24 ± 2 hours. Their length was measured and recorded as the dry measurement. Finally, the actual length of the prisms adjacent to the balls was measured to the nearest mm and recorded as the dry length. The excess drying shrinkage S of the concrete was attributed to the aggregate and was determined by the expression:

$$\mathbf{S} = \frac{\mathbf{w} - \mathbf{d}}{\mathbf{l}}(\mathbf{100}) \qquad (21)$$

Where:

w	is the wet measurement (mm)
d	is the dry measurement (mm)
l	is the dry length (mm)

Finally, it should be noted that [13] sets a maximum limit of 0.075% on the aggregate (virgin or recycled) drying shrinkage, when measured using the above test method.

Table 8 Required vs adopted grading of aggregate used for making drying shrinkage test concrete prisms.

Sieve size (mm)	**Overall grading limits** [32]			**Adopted grading**
	Lower % passing	Preferred % passing	Upper % passing	% passing
20	100	100	100	n/a
16	76	82	92	100
14	65	69	83	69
12.5	60	64	78	n/a
11.2	56	60	76	n/a
10	50	55	70	55
8	41	46	61	46
6.3	n/a	n/a	n/a	40
5.6	32	38	52	n/a
5	n/a	n/a	n/a	35
4	26	30	53	30
2	20	22	33	22
1	14	17	25	17
0.5	10	12	18	12
0.25	5	8	12	8
0.125	0	2	6	2

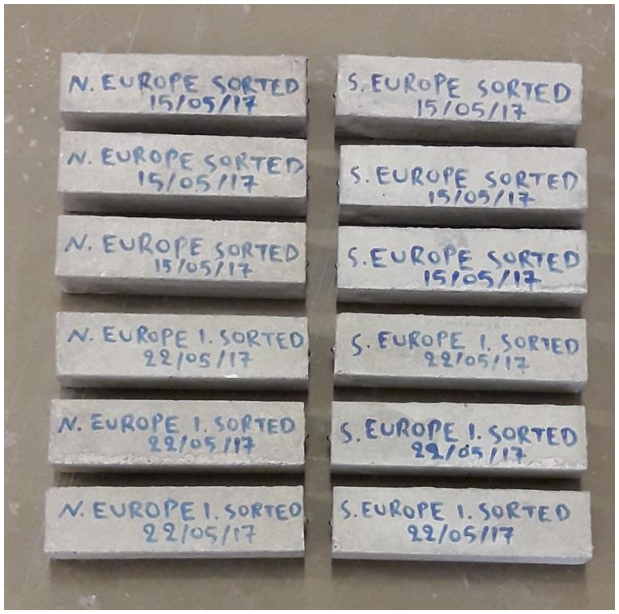

Figure 15 CDW concrete prisms for drying shrinkage testing.

Figure 16 Concrete prisms for drying shrinkage testing (control specimens).

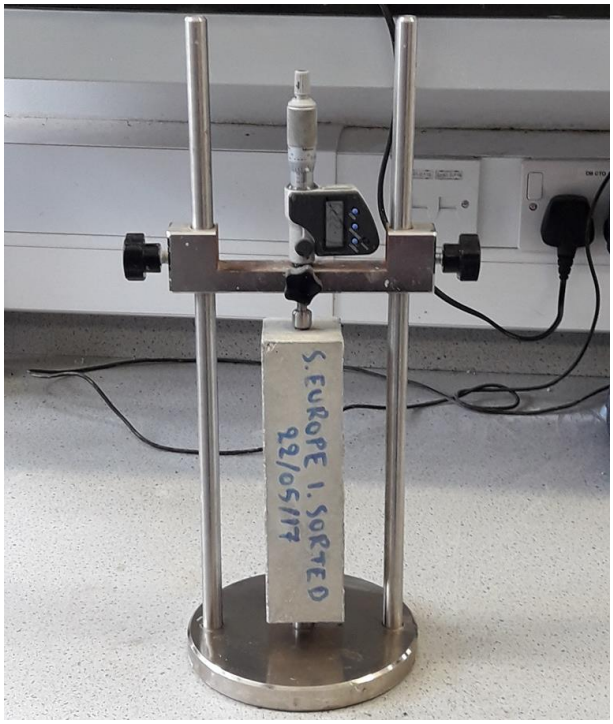

Figure 17 Comparator for measuring drying shrinkage of concrete samples.

3.2.12 Alkali-Silica Reactivity

Background Information

In most cases, virgin aggregates used in the production of concrete are chemically inert. However, in the presence of moisture, some types of aggregate react with alkali hydroxides in pore water derived from the alkalis of cement. The result of this deleterious reaction is the formation of a gel, either in planes of weakness or pores of reacting aggregates, or on the surface of reacting aggregates [19]. This alkali-silica gel attracts water by absorption or osmosis and thus increases in volume, creating tensile forces causing tension cracking around the aggregates. When cracks form, more moisture penetrates the concrete, accelerating the alkali aggregate reaction.

Experimental Procedure

The [33] test method was employed in order to assess the potential alkali-reactivity of the following mineral fractions:

- N.E.S. (0/2 mm)
- S.E.S. (0/2 mm)
- N.E.I.S. (0/2 mm)
- S.E.I.S. (0/2 mm).

This test method was developed by RILEM as a faster and more reliable alternative to [34]. Three mortar prism specimens (285 x 25 x 25 mm) were cast using saturated surface dry recycled aggregate from each of the above four fractions, CEM I 52.5 N Portland cement and w/c 0.47. The recycled aggregate (0.125-4 mm) was graded as shown in **Table 9**. The prisms were cast in steel moulds (with 8 mm diameter stainless steel balls securely fixed to the centre of the inside faces of the 25 x 25 mm ends of the mould) and compacted using a vibrating table. Special care was taken to keep the trowelled face of the prisms smooth and level. The compacted prisms were covered with polyethylene sheets and kept in a laboratory environment (20 °C at 60% RH) for 24 hours after mixing. The prisms were then de-moulded and their initial length was measured using a digital length comparator. Next, the prisms were placed in water and transferred to an oven at 40 °C for a period of 24 hours. The standard stipulates a temperature of 80 ± 2°C, but since the recycled aggregates contain bitumen this major deviation from the standard was chosen). Following the above period, the prisms were removed from water and their length was immediately measured before a significant drop in temperature took place (zero reading). The prisms were then placed in a container with a 1 M solution of NaOH already at 40 °C (instead of stipulated 80 ± 2 °C) as shown in **Figure 18**. The container was sealed and placed in the oven at 40 °C (instead of specified 80 ± 2 °C) for 14 days. During this period, frequent length measurements at 24 or 72 hours were taken. The results were compared with control mortar prisms with virgin aggregate (N. Ireland Lough Neagh Sand) (**Figure 19**).

Table 9 Aggregate grading requirements adopted from RILEM TC106-2.

Sieve Size		Mass retained (%)
Passing	Retained	
4 mm	2 mm	10
2 mm	1 mm	25
1 mm	500 µm	25
500 µm	250 µm	25
250 µm	125 µm	15

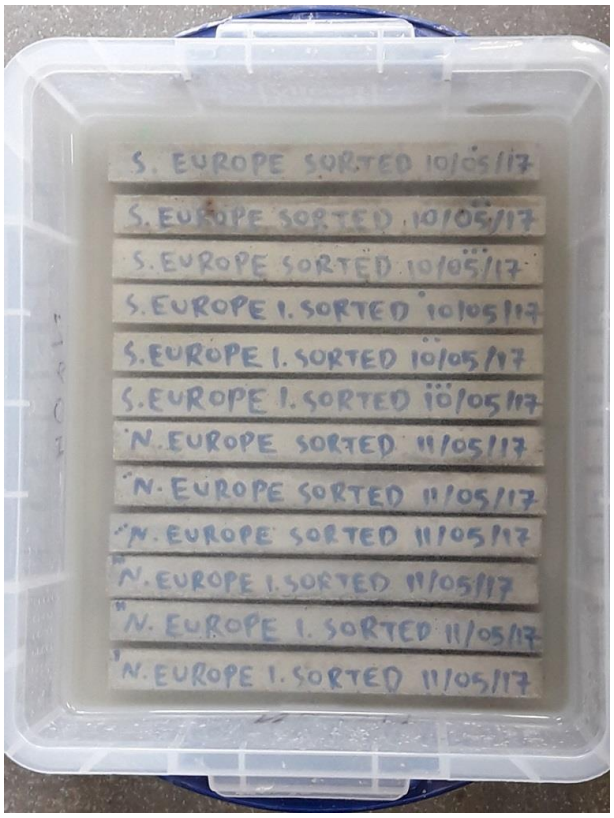

Figure 18 Mortar prisms for ASR testing, immersed in 1 M NaOH solution. Prisms made using CDW sand (0/2 mm).

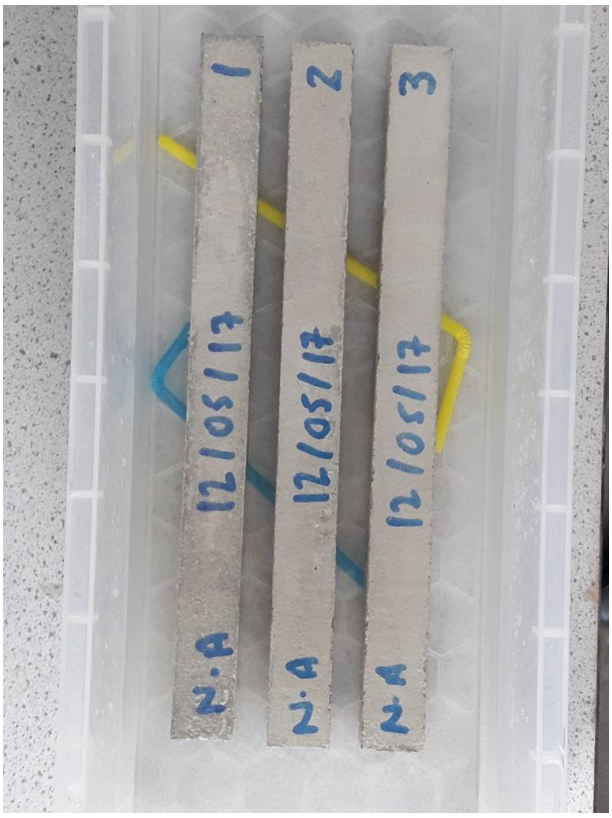

Figure 19 Mortar prisms for ASR testing, immersed in 1 M NaOH solution. Prisms made using virgin sand (0/2 mm).

3.2.13 Grading – following EN 933-1:2012

Following [35], an aggregate test portion is divided into several particle sizes by using a series of test sieves, stacked on top of each other from top to bottom in decreasing aperture size order, and placed in a sieving machine. After sieving, the material retained on each sieve is weighed and related to the total mass of the test portion. Knowledge of the particle size distribution of each aggregate

fraction is important, when for example designing an optimal grading curve for the total aggregate content to be used in a concrete mix.

Before sieving, the sample was dried at 110 °C and weighed, then washed and dried again at 110 °C. The size-fractions tested were 0/2, 2/8 and 8/16, and the amount of material used for each of these size-fractions was 500 g, 1200 g and 2900 g, respectively. Each sample was sieved for 12 minutes, with an oscillation amplitude of 1.9 mm, using a Haver EML Digital Plus test sieve shaker from Haver & Boecker.

3.2.14 Flakiness Index – following EN 933-3:2012

Following [36], Flakiness Index (FI) gives a measure of the aggregate particle shape, by sieving of aggregates on bar sieves. The particle shape is important to know in order for a first estimation on how the aggregates will affect the behaviour of the fresh concrete. The test is conducted by two sieving steps. In the first, the tested aggregate fraction is divided into sub-fractions using squared test sieves (d_i/D_i). In the second step, each of these sub-fractions is sieved on bar sieves (bar width = $D_i/2$). The overall FI (dimensionless) for a particular size-fraction is calculated by the expression:

$$\mathbf{FI} = \frac{\mathbf{M2}}{\mathbf{M1}}\ (\mathbf{100}) \qquad (22)$$

Where
M1 is the sum of the sub-fraction masses (g)
M2 is the sum of the sub-fraction masses, passing the bar sieve of slot width $D_i/2$ (g)

The size-fractions 2/8 and 8/16 were tested. The sub-fractions obtained in the first step and the bar sieve widths used in the second step are shown in **Table 10**. Note that for size-fraction 2/8, because FI is not measured on particles < 4 mm only the 4-8 mm portion was included in the analysis (using sub-fractions 4-5, 5-6.3 and 6.3-8 mm).

Table 10 Flakiness Index – sub-fractions and bar sieve widths.

Size-fraction, d/D (mm)	Step 1: Sub-fractions, d_i/D_i (mm)	Step 2: Bar sieve width, $D_i/2$ (mm)
8/16	12.5-16	8
	10-12.5	6.3
	8-10	5
2/8 (excluding < 4 mm)	6.3-8	4
	5-6.3	3.15
	4-5	2.5

3.2.15 Flow coefficient of Fine Aggregates – following EN 933-6:2014

In this test [37], the time for a specified volume of sand (0/2) loaded in a standardised cone to flow through its lower circular opening is measured. The resulting value corresponds to the flowability of

the sand and thus gives an indication of how it will affect the rheology of the fresh concrete. A shorter flow time indicates better flowability and thus better concrete rheology.

The sample is prepared by washing, drying for 24 h at 110 °C and sieving using aperture sizes 0.063 and 2 mm. All material retained on the 2 mm sieve or passing the 0.0063 mm sieve is discarded. Since the sample volume is specified and always should be the same, the amount of sample (mass in g) requested for the analysis is calculated according to the relation:

$$\mathbf{m_{sample}}\ (\mathrm{g}) = \mathbf{1000}\left(\frac{\boldsymbol{\rho_p}}{\mathbf{2.70}}\right) \qquad (23)$$

Where

ρ_p is the pre-dried particle density of the aggregate to be tested (Mg/m^3)

2.70 is a constant (Mg/m^3)

For most normal aggregates, the amount of sample is approximately 1 kg.

A standardised cone with specified dimensions is filled with the sample material. The lower opening is 11.99 mm in diameter and closed with a cover plate during sample loading. Synchronized with the opening of the hatchet, a stopwatch is started and the time for all sand to run through the lower opening is measured. The sand is collected in a container below the cone and the measurement is repeated using the same test portion. The flow coefficient is expressed in *seconds*, as the mean value of five such measurements. Usually a reference sand with pre-dried particle density 2.70 Mg/m^3 and flow time 32 ± 2 s is measured at the same time, but as such sand was not available this was not done and the results can thus only be compared relative each other.

3.2.16 Resistance to Fragmentation – following EN 1097-2:2011

Resistance to fragmentation is measured using the Los Angeles test [1], with result expressed as LA coefficient. An amount of 5000 g aggregate in the size-range of 10-14 mm is rolled with 11 steel balls in a rotating hollow steel drum (500 revolutions using a rotational speed of 31-33 revolutions/min). Next, the tested material is washed and sieved using a 1.6 mm sieve and dried to a constant mass at 110 °C (instead of 40 °C stipulated in standard for temperature sensitive recycled aggregates). The LA coefficient is calculated using the expression:

$$\mathbf{LA} = \frac{(\mathbf{5000} - \mathbf{m})}{\mathbf{50}} \qquad (24)$$

Where

m is the material retained on the 1.6 mm sieve, measured in grams

In order to obtain the correct sample size-range from the tested 8/16 size-fraction, the particles were sieved using sieves with aperture size 14, 11.2 and 10 mm. Only material passing the 14 mm

and retained on the 11.2 and 10 mm sieves was used for the test, in such proportions that 35 % of the sample (i.e. 1750 g) was in the size-range of 10-11.2 mm and 65 % (i.e. 3250 g) in the size-range of 11.2-14 mm. Each fraction was washed and dried to constant temperature individually, before being mixed into a combined 10-14 mm fraction. The drying was at 110 °C and not the 40 °C stipulated for temperature sensitive recycled aggregates in EN 1097-2, and is thus a deviation.

3.2.17 Resistance to Wear – following EN 1097-1:2011

The resistance to wear is tested using the micro-Deval method [38], in which an aggregate sample is rotated in a steel drum with grinding agents (steel balls) and the amount of material retained on the 1.6 mm sieve after the test is weighed and related to the initial sample amount.

Two samples, each consisting of 500 g aggregate particles in the size-range of 10-14 mm, are sieved from the 8/16 fraction to be tested. The sieving was performed so that the two fractions 10-11.2 and 11.2-14 mm were obtained, weighing 175 g (35% of sample) and 325 g (65% sample), respectively. Each fraction was separately washed and dried to constant mass at 110 °C, before being mixed to one sample ready for testing.

The two 500 g samples were placed in two separate steel drums. To each drum, steel balls (5000 g) and water (2.5 l) were added. The drums were placed on shafts and rotated 12 000 revolutions with a rotational speed of 100 ± 5 revolutions/min. The material was washed on a 1.6 mm sieve and then dried to a constant mass at 110 °C.

The result is expressed as the mean value of the individual M_{DE} values from the two measurements, calculated using the following expression:

$$\mathbf{M_{DE}} = \frac{(\mathbf{500} - \mathbf{m})}{\mathbf{5}} \qquad (25)$$

Where

m is the material retained on the 1.6 mm sieve, measured in grams

3.2.18 Particle Density and Water Absorption – following EN 1097-6:2013

Particle density (apparent, saturated surface dry and oven-dried) and water absorption were determined according to [39], using the pycnometer method on 8/16 and 2/8 (Clause 8), and 0/2 (Clause 9) fractions. Air bubbles were removed by gently jolting/rolling the pre-calibrated pycnometer, before as well as after the 24 h aggregate soaking period. Saturated 8/16 and 2/8 mm aggregates were surface dried using Wettex cloth (Clause 8), until the aggregates looked matte but still moist.

In excess of measuring after 24 h water soaking time and using drying temperature of 110 °C (both according to standard), measurements were also conducted for long-time water absorption (at

intervals from 1 h up to 14 days) as well as using drying temperature of 40 °C (due to presence of bituminous materials in the CDW).

For size-fraction 0/2 (Clause 9), instead of Wettex cloth, a metal cone was used in order to determine when the aggregates were water saturated but surface dry. The metal cone is filled with the specified amount of aggregate and gently stamped 25 times. The cone is lifted and the shape of the unsupported aggregate pile is compared with the pictures in EN 1097-6 Annex F, showing different sand pile shapes in relation to drying status. If the sand was considered to still be wet (i.e. not surface dry), the sand was placed in the oven again for further drying, before making the test again.

3.3 Methods for Fine materials

During the wet processing and sorting of CDW using CDE's recycling plant equipment, all the washings are collected on fine filters. This filter cake consists of very fine materials, typically smaller than 63 µm in size (i.e. silt and clay fraction), and may consist of top soil and other organic matter. This material is considered inert but published literature suggests that it can in effect be reactive as clay and soil can be present [40]. The aim on this subtask is to assess the potential of using this filter cake in the development of building products.

25 kg of fine material was obtained from the Northern Europe recycling plant only. Upon reception, several kilos of the fine material were placed in the oven at 40 °C to dry until constant mass for subsequent testing. A small portion was also calcined at 700 °C for 6 hours [41]. The principle of calcining the fine material (i.e. removal of structural water) was to investigate its potential use as a precursor for geopolymer materials [42].

The relevant methods for the chemical and physical characterization of CDW fine mineral fraction (< 0.063 mm) are summarized in **Table 11**. The methods are according to EN standards and are generally developed and designed for natural aggregates (sand, gravel and crushed rocks).

Table 11 Test methods for CDW fine materials fraction.

Property	Standard	Laboratories
Physical Testing		
Liquid Limit	BS 1377-2:1990	QUB
Plastic Limit	BS 1377-2:1990	QUB
Plasticity	BS 1377-2:1990	QUB
Chemical Testing		
XRF Analysis	n/a	QUB
XRD Analysis	n/a	QUB

Property	Standard	Laboratories
FTIR Spectroscopy	n/a	QUB
DTA-TGA	n/a	QUB
Soluble components (humus, fulvo acid, sulphates & chlorides) Soluble components (alkalis)	EN 1744-1:2009+A1 :2012 ICP MS	QUB
Activity Index	n/a	QUB
Reactivity/Isothermal calorimetry	CEN/TR 16632	QUB

The used methods are shortly described below, with emphasis on special procedures and deviations used for the CDW.

3.3.1 Liquid Limit (w_L) – following BS 1377-2:1990

The liquid limit of the fine material was determined following the cone penetrometer method described in BS 1377-2:1990 [43]. Physically, the liquid limit is the moisture content at which the soil passes from a plastic state (below the limit) to a liquid state (above the limit). The liquid limit is taken as the moisture content (in %) when the cone penetrometer penetrates the paste by 20 mm. A picture of the cone penetrometer can be seen in **Figure 20**. The penetrometer is also fitted with an automatic release and locking device as to lock the cone into position.

Figure 20 Penetrometer and sample holder.

For the test, 400 g material passing a 425 µm sieve was collected. Water was added to the soil and mixed using a palette knife as to produce a workable paste. The paste was subsequently wrapped in cling film and was allowed to rest for 24 hours for the water to fully permeate through the soil.

Following the rest period, the fine material was mixed thoroughly with little added water so that the moisture content of the paste allowed a 15 mm penetration depth by the penetrometer for the first reading. A portion of the paste was transferred into the sample holder in such a way as to avoid the creation of air voids. Any excess paste was removed as to produce a level surface. The specimen was placed underneath the cone, which was subsequently lowered to be just in contact with the soil specimen. The cone was released and allowed to penetrate the soil under its own weight for 5 seconds, before being locked into position again. The penetration depth was then recorded. A portion of the paste was weighed in a container of mass m_1 and placed in the oven at 105 °C to dry until constant mass. The moisture content (MC) of the paste was calculated according to the equation:

$$\mathbf{MC} = \frac{\mathbf{m_2 - m_3}}{\mathbf{m_3 - m_1}}(\mathbf{100}) \qquad (26)$$

Where:

m_1 is the mass of container (g)

m_2 is the mass of the wet soil (paste) (g)

m_3 is the mass of the dry soil (g)

3.3.2 Plastic Limit (w_p) – following BS 1377-2:1990

The plastic limit is taken as the moisture content that allows for the paste to be rolled to thin strips 3 mm in diameter before cracking. A small amount of soil paste initially prepared for determining the elastic limit (with sufficient moisture content as to achieve a penetration depth of 15 mm) was allowed to dry on a glass plate until a smooth ball could be formed. The paste was continuously handled as to allow moisture to escape until cracks appeared. The paste was divided into several pea size pieces. Each piece was rolled to a thread, 3 mm in diameter, in 10-15 back and forth rolling motions against a glass plate. This process was repeated until the threads just started to shear when approaching a diameter of 3 mm (using a rod of 3 mm in diameter as visual reference). The threads were split into 2 lots of 4 threads and were weighed before and after drying at 105 °C in order to determine the moisture content and the plastic limit.

3.3.3 Plasticity – following BS 1377-2:1990

The plasticity index (I_P) is the difference between the liquid limit (w_L) and the plastic limit (w_p):

$$\mathbf{I_p = w_L - w_p} \qquad (27)$$

3.3.4 XRF Analysis

For a brief description of XRF, please refer to XRF of 0/2 mm, 2/8 mm and 8/16 mm mineral fractions (Section 3.2.8).

3.3.5 XRD Analysis

For a brief description of XRD, please refer to XRD of fine mineral fractions (Section 3.2.5).

3.3.6 FTIR Spectroscopy

Fourier Transform Infrared Spectroscopy (FTIR) is a technique used to obtain an infrared spectrum of absorption or emission of sample. When a solid, liquid or gas sample is exposed to infrared radiation, part of it is absorbed and the rest is transmitted. The resulting signal can be processed using the Fourier Transform method in order to get an infrared spectrum, which represents a molecular "fingerprint" of the sample. Since different molecules create different spectras, information regarding the chemical composition of the sample can be obtained [44].

3.3.7 DTA-TGA

For a brief description of TGA, please refer to TGA of fine mineral fractions (Section 3.2.5).

3.3.8 Soluble components – following EN 1744-1:2009+A1:2012 and ICP-MS

For a description on the determination of humus, please refer to Section 3.2.6.

For a description on the determination of fulvo acid, please refer to Section 3.2.6.

For a description on the determination of water-soluble sulphate content, please refer to Section 3.2.4.

For a description on the determination of water-soluble chloride content, please refer to Section 3.2.3.

Soluble alkali content was determined by Inductively Coupled Plasma Mass Spectroscopy (ICP-MS). An ICP instrument works by generating plasma, i.e. an electrically charged gas in which atoms are present in an ionised state. The plasma is maintained through inductive heating of flowing gases using a coil that creates a magnetic field. The plasma is surrounded and contained by argon gas to prevent it from touching any surfaces, which would damage the instrument. The sample to be tested is dissolved in an aqueous solution, which is atomised using a nebuliser and passed into the plasma torch. Light is emitted from the atoms of an element in the ICP instrument. This light is converted into an electrical signal by resolving the light into its component radiation, (using diffraction grating),

and then measuring the intensity of the light with a photomultiplier tube. Each element has a specific wavelength and the measured wavelengths are compared to known standards and the elemental concentrations are calculated.

For analysis, a sample of known volume/mass was placed in a beaker and deionised water was added in a ratio of 1:2 (sample to water). The mixture was shaken for 24 hours after which the sample was left to settle and the liquid was decanted off. This solution was acidified and fed into the ICP instrument. This defined the leached chemical make-up of the sample with a few simple calculations.

3.3.9 Activity Index

The activity index (A) of a soil is equal to the plasticity index (I_p) divided by the percent of clay-sized particles (less than 2 μm) present as shown below:

$$\mathbf{A} = \frac{\mathbf{I_p}}{\%\ \mathbf{clay\ particles}} \qquad (28)$$

In order to determine the activity index, the amount of clay present in the fine material must first be determined. This was achieved by wet sieving 500 g of the fine material according to BS 1377-2:1990 [43], to separate silt and clay particles from the bulk. Before wet sieving, the fine fraction was mixed in excess water for 1 hour to loosen the particles. The wet fine fraction was transferred to a 2 mm sieve nestled in a 0.063 mm sieve and washed thoroughly until water passing the finer sieve ran clear. The retained portion was spread evenly in trays to dry at 105 °C until constant mass. Once dry, the fine fraction was broken gently in a pestle and mortar to loosen the particles before being sieved dry through the available sieves ranging from 4 mm down to 0.063 mm.

A small amount of the fine material passing the 0.063 mm sieve was retained and dried until constant mass. This very fine fraction was measured using a Malvern particle size to determine the amount of silt and clay.

3.3.10 Reactivity/Isothermal calorimetry

The heat associated with the hydration of fine materials was measured with a TAM-air 8 channel calorimeter conforming to [45], as shown in **Figure 21**. Both uncalcined and calcined fine material samples were tested, and their hydration was activated either by using deionized water or NaOH/KOH solutions (1 M and 2 M for uncalcined fine material, and 1 M, 2 M and 8 M for calcined fine material). 5 g of fine material was mixed with 5 g of deionized water or alkali solution for 1 minute. 5 g of the resulting paste was transferred in a plastic vial before being placed in the calorimeter, set at 20 °C. The heat released during hydration was measured for a total of 7 days.

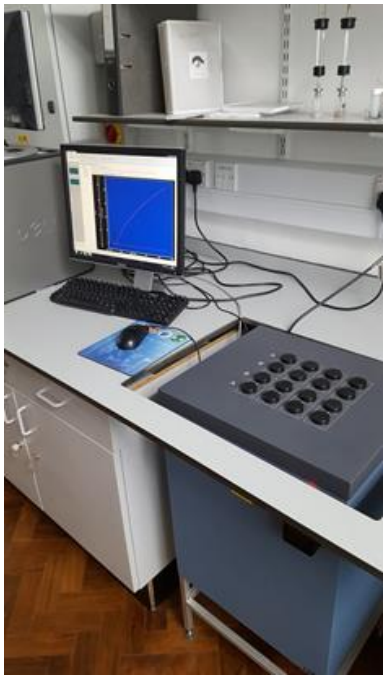

Figure 21 TAM-air 8 channel calorimeter.

3.4 Methods for Lightweight materials

3.4.1 Materials overview

As reported in **Table 1** the following lightweight (LW) fractions from CDW have been selected for the experimental activities:

- mixed Wood and Plastic (WP) and mixed Rigid Plastic (RP) scraps to be assessed as aggregates for LW concretes development (Subtask 5.1.3);
- RP and Wood (W) scraps for LW insulation panels development (Subtask 5.2.4).

The partner CDE has provided to CETMA two different batches of LW materials in different size fractions coming, respectively, from Southern Europe (S-EU) and Northern Europe (N-EU) source. Among the received materials, the sizes considered suitable for the Project purposes are:

- WP 0-4 mm scraps – a typical by-product of the CDW processing plant, which results as floating material of washing steps required for CDW cleaning and that, currently, is discarded since it has not a specific application; this scrap has by itself suitable size to be tested as fine aggregate for mortars/concretes without any further process (**Figure 22**);
- RP and W < 100 mm scraps – LW fractions separated before mineral CDW fractions processing; these scraps need a further grinding process to allow size reduction in the view of their assessment as aggregates for mortars/concretes (RP fine/medium fractions) and insulating panels production (RP medium/coarse fractions, W chips/fibres).

Figure 22 Wood and Plastic fractions rejected from CDW processing plants and relevant magnification (on the right) showing polystyrene particles and cortex pieces.

RP from S-EU and N-EU were ground by a grinder equipped with sieves having size up to 10 mm; the resulting material was then sieved in 0-4 mm and 4-10 mm fractions to comply with the size range reported in the standards for characterization (**Figure 23**, **Figure 24**).

Figure 23 Rigid Plastic fractions from S-EU source as received, grinder and after the grinding process (coarse fraction).

Figure 24 Rigid Plastic fractions from N-EU source as received, grinding process and resulting material (fine fraction).

W from S-EU arrived as pieces of dimensions in the range 100-200 mm. Thus it was necessary a further grinding process in order to reduce the material in fibres. A grinder with a sieve with a circular mesh of 20 mm was used (**Figure 25**). W from N-EU was delivered already in chips and fibres shape, so no further grinding process was necessary (**Figure 26**).

Figure 25 Wood fractions from S-EU source as received, grinder, 20 mm circular mesh sieve and wood after grinding process (size <20 mm).

Figure 26 Wood fractions from N-EU source (as received).

3.4.2 Characterization methods

Methods for the geometrical and physical characterization of CDW LW fractions are summarized in **Table 12**. Note that, depending on the intended application (e.g. concretes, panels), for each CDW-derived material specific characterization tests were selected. The CDW-derived materials to assess as concrete aggregates (WP, RP) were tested according to EN relevant standards, whereas for the CDW-derived materials allocated to panels (RP, W) there are no EN standards that establish a way of characterization. For this reason, RP was considered characterized by means of the characterization work made for concrete aggregates, while W was geometrically and physically characterized using technical procedures reported by wood panel producers.

Table 12 Physical and geometrical test methods for CDW LW fractions.

Property	Standard	Laboratories
Mixed Wood and Plastic (WP) intended as LW aggregate for concretes		
Grain Size	EN 933-1 | Determination of particle size distribution	CETMA
Density	EN 1097-3 | Determination of loose bulk density and voids; EN 1097-6 | Determination of particle density and water absorption (Chapters 8, 9 and Appendix C)	CETMA
Water Absorption	EN 1097-6 | Determination of particle density and water absorption (Chapters 8, 9 and Appendix C)	CETMA
Mixed Rigid Plastic (RP) intended as LW aggregate for concretes and component material for LW panels		
Grain Size	EN 933-1 | Determination of particle size distribution	CETMA
Density	EN 1097-3 | Determination of loose bulk density and voids; EN 1097-6 | Determination of particle density and water absorption (Chapters 8, 9 and Appendix C)	CETMA
Water Absorption	EN 1097-6 | Determination of particle density and water absorption (Chapters 8, 9 and Appendix C)	CETMA
Wood (W) scraps intended as component material for LW panels		
Grain size	EN 933-1 | Determination of particle size distribution	CETMA
Density	n.a.	CETMA

Moisture content	n.a.	CETMA

The used methods are shortly described below, with emphasis on special procedures and deviations used for the CDW LW fractions.

Grain size

The method applied for testing WP and RP consists in the determination of particle size distribution by the sieving method. This method is suitable for natural aggregates, artificial aggregates included lightweight materials such as WP and RP. The fraction WP was tested as received, while RP was grinded and separated into 0-4 mm and 4-10 mm fractions to comply with the size range reported in such standard. No specific deviations, with respect to the standard protocol UNI EN 933-1, were necessary. The materials were sampled according to UNI EN 932-2, amounts of samples for testing were those recommended for normal weight aggregates (based on the maximum aggregate size), no washing was applied (being both materials free of agglomerate particles and to avoid physical deterioration, especially for WP), the materials were oven dried at 80°C (against the 110±5°C suggested by the standard, to avoid material deterioration) up to the mass stabilization and then sieved.

W fraction has been characterized to define particle sizes. Two different characterizations have been carried out. The first one is a type of determination of particle size distribution of wood chips described in a number of standards (ANSI/ASAE S424.1 MAR98, SCAN-CM 40:94), which are referred to wood chips materials and is similar to the methodology described in EN 933-1. It has been a one-dimensional sorting, in order to determine the ratio of powder (or near powder sized particles) on the total amount of material. Moreover, first data on size distribution have been acquired. In this sorting method, squared-shaped meshes sieves, with mesh dimensions varying from 32 mm to 0.63 mm, are used. The screens are usually arranged in a tower of several sieves, which are clamped to each other, starting with the largest aperture size on top. They are operating in a one-, two- or three-dimensional screen shaking movement sorting the particles by decreasing size. For each batch of wood fraction, 8 l volumes have been sieved with this method. These quantities are the only variation to the EN 933-1 standard, where 10 kg of materials are required. Such quantity corresponds to a too high value of volume of material to be characterized.
In order to better define the particles geometry of wood fraction a second manual sorting of the particle has been carried out, separating particles as a function of the length. This work was aimed to define the typology of particles present in the wood fraction (i.e. chips, fibres, wood wool) and their range of length. The method, which has not a reference standard, consisted in dividing three times in quarter an 8 l volume of wood fraction for each batch, obtaining 4 samples of 0.125 l to be sorted. Four different classes of length have been used for the characterization: 0-2 cm; 2-4 cm; 4-6 cm; 6-8 cm.

Density, water absorption and moisture content

Two different methods were applied for testing WP and RP: UNI EN 1097-3 for loose bulk density (ρ_b) and UNI EN 1097-6 for the evaluation of apparent density (ρ_a), particle density on an oven dried basis (ρ_{rd}), particle density on a saturated and surface-dried basis (ρ_{ssd}) as well as water uptake (WA_{24h}) of aggregates.
UNI EN 1097-3 is suitable for natural and artificial aggregates, while UNI EN 1097-6 includes methods for testing both normal weight and lightweight aggregates. These standards seemed close to the specifications of the materials at issue. No specific deviations, with respect to standard protocol UNI EN 1097-3, were necessary; the materials were oven dried at 80°C (against the 110±5 °C suggested by the standard, to avoid material deterioration) up to the mass stabilization and then tested. In the case of UNI EN 1097-6, different methods suggested by the standard were applied (pycnometer methods). At first, the method reported in Appendix C was followed, being specific for LW-aggregates; this protocol is however suitable for aggregates over than 4 mm (this is, for instance, not the case of WP and RP below 4 mm) and allows only the evaluation of apparent density (ρ_a) and water uptake after 5 min and 24 h of water immersion. In addition, based on indirect evidence from LW-mortars investigated in WP5, densities of WP and RP seemed not consistent with those measured according to the protocol (possibly due to the specific nature of the materials under investigation). It was, therefore, decided to apply the procedures included in the same standard but suggested for NW-aggregates that are Chapter 9 for 0.063-4 mm fractions and Chapter 8 for 4-31.5 mm fractions. The materials were sampled according to UNI EN 932-2, samples of 0.5-0.6 l were prepared for testing as suggested by Appendix C for LW-aggregates. No specific deviations, with respect to the standard protocol UNI EN 1097-6, were necessary. Once the condition of aggregates saturated with dried surface was reached (the cone method was used to assess the non-adherence of granules), such aggregates were oven dried at 80°C (against the 110±5 °C suggested by the standard to avoid material deterioration) up to the mass stabilization.

The density of W fraction is obtained by the ratio between the mass of wood particles and their apparent volume, at a pre – determined moisture content value. The determination of moisture content is necessary because of the direct proportionality between the two parameters, density and moisture content.
The moisture content in W fraction was calculated as the ratio between the mass of water in the wood fraction under examination and the same anhydrous wood fraction. In order to obtain the anhydrous wood fraction, the exsiccation method has been carried out. The wood fraction, after being weighted, is oven dried at 103±2 °C, until the mass stabilization.

Considerations on thermal tests

With respect to thermal properties (e.g. thermal conductivity, heat capacity), it was decided to measure them when WP, RP and W materials will be incorporated into the final components (LW mortars/concretes, LW insulation panels) to develop within WP5. This decision moved from the assumption that such characterizations tests can provide more meaningful info if directly assessed

for the final components, which will be produced later in the Project once the concerning formulations will be optimized.

3.5 Methods for Timber materials

The relevant methods for the procurement and characterization of CDW timber are summarized in **Table 13**. Methods focus on strategies to increase the reuse of complete or reprocessed timbers in order to develop a separate material stream for this purpose. Aim is to generate raw materials from salvaged timber that can be strength graded according to existing norms and processed along existing production lines. The applied methods are briefly described in the following paragraphs, with emphasis on special procedures and deviations used for the CDW.

Table 13 Test methods for CDW timber elements.

Property	Standard	Laboratories	Specimen size
In situ strength assessment	No existing standard	On-site	Complete members
Visual on-site inspection	No existing standards	On-site	Complete building
Assessment on chemical contamination	EN ISO 11969 EN ISO 11885 EN ISO 5961 EN 1233 EN 1483 EN ISO 12338 Further special procedures according to accreditation of the laboratories	Accredited laboratory	Minimum 2 g
On-site separation	EU Waste Framework Directive 2008/98/EC and national implementations	On-site	Complete members
Reprocessing and strength grading	EN 14081-1/2, EN 14080	Sawmill or recycling facility	Minimum 6 mm

3.5.1 In situ strength assessment

In situ strength assessment is used for the preservation of heritage structures; it is not feasible for the intended purpose of assessing large quantities of aged timber. For completeness, the most common procedures are briefly described below.

Resistance drilling

Resistance drilling is a widely used method to detect defects and decay in timber elements. Resistance drilling devices record the energy needed to drill a small needle with constant feed and rotation rate into the timber investigated. The measured energy used for drilling is proportional to the density of the wood. The method can detect defects, knots, fissures and decay by recording

differences in the density of the wood. Results are limited to the examined areas and cannot provide mechanical properties valid for the complete timber element.

Wave velocity tests

For wave velocity tests a transmitter and receiver are placed at a specific distance on the timber to be assessed. The output parameter is wave velocity. Wave velocity, combined with tested density of the timber, is used to calculate the dynamic modulus of elasticity. The correlations between the calculated dynamic modulus of elasticity and mechanical or physical parameters of timber are not always reliable due to natural variability of timber properties [46].

Penetration tests

Penetration test devices use a pin that is shot into the wood by an exact amount of energy. The penetration depth can be read on a scale and makes it possible to draw conclusions on the superficial density, resistance and decay. The method is limited to superficial areas and the results do not apply for the complete cross section.

3.5.2 Visual on-site inspection

CDW timber needs to be specified according to wood species by visual inspection. If no exact determination is possible, a minimum categorisation into softwood and hardwood is necessary. The cross sections need to be measured and the amount of timber roughly estimated. The extent of decay, defects and damages needs to be assessed.

3.5.3 Assessment on chemical contamination

Unless other information can prove that no harmful contamination exists, sampling needs to be made to determine if harmful chemical contamination exists. According to state of the art of today, samples are tested in accredited laboratories.

3.5.4 On-site separation

According to the results of the visual inspection and assessment of chemical contamination, the timber is categorised in different sorting categories. Categories differ according to national standards and regulations.

3.5.5 Reprocessing and strength grading

For further processing, all impurities, such as nails, screws, paints, coatings or other non-wooden substances need to be removed. The aim is to obtain clean raw material that can be cut and planed into rectangular cross sections. For strength grading, the timber needs to be dry, on average less than 20% relative moisture content and cut into final dimensions. Strength grading for timber with rectangular cross section is carried out according to harmonized standards [47], [48], [49], and national grading rules.

Additional requirements for lamellas, designated for glued laminated timber are regulated in superior standard [49].

4. RESULTS AND COMMENTS ON THE RESULTS

4.1 Mineral materials

The results from the mineralogical, chemical and physical characterization of the CDW mineral fraction are summarized and commented below.

4.1.1 Petrographic Description

N.E.I.S. (8/16 mm)
A sample of 2038 g was used for performing qualitative and quantitative analysis of N.E.I.S. (8/16 mm) mineral fraction. **Figure 27**, **Figure 28**, **Figure 29**, **Figure 30** and **Figure 31** show the various types of N.E.I.S. coarse aggregates (8/16 mm) separated according to shape and colour. Petrographic descriptions were carried out following the guidelines set in [50], with additional information regarding the quality of the aggregates taken from [19] and [51]. Qualitatively, 5 types of aggregates were found and sorted by shape, size and colour. A brief description of each fraction can be found in **Table 14**. General observations showed that the majority of the aggregates was covered in cement paste, making direct determination of the type of aggregate generally difficult. By far, most of the aggregates were of Type 2 (**Figure 28**) and Type 3 (**Figure 29**), whereas the remaining types of aggregates were present only in small amounts.

To determine the dominant mineral of each aggregate type, most of the aggregates were cracked open with the aid of a hammer. The inside of the aggregates was analysed with the help of a magnifying glass to better observe discreet crystals, if discernible, and the exposed surface was scratched to assess hardness. A drop of acid was placed at the centre of the exposed surface with the aid of a syringe, avoiding any contact with the external surface, to detect the presence of carbonates. It should be noted that an aggregate particle is unlikely to be composed of a single mineral compound but rather a combination of them. For the purpose of this study, only the dominant mineral compound was determined for each type of aggregate.

Close observation of the N.E.I.S. Type 1 aggregate revealed a mixture of quartzite, limestone, marble and granite. N.E.I.S. Type 2 and 3 were found to be marble and limestone respectively. The red, rough textured particles, shown in **Figure 30**, easily gave way with a light hit from a hammer and were identified as sandstone. Finally, N.E.I.S Type 5 aggregates were mostly found to be quartzite. **Table 15** summarises the above results.

Figure 27 N.E.I.S. aggregate Type 1.

Figure 28 N.E.I.S. aggregate Type 2.

Figure 29 N.E.I.S. aggregate Type 3.

Figure 30 N.E.I.S. aggregate Type 4.

Figure 31 N.E.I.S. aggregate Type 5.

Table 14 Physical classification of N.E.I.S. (8/16 mm) aggregates.

N.E.I.S. (8/16 mm)			
Type of aggregate	**Mass (g)**	**Description**	
		Shape	**Colour**
1	326	Rounded, smooth	Various shades of grey/brown
2	515	Angular/irregular	Off white to light grey
3	994	Angular/irregular	Dark grey
4	102	Irregular	Red (very rough texture)
5	101	Rounded/angular/irregular	White

Table 15 Mineralogical classification of N.E.I.S (8/16 mm) aggregates.

Name	Dominant mineral	Rock type	Mass (g)
Limestone	Calcite	Sedimentary	984
Marble	Calcite	Metamorphic	707
Sandstone	Quartz	Sedimentary	99
Granite	Quartz/Feldspar	Igneous	73
Quartzite	Quartz	Metamorphic	165

S.E.I.S. (8/16 mm)

A sample of 2714 g was used for performing qualitative and quantitative analysis of S.E.I.S. (8/16 mm) mineral fraction.

Qualitative separation of this mineral fraction is shown in figures below and summarized in **Table 16**. S.E.I.S Type 1 and 2 were by far the most dominant groups, with Type 1 being angular (**Figure 32**) and Type 2 being rounded in shape (**Figure 33**). Type 3 (**Figure 34**) remained undefined at this

stage and did not fit the visual cues of Types 1 and 2. Type 4 aggregates were grouped based on their white shade (**Figure 35**), whereas Type 5 resembled the red sandstone seen previously in the Northern fraction (**Figure 36**). Similar in texture to Type 5, white rough particles were also found during the qualitative assessment of the mineral aggregates and grouped as Type 6 (**Figure 37**).

Type 1 was found to be exclusively limestone, with the drop of hydrochloric acid always fizzing when put in contact with the internal surface of the aggregates. Similarly, Type 2, the rounded aggregates, was exclusively limestone. Type 5, the red rough aggregates was confirmed to be sandstone, whereas the white porous and rough textured aggregates (Type 6) were found to be chalk. Type 3 was found to be a mixture of limestone and mudstone, the latter being a sedimentary rock originating from clays or muds. Finally, Type 4 aggregates were predominately quartzite. **Table 17** summarises the above results.

Table 16 Physical classification of S.E.I.S. (8/16 mm) aggregates.

S.E.I.S. (8/16 mm)			
Type of aggregate	**Mass (g)**	**Description**	
		Shape	**Colour**
1	1254	Angular/irregular	Various shades of grey
2	997	Rounded, smooth	Various (light grey, dark grey & brown)
3	319	Angular/irregular	Various (black, dark grey, light grey & white)
4	54	Rounded/irregular	White
5	28	Irregular	Red (very rough texture)
6	62	Irregular	White to grey (very rough texture)

Table 17 Mineralogical classification of S.E.I.S. (8/16 mm) aggregates.

Name	Dominant mineral	Rock type	Mass (g)
Limestone	Calcite	Sedimentary	2415
Chalk	Calcite	Sedimentary	62
Sandstone	Quartz	Sedimentary	72
Quartzite	Quartz	Metamorphic	59
Mudstone	Quartz/Mica	Sedimentary	61

Figure 32 S.E.I.S. aggregate Type 1.

Figure 33 S.E.I.S. aggregate Type 2.

Figure 34 S.E.I.S. aggregate Type 3.

Figure 35 S.E.I.S. aggregate Type 4.

Figure 36 S.E.I.S. aggregate Type 5.

Figure 37 S.E.I.S. aggregate Type 6.

N.E.S. & S.E.S. (0/2 mm)

The fine fraction (0/2 mm) was observed using thin sections. The sections were first observed qualitatively to determine the nature of the minerals present, under both polarized (light waves pass through a single polarizing filter) and cross-polarized light (light waves pass through two polarizing filters). Under cross-polarized light, only anisotropic minerals who exhibit birefringence become visible. A typical cross-section under both polarized and cross-polarized light for both N.E.S. and S.E.S. mineral fractions is shown in **Figure 38**, **Figure 39**, **Figure 40** and **Figure 41**.

Quartz (Q) was by far the most common mineral present. Under cross-polarized light, quartz appears either black, white or in any shade of grey. Upon rotating the stage, and therefore changing the orientation of the mineral grain with respect to the two polarising filters, quartz will vary in shades of grey, and may oscillate from black to white. Limestone (L) was the second most common mineral present and appeared as shades of pink-brown under cross-polarized light. In many cases, minerals were clumped together to form a discreet particle with well-defined borders. These particles were typically made of limestone and quartz and were most likely pieces of mortar (M). Feldspar (F) was also identified, but was much less common. Finally, the rest of particles, including brick and tiles (B), was grouped as "other".

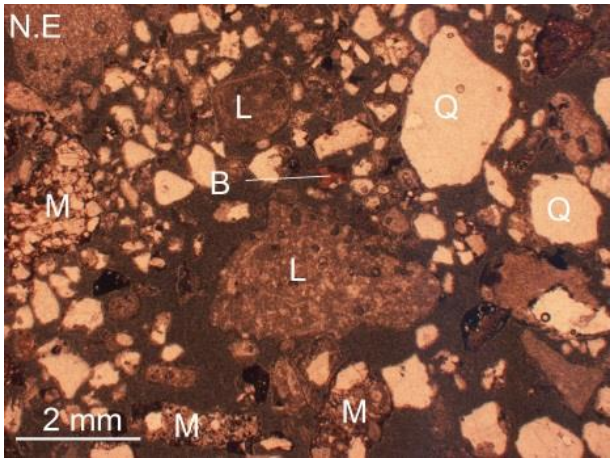

Figure 38 Typical cross-section of N.E.S. (0/2 mm) under polarized light.

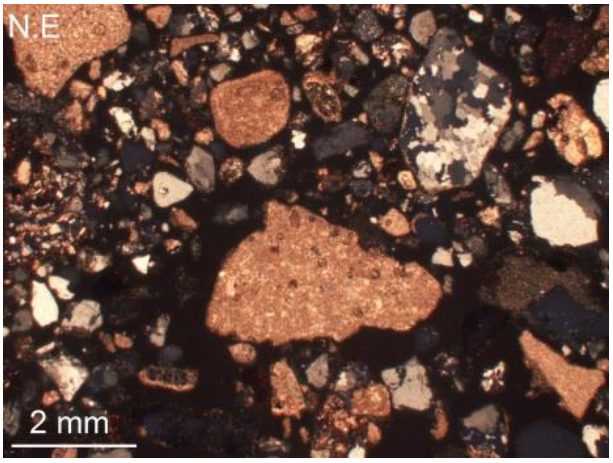

Figure 39 Typical cross-section of N.E.S. (0/2 mm) under cross-polarized light.

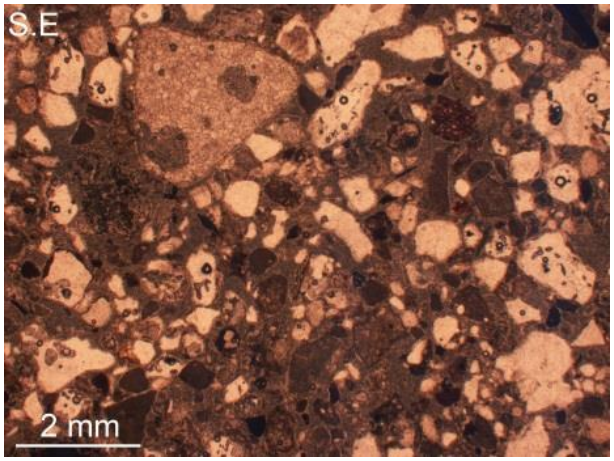

Figure 40 Typical cross-section of S.E.S. (0/2 mm) under polarized light.

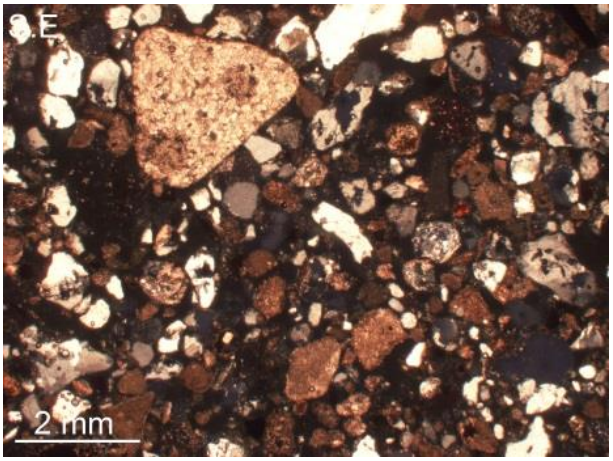

Figure 41 Typical cross-section of S.E.S. (0/2 mm) under cross-polarized light.

Quantification of the mineral fraction was only carried out by spatial analysis, whereby for a single still image, the total number of particles was counted and distributed between their respective mineral constituents. This approach was used as the optical microscope was not fitted with a point counting stage. The "other" category included all particles not considered to be minerals, e.g. mortars, bricks, tiles and bitumen. A total of 1061 and 885 particles were counted for the S.E.S. and N.E.S. fractions, respectively, across 6 to 8 sites. The results are shown in **Table 18**.

The N.E.S. fraction showed to be comprised of 61% quartz and 30% limestone. The quartz content seemed overestimated when compared to the XRD analysis results (56.7% quartz) presented in the relevant section of the report. However, the limestone content determined by petrographic analysis seemed to be underestimated compared to XRD analysis (24.8% calcite plus 9.4% dolomite equals 34.2% total carbonate content). The S.E.S. fraction on the other hand, was shown to be made of

62% of quartz and 25% of limestone. Again, the quartz content was overestimated by means of petrographic analysis (56% was measured by XRD). However, the limestone content seemed underestimated when compared to XRD findings (10.2% calcite plus 4.5% dolomite equals 14.7% total carbonate content).

Table 18 Quantification of N.E.S. and S.E.S. 0/2 mm mineral fractions observed under microscope.

Mineral	N.E.S. (0/2 mm)		S.E.S. (0/2 mm)	
	Number of particles	Percentage	Number of particles	Percentage
Quartz	542	61.2	655	61.7
Limestone	266	30.1	263	24.8
Feldspar	1	0.1	2	0.2
Other	76	8.6	141	13.3
Total	885	100	1061	100

Finally, an interesting section, which shows a thin layer of carbonated cement paste (resembling limestone in colour under polarized light) coating a quartz particle, can be seen in **Figure 42**.

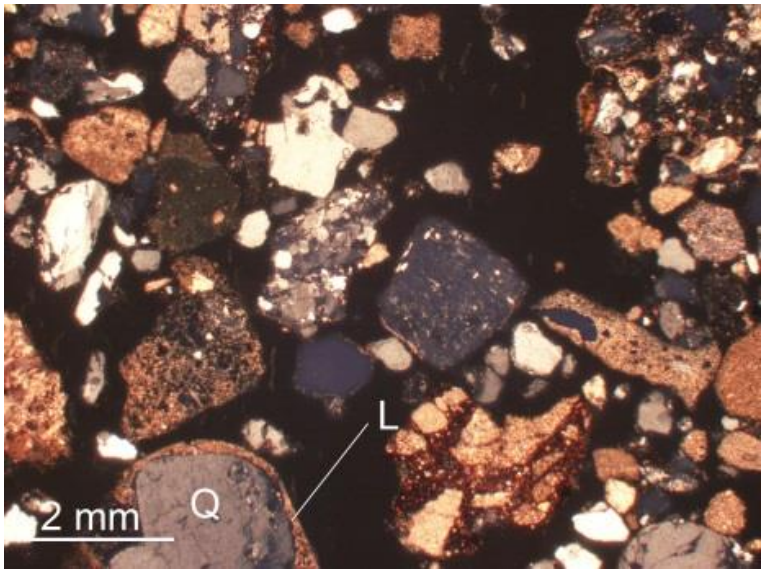

Figure 42 Quartz particle coated with thin layer of carbonated cement paste.

4.1.2 Constituent Classification of coarse aggregate

The estimated composition of N.E.S. (8/16 mm) mineral fraction in terms of FL, X, Rc, Ru, Rb, Ra and Rg is given in **Table 19** and **Figure 43**, whereas that of S.E.S. (8/16 mm) mineral fraction is given in **Table 20** and **Figure 44**. These results are then compared with the requirements set by [2] and [13] for the use of either Type A/B recycled aggregates or Crushed Concrete Aggregate (CCA) in structural Concrete as shown in **Table 21**.

Table 19 Coarse recycled aggregate composition of N.E.S. mineral fraction.

Symbol	Description	Mass or Volume	Percentage
M_1	Mass of oven-dried portion	19.981 kg	n/a
M_{FL}	Mass of floating particles in M_1	0.002 kg	n/a
M_X	Mass of clay and soil, ferrous and non-ferrous metals, non-floating wood, plastic, rubber and gypsum in M_1	0.016 kg	n/a
M_2	Mass of non-floating particles in M_1	19.963 kg	n/a
M_3	Mass of test sample obtained from M_2 and analysed	5.082 kg	n/a
M_{Rc}	Mass of concrete, concrete products, mortar and concrete masonry units detected in M_3	0.275 kg	n/a
M_{Ru}	Mass of unbound aggregate, natural stone and hydraulically bound aggregate detected in M_3	4.328 kg	n/a
M_{Rb}	Mass of clay masonry units, calcium silicate units and aerated-no floating concrete detected in M_3	0.184 kg	n/a
M_{Ra}	Mass of bituminous materials detected in M_3	0.287 kg	n/a
M_{Rg}	Mass of glass detected in M_3	0.004 kg	n/a
FL	Estimated volume of floating particles in M_1	negligible	0%
X	Estimated percentage of clay and soil, ferrous and non-ferrous metals, non-floating wood, plastic, rubber and gypsum in M_1	n/a	0.1%
Rc	Estimated percentage of concrete, concrete products, mortar and concrete masonry units in M_1	n/a	5.4%
Ru	Estimated percentage of unbound aggregate, natural stone and hydraulically bound aggregate in M_1	n/a	85.0%
Rb	Estimated percentage of clay masonry units, calcium silicate units and aerated-no floating concrete detected in M_1	n/a	3.6%
Ra	Estimated percentage of bituminous materials detected in M_1	n/a	5.6%
Rg	Estimated percentage of glass detected in M_1	n/a	0.1%

Table 20 Coarse recycled aggregate composition of S.E.S. mineral fraction.

Symbol	Description	Mass or Volume	Percentage
M_1	Mass of oven-dried portion	19.40 kg	n/a
M_{FL}	Mass of floating particles in M_1	0.01 kg	n/a
M_X	Mass of clay and soil, ferrous and non-ferrous metals, non-floating wood, plastic, rubber and gypsum in M_1	0.01 kg	n/a
M_2	Mass of non-floating particles in M_1	19.38 kg	n/a
M_3	Mass of test sample obtained from M_2 and analysed	6.33 kg	n/a
M_{Rc}	Mass of concrete, concrete products, mortar and concrete masonry units detected in M_3	1.49 kg	n/a

Symbol	Description	Mass or Volume	Percentage
M_{Ru}	Mass of unbound aggregate, natural stone and hydraulically bound aggregate detected in M_3	4.16 kg	n/a
M_{Rb}	Mass of clay masonry units, calcium silicate units and aerated-no floating concrete detected in M_3	0.51 kg	n/a
M_{Ra}	Mass of bituminous materials detected in M_3	0.16 kg	n/a
M_{Rg}	Mass of glass detected in M_3	0.01 kg	n/a
FL	Estimated volume of floating particles in M_1	negligible	0%
X	Estimated percentage of clay and soil, ferrous and non-ferrous metals, non-floating wood, plastic, rubber and gypsum in M_1	n/a	0.1%
Rc	Estimated percentage of concrete, concrete products, mortar and concrete masonry units in M_1	n/a	23.6%
Ru	Estimated percentage of unbound aggregate, natural stone and hydraulically bound aggregate in M_1	n/a	65.6%
Rb	Estimated percentage of clay masonry units, calcium silicate units and aerated-no floating concrete detected in M_1	n/a	8.0%
Ra	Estimated percentage of bituminous materials detected in M_1	n/a	2.6%
Rg	Estimated percentage of glass detected in M_1	n/a	0.1%

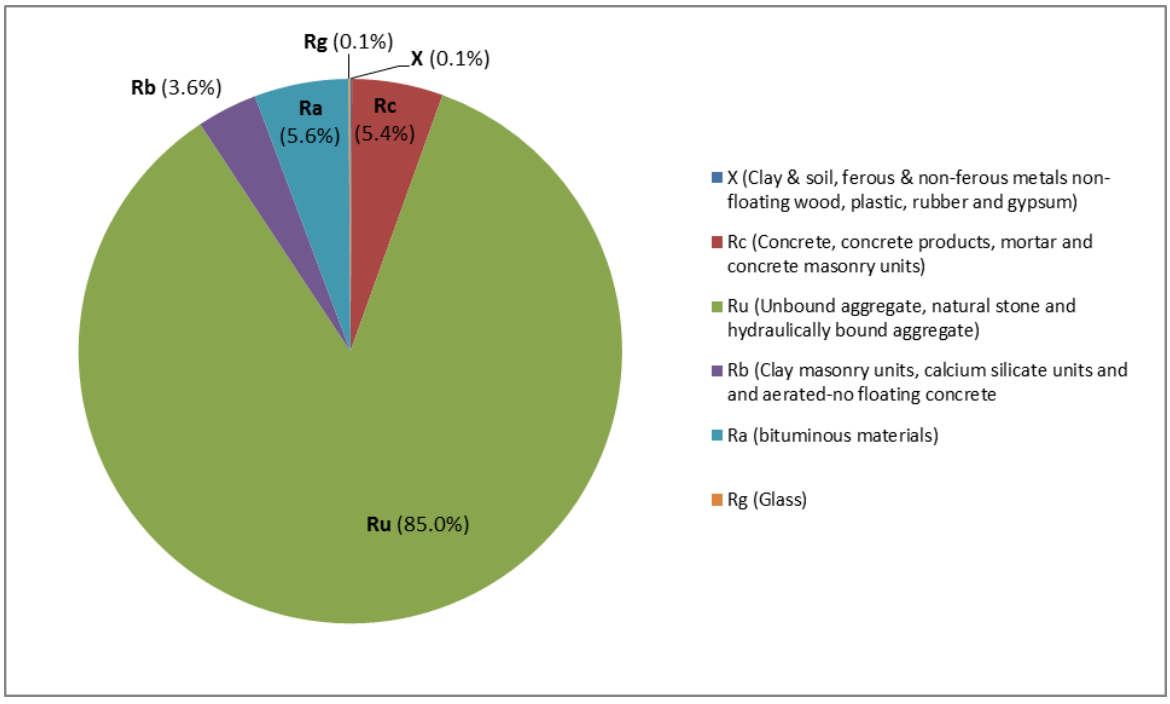

Figure 43 Coarse recycled aggregate composition of N.E.S. mineral fraction.

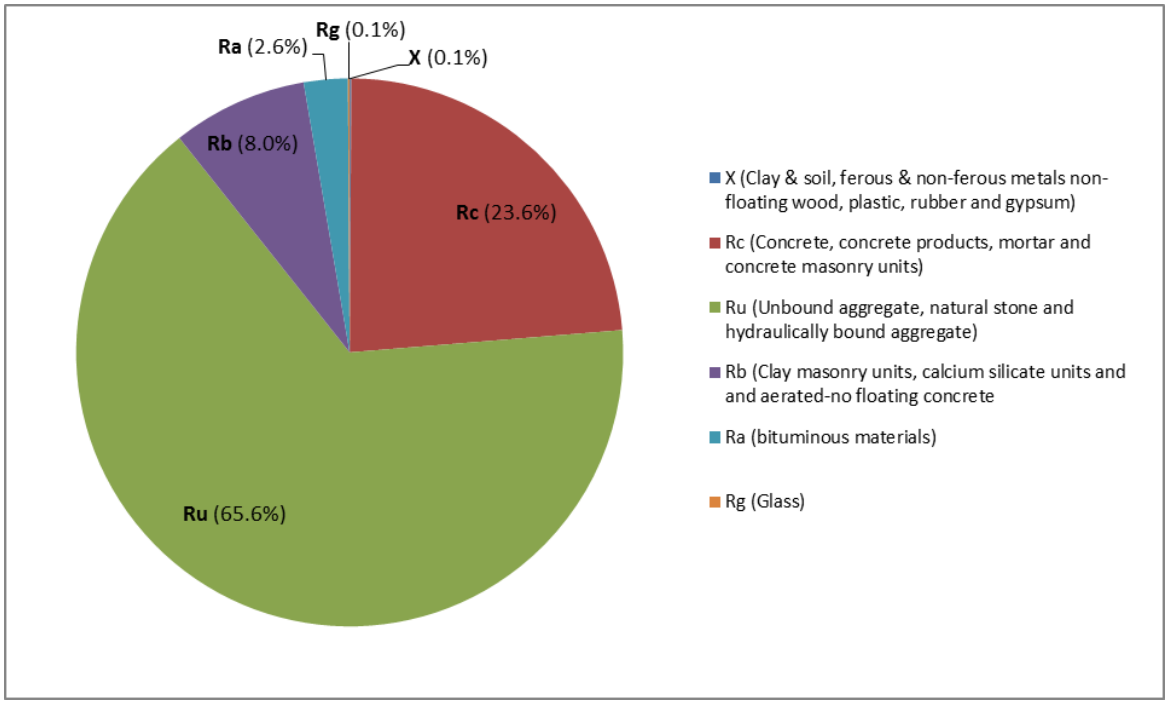

Figure 44 Coarse recycled aggregate composition of S.E.S. mineral fraction.

Table 21 Comparison of N.E.S. and S.E.S. compositions against requirements set by EN 206 and BS 8500-2.

Type of aggregate	Rc + Ru (wt%)	Rb (wt%)	Ra (wt%)	X + Rg (wt%)	FL (cm^3/kg)
Type A [2]	≥ 95	≤ 10	≤ 1	≤ 1	≤ 2
Type B [2]	≥ 70	≤ 30	≤ 5	≤ 2	≤ 2
CCA [13]	≥ 90	≤ 10	≤ 5	≤ 1	≤ 2
N.E.S. (8/16 mm) mineral fraction	90.4	3.6	5.6	0.2	negligible
S.E.S. (8/16 mm) mineral fraction	89.2	8	2.6	0.2	negligible

As shown in **Table 21**, N.E.S. (8/16 mm) mineral fraction complies with all requirements set by [2] (Type B) and [13] (CCA) with the exception of Ra content (5.6% as opposed to 5%). S.E.S. (8/16 mm) mineral fraction on the other hand, complies with all requirements set by [2] (Type B). It also complies with all requirements set by [13] (CCA) with the exception of minimum Rc + Ru content (89.2% as opposed to 90%). Since the observed deviations from the above requirements are very small, both mineral fractions are deemed to be suitable for use in the production of structural concrete. Finally, the above results demonstrate the ability of CDE's wet treatment and sorting equipment to effectively remove FL, X and Rg particles from the above mineral fractions.

4.1.3 Water-Soluble Chloride Salt Content

The water-soluble chloride content of N.E.S., N.E.I.S., S.E.S. and S.E.I.S. 0/2 and 8/16 mm fractions, obtained using the Volhard and potentiometry methods, is shown in **Table 22** and **Table 23**.

Table 22 Water-soluble chloride content of 0/2 mm mineral fractions.

0/2 mm Size Fraction					
Test method	**Unit**	**N.E.S.**	**S.E.S.**	**N.E.I.S.**	**S.E.I.S.**
Volhard	mol/l	0.000024	0.000014	0.000024	0.000034
	g/l	0.00085	0.0005	0.00085	0.0012
	wt%	0.00085	0.0005	0.00085	0.0012
Potentiometry	mol/l	0.000026	0.000016	0.000025	0.000018
	g/l	0.00091	0.00057	0.00089	0.00064
	wt%	0.00091	0.00057	0.00089	0.00064

Table 23 Water-soluble chloride content of 8/16 mm mineral fractions.

8/16 mm Size Fraction					
Test method	**Unit**	**N.E.S.**	**S.E.S.**	**N.E.I.S.**	**S.E.I.S.**
Volhard	mol/l	0.000004	0.000054	0.000014	0.000034
	g/l	0.00014	0.0019	0.0005	0.0012
	wt%	0.00014	0.0019	0.0005	0.0012
Potentiometry	mol/l	0.000026	0.000051	0.000017	0.000034
	g/l	0.00091	0.0018	0.00059	0.0012
	wt%	0.00091	0.0018	0.00059	0.0012

As shown in **Table 22** and **Table 23**, all tested mineral fractions contain very low levels of water-soluble chlorides. This can be attributed to the various washing stages of CDE's processing and sorting equipment, which effectively removes water-soluble chlorides. However, requirements in [2] set a limit on chloride ion content at either 0.20 or 0.40 % by mass of cement for reinforced concrete. Assuming that the w/c ratio of a typical structural concrete mix is 0.5 (180 kg of water and 360 kg of cement per m^3) and its fresh density is 2400 kg/m^3, the mix will contain 1860 kg aggregates per m^3 fresh concrete. If 40% of the total aggregate content is fine and the rest coarse, the amount of chlorides expressed as % by mass of cement is still well below the 0.2% limit.

4.1.4 Water-Soluble Sulphate Content

The water-soluble sulphate content of N.E.S., N.E.I.S., S.E.S. and S.E.I.S. 0/2 and 8/16 mm mineral fractions are shown in **Table 24**.

Table 24 Water-soluble sulphate content of fine and coarse mineral fractions at room temperature.

Mineral fraction	wt% water soluble SO_3
N.E.S. (0/2 mm)	0.025
N.E.I.S. (0/2 mm)	0.027
N.E.S. (8/16 mm)	0.014
N.E.I.S (8/16 mm)	0.015
S.E.S. (0/2 mm)	0.229

Mineral fraction	wt% water soluble SO_3
S.E.I.S. (0/2 mm)	0.194
S.E.S. (8/16 mm)	0.090
S.E.I.S. (8/16 mm)	0.093

Based on **Table 24**, the water-soluble sulphate content (by mass of aggregate) of all coarse mineral fractions is well below the 0.2% limit set by [3]. The same can be said for all fine mineral fractions with the exception of S.E.S. (0/2 mm). The high levels of water-soluble sulphates in S.E.S. (0/2 mm) are in line with its chemical composition obtained by XRF (see relevant section of the report).

Based on **Table 25** S.E.S and N.E.S. tested at 60 C have leached more sulphates compared to **Table 24**. Nonetheless, in all cases S.E.S. (0/2 mm) is the only mineral fraction that still fails to meet the sulphate criteria set by [3].

Table 25 Water-soluble sulphate content of fine mineral fractions at 60 °C.

Mineral fraction	wt% water soluble SO_3
S.E.S. (0/2 mm)	0.274
N.E.S. (0/2 mm)	0.036

4.1.5 Carbonate Content of Fine Aggregates

XRD

Results of XRD for N.E.S. and S.E.S. mineral fractions are shown in **Figure 45** and **Figure 46**, respectively**.**

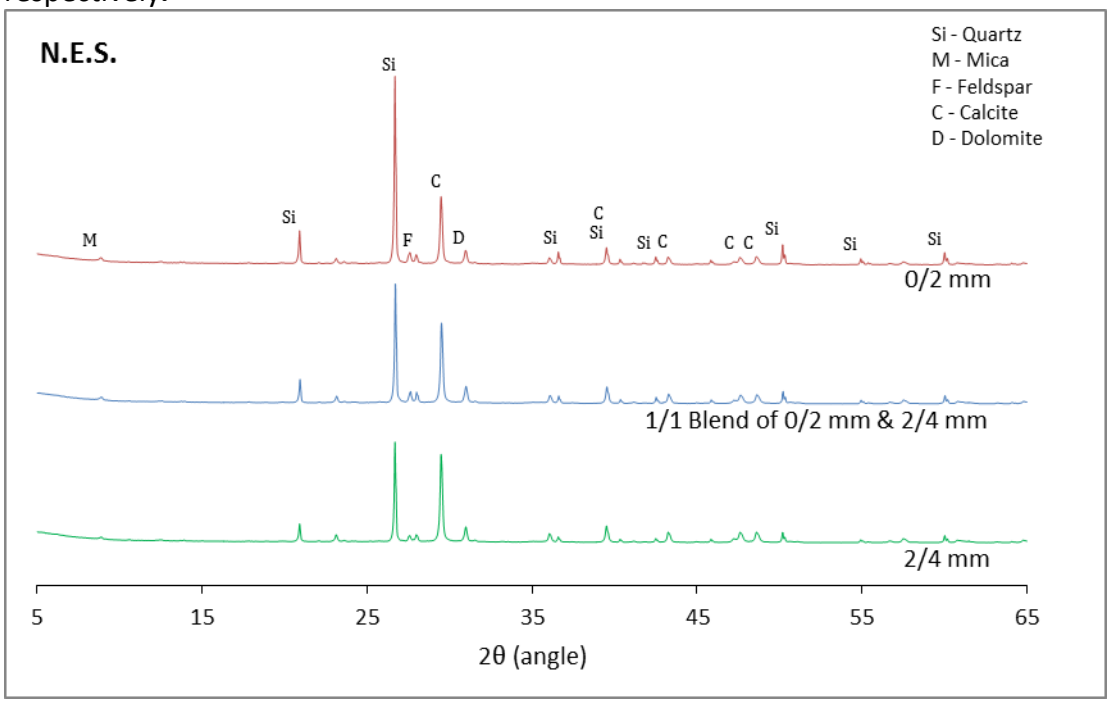

Figure 45 XRD results for N.E.S. fine mineral fractions.

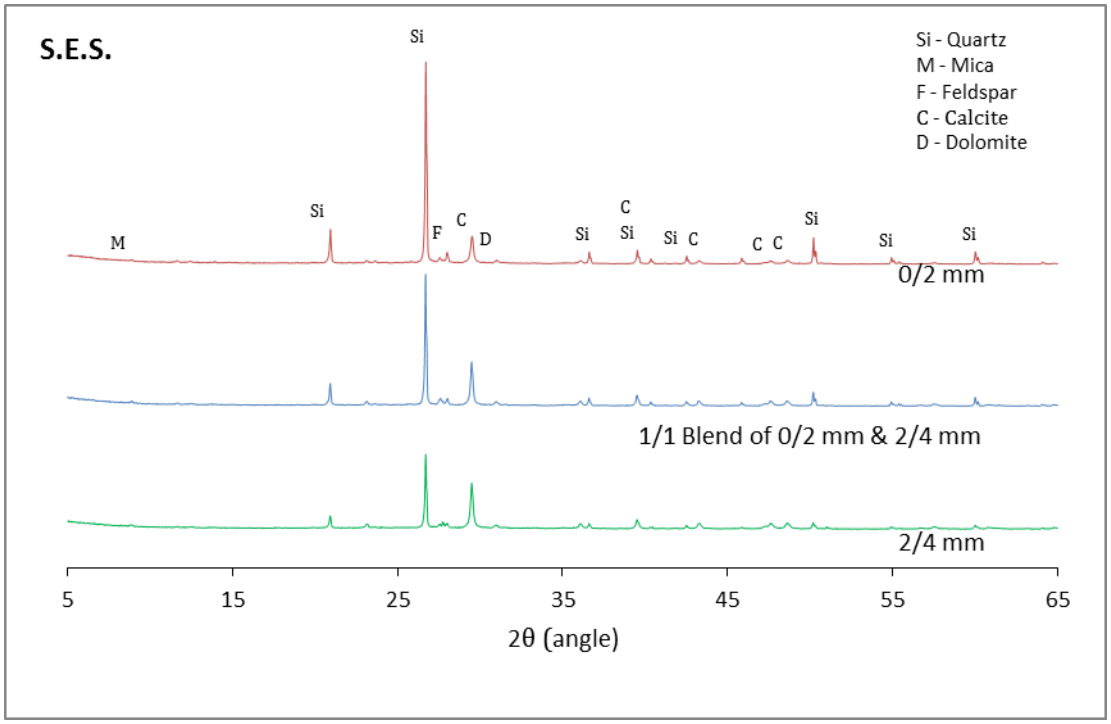

Figure 46 XRD results for S.E.S. fine mineral fractions.

Based on the above results, the main minerals of the various N.E.S. and S.E.S. fine mineral fractions are given in **Table 26.** As the size of the fine fraction rises from 0/2 mm to 2/4 mm, a significant increase in calcite content accompanied by a significant decrease in quartz content are observed for both N.E.S. and S.E.S.

Table 26 Mineral composition of N.E.S. and S.E.S. fine mineral fractions based on XRD.

Mineral	N.E.S.			S.E.S.		
	0/2 mm (wt%)	Blend 0/2 & 2/4 mm (wt%)	2/4 mm (wt%)	0/2 mm (wt%)	Blend 0/2 & 2/4 mm (wt%)	2/4 mm (wt%)
Quartz (SiO_2)	56.7	40.8	34.7	56.0	42.9	30.5
Calcite ($CaCO_3$)	24.8	32.8	38.9	10.2	22.1	30.2
Dolomite ($CaMg(CO_3)_2$)	9.4	8.9	10.6	4.5	4.0	2.7
Other	9.1	17.5	15.8	29.3	31.0	36.6

TGA

Results of TGA for N.E.S. fine mineral fractions are shown in **Figure 47** and **Figure 48**, whereas those for S.E.S. fine mineral fractions are shown in **Figure 49** and **Figure 50**.

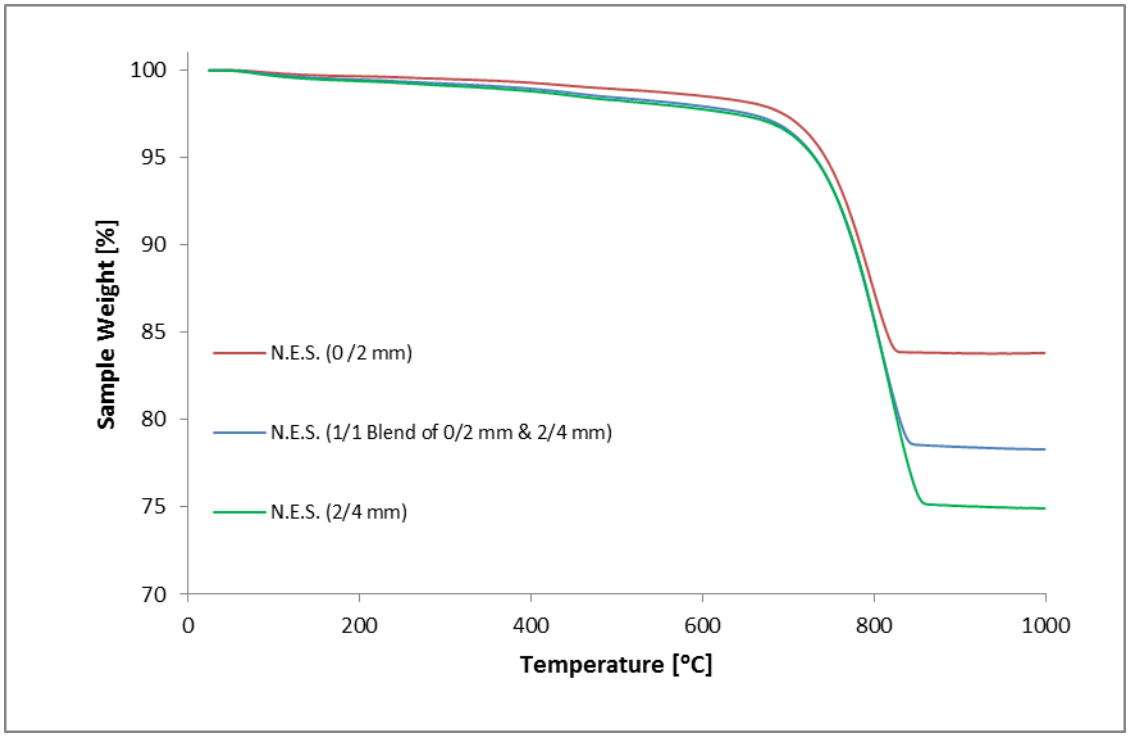

Figure 47 N.E.S. sample weight (%) versus heating temperature (°C).

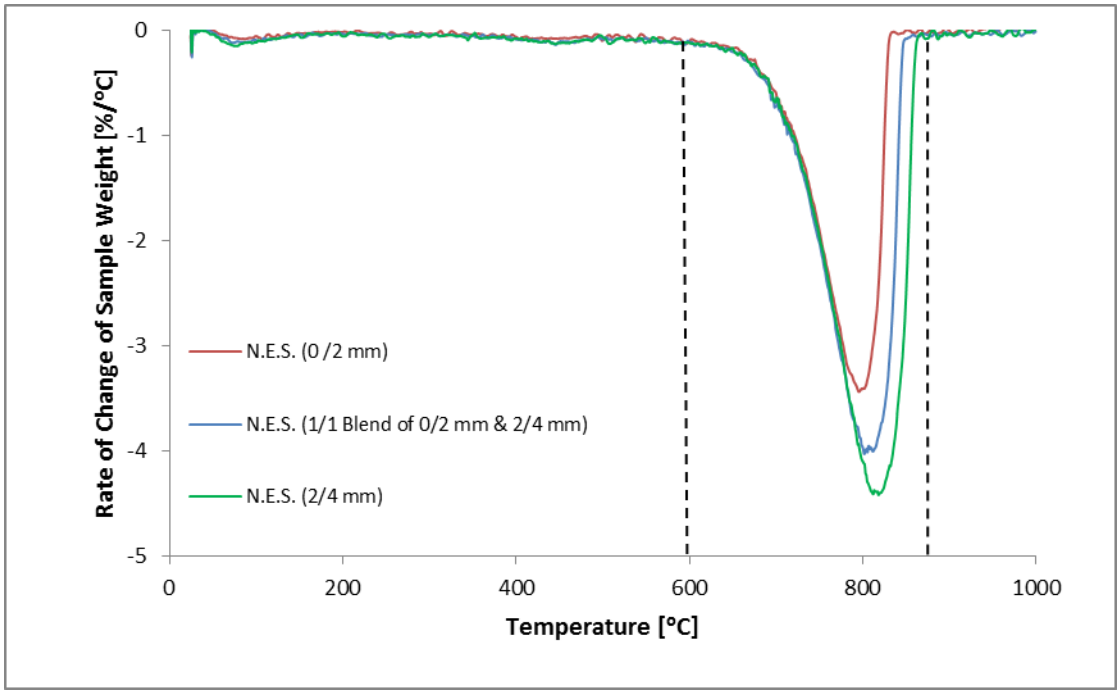

Figure 48 N.E.S. rate of change of sample weight (%/°C) versus heating temperature (°C).

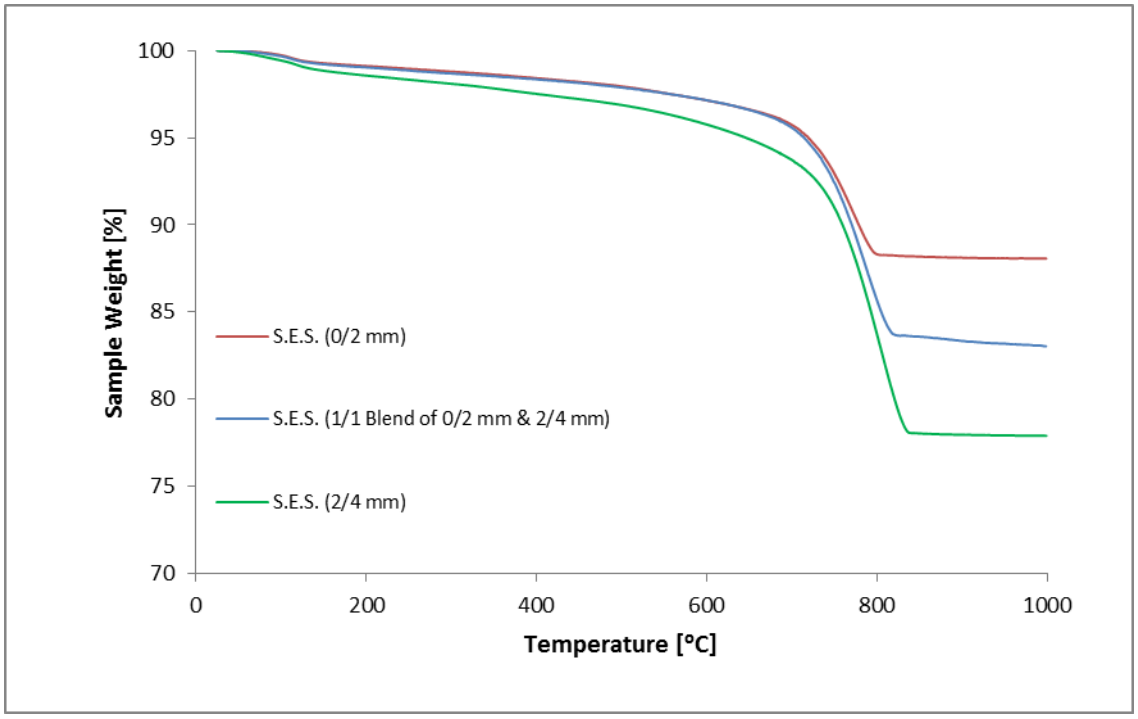

Figure 49 S.E.S. sample weight (%) versus heating temperature (°C).

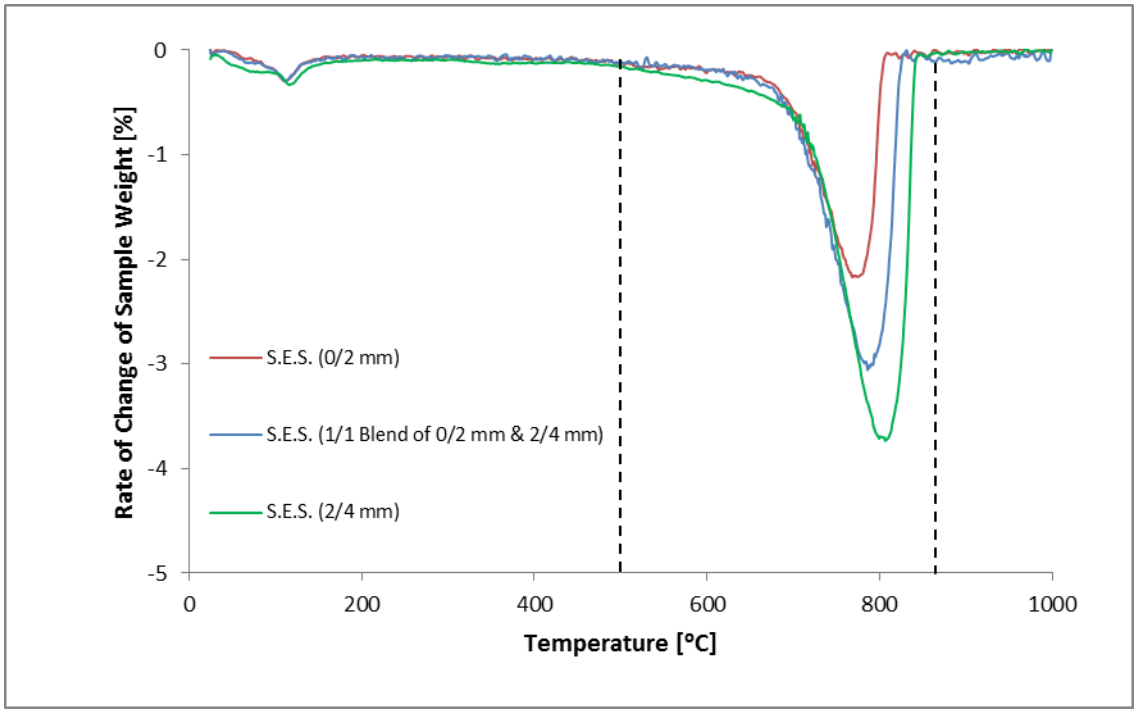

Figure 50 S.E.S. Rate of change of sample weight (%/°C) versus heating temperature (°C).

Based on the above results, the percentage mass loss of CO_2 in the various fine fractions of N.E.S. and S.E.S. are given in **Table 27**. It should be noted that these values are due to the decomposition of calcite and dolomite present in the mineral fractions. However, XRD values for calcite and dolomite contents (shown above), allow the calculation of maximum theoretical CO_2 mass loss, which is also shown in **Table 27**. The estimated values based on XRD are in good agreement with the actual ones obtained from TGA.

Table 27 Actual and estimated CO_2 mass loss using TGA and XRD.

CO_2 mass loss	**N.E.S.**			**S.E.S.**		
	0/2 mm (wt%)	Blend 0/2 & 2/4 mm (wt%)	2/4 mm (wt%)	0/2 mm (wt%)	Blend 0/2 & 2/4 mm (wt%)	2/4 mm (wt%)
Determined by TGA	14.9	19.8	23.0	9.4	14.2	18.4
Estimated from XRD results	15.4	18.7	22.2	6.6	11.6	14.6

4.1.6 Organic Matter (Humus and Fulvo Acid Content)

Humus

All analysed samples are shown in **Figure 51**. Both N.E.S. and S.E.S. mineral fractions tinted the NaOH solution. However, compared to the standard colour solution, the intensity of the tinted hydroxide solution was faint at best. The amount of humus present in the solution was therefore minimal. The NaOH soaking the improved sorted material from both geographical regions did not tint. It should be remembered that the improved sorted fractions were produced by manually sorting the coarse (8/16 mm) fractions and then crushing them to a size < 4 mm. It may be that differences during the various washing steps of a typical CDW processing plant between the fine (0/2mm) and coarse (2/8 mm & 8/16 mm) fractions led to differing amounts of organic matter present in the above size fractions.

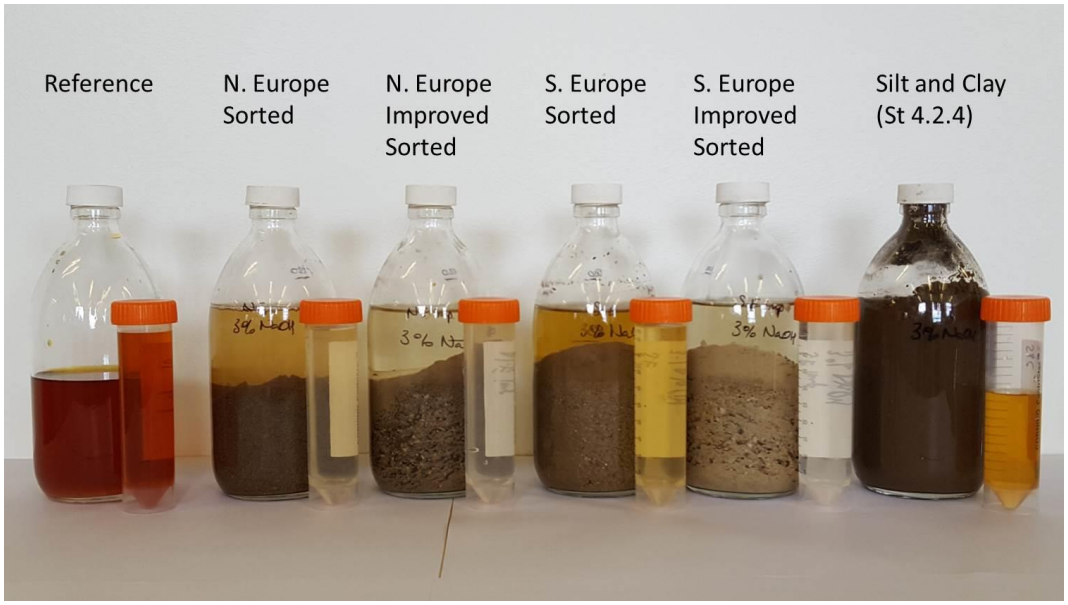

Figure 51 Colorimetric identification of the presence of humus in all 0/2 mm mineral fractions & fine fraction.

Fulvo Acid

All analysed samples are shown in **Figure 52**. None of the tested mineral fractions tinted the HCl solution. Like in the case of humus, washing of CDW material during its various processing and sorting stages effectively removed all fulvo acid present.

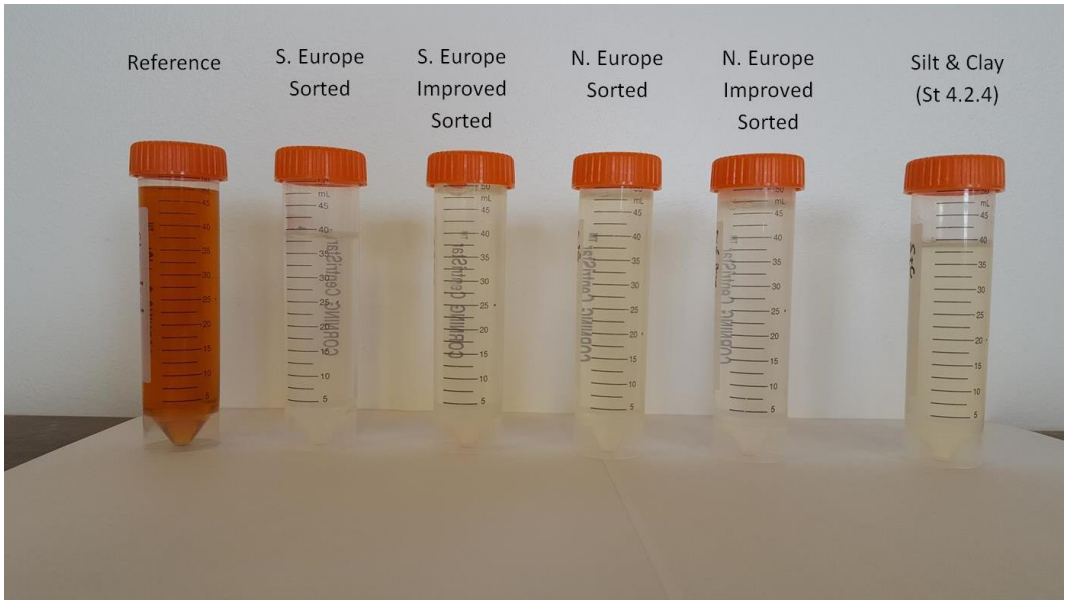

Figure 52 Colorimetric identification of the presence of fulvo acid in all 0/2 mm mineral fractions & fine fraction.

4.1.7 Water Soluble Components from Recycled Aggregate

Figure 53 shows how the penetration depth of the Vicat apparatus needle varies over time on pastes prepared with (a) tap water, (b) S.E.S. aggregate leachate water and (c) N.E.S. aggregate leachate water. No setting was observed during the first 2 hours (120 min) after the start of mixing cement with water in all 3 mixes. Following the above period, all pastes started to show signs of stiffening and reached initial setting state after between 141 and 144 minutes (**Table 28**). Next, all pastes continued to set at a similar rate and reached final setting state between 192 and 204 minutes from the start of hydration (**Table 28**).

Table 28 Initial and final setting times of cement pastes.

Source of water used	w/c	Initial setting time (min)	Final setting time (min)
Tap water	0.296	141	192
N.E.S. aggregate leachate water	0.296	144	204
S.E.S. aggregate leachate water	0.296	141	195

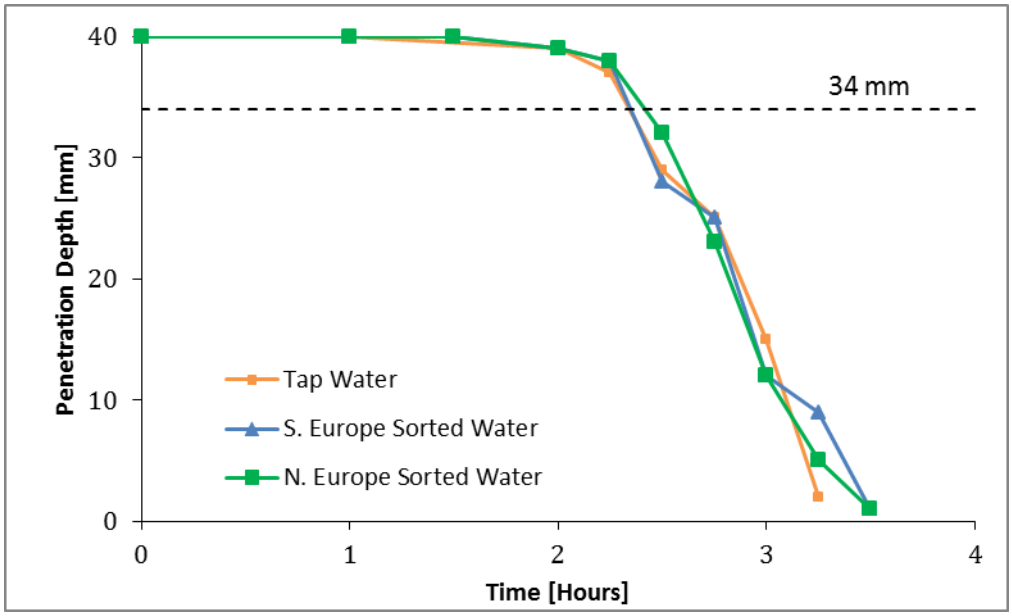

Figure 53 Penetration depth of Vicat apparatus needle versus time. Height of cement paste sample is 40 mm.

Any foreign elements present on the recycled aggregates and leached into the mixing water had no influence on the setting time of the cement pastes. This is consistent with the low levels of humus and fulvo acid detected in S.E.S. and N.E.S. mineral fractions as shown above.

4.1.8 Total/bulk chemistry of the material

The chemical composition of N.E.S. and S.E.S. 0/2, 2/8 and 8/16 mm as well as N.E.I.S. and S.E.I.S. 8/16 mm mineral fractions, obtained from the XRF analysis, is shown in **Table 29** and **Table 30**.

Table 29 Chemical composition of N.E.S. and N.E.I.S. mineral fractions.

Chemical compound	N.E.S.			N.E.I.S.
	0/2 mm (wt%)	2/8 mm (wt%)	8/16 mm (wt%)	8/16 mm (wt%)
SiO_2	51.1	37.4	30.0	34.8
CaO	19.3	28.3	31.7	29.2
Al_2O_3	4.6	3.9	3.8	4.5
Fe_2O_3	1.9	1.6	1.4	1.9
SO_3	0.6	0.1	0.6	0.1
MgO	1.5	2.0	2.9	2.4
Na_2O	0.5	0.4	0.2	0.3
K_2O	1.4	1.0	1.1	1.3
Loss of Ignition	17.1	23.7	27.5	24.7
Total	96.6	96.2	96.3	96.8

Table 30 Chemical composition of S.E.S. and S.E.I.S. mineral fractions.

Chemical compound	S.E.S.			S.E.I.S.
	0/2 mm (wt%)	2/8 mm (wt%)	8/16 mm (wt%)	8/16 mm (wt%)
SiO_2	60.2	30.1	23.1	17.0
CaO	13.5	31.8	38.1	43.6
Al_2O_3	5.7	4.9	4.0	2.4
Fe_2O_3	1.9	3.4	2.0	2.1
SO_3	2.4	0.4	0.6	0.3
MgO	1.0	1.2	1.1	0.8
Na_2O	0.7	0.5	0.4	0.2
K_2O	1.3	1.0	0.9	0.5
LOI	11.6	25.4	29.5	33.7
Total	97.5	97.6	98.6	99.7

XRF results suggest that the mineral fractions obtained from both Northern and Southern Europe recycling centres are rich in calcium as opposed to results reported by other researchers [52], [53] and [54]. Combined with the high loss of ignition, the data suggests that the mineral fractions contain high levels of limestone aggregates. The above results are in line with the ones obtained from petrography, which indicate high levels of limestone aggregates present in all mineral fractions. Higher levels of CaO present in S.E.S. and S.E.I.S. (8/16 mm) compared to N.E.S. and N.E.I.S. (8/16 mm) mineral fractions can be attributed to greater amounts of cement paste (rich in Ca) adhered to them. This result is in line with the results obtained from the constituent classification of aggregates as shown above.

4.1.9 Resistance to Weathering

Resistance to Freezing and Thawing (Magnesium Sulphate Test)

Although the magnesium sulphate test is not suitable for recycled aggregates coated with cement paste [3], it was carried out for comparing the performance of the various mineral fractions exposed to it. **Figure 54** shows the mass loss of the various mineral fractions exposed to 5 cycles of $MgSO_4$ solution. N.E.S. and N.E.I.S. mineral fractions showed a mass loss of 9.8% and 6.2%, respectively. S.E.S. and S.E.I.S. mineral fractions on the other hand, experienced a mass loss of 8.6% and 8%, respectively. Clearly, N. Europe mineral fractions were more susceptible to damage caused by repeated exposure to $MgSO_4$, compared to actual freeze-thaw testing.

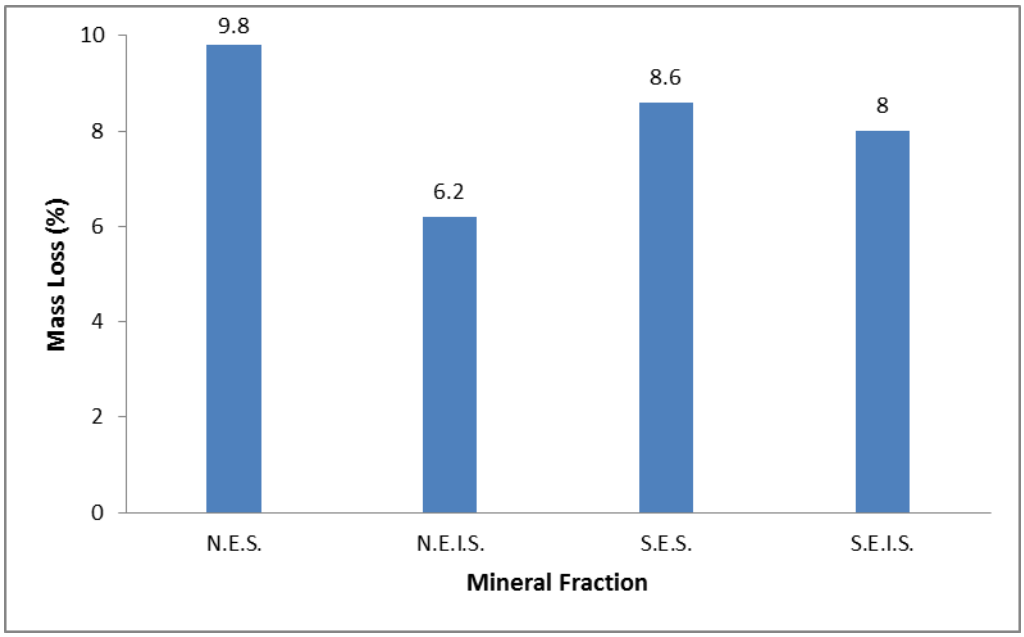

Figure 54 Percentage mass loss of different mineral fractions exposed to 5 cycles of $MgSO_4$ solution.

4.1.10 Resistance to freezing and thawing

Figure 55 shows the mass loss of the various mineral fractions subjected to 10 cycles of freezing and thawing. Control (N. Ireland Virgin Basalt) aggregates showed minimal mass loss (less than 1%). N.E.S. and N.E.I.S. fractions showed a mass loss of 3.4% and 4.1%, respectively. Finally, S.E.S. and S.E.I.S. mineral fractions experienced a mass loss of 11.7% and 10%, respectively. Clearly, S. Europe mineral fractions were more susceptible to damage caused by repeated freeze-thaw cycles. This result indicates that S. Europe mineral fractions contain significantly more cement paste and is in line with the results obtained from the constituent classification of aggregates as shown above.

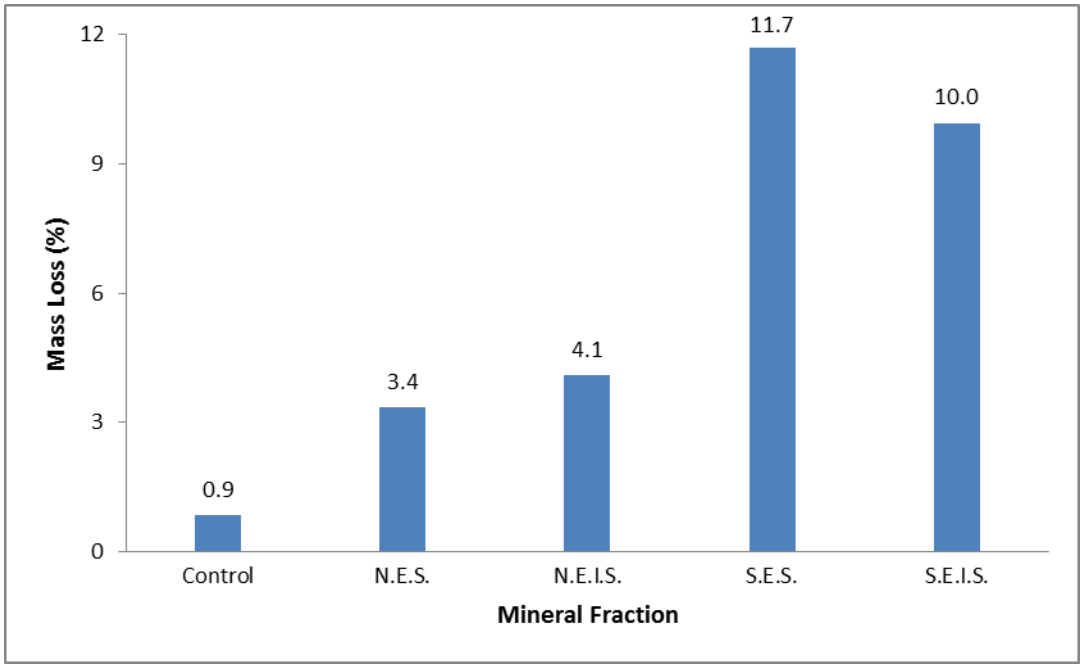

Figure 55 Percentage mass loss of different mineral fractions subjected to 10 freeze-thaw cycles.

Visual inspection of the aggregates after testing revealed that they were noticeably cleaner as shown in **Figure 56**, **Figure 57**, **Figure 58** and **Figure 59**. The stresses developed due to the repeated freeze-thawing cycles led to the descaling of the cement paste attached to the coarse aggregates.

Figure 56 State of N.E.S mineral fractions after 10 freeze-thaw cycles.

Figure 57 State of N.E.I.S. mineral fractions after 10 freeze-thaw cycles.

Figure 58 State of S.E.S. mineral fractions after 10 freeze-thaw cycles.

Figure 59 State of S.E.I.S. mineral fractions after 10 freeze-thaw cycles.

The mass loss (< 4 mm) from each of the S. Europe and N. Europe mineral fractions, after the end of 10 freeze-thaw cycles, is shown in **Figure 60**, **Figure 61**, **Figure 62** and **Figure 63**. Visual inspection of the above masses showed that brick, sandstone, concrete and even some natural aggregate particles were damaged during freeze thaw testing.

Figure 60 N.E.S. fine particles (< 4 mm) collected after the end of 10 freeze-thaw cycles.

Figure 61 N.E.I.S. fine particles (< 4 mm) collected after the end of 10 freeze-thaw cycles.

Figure 62 S.E.S. fine particles (< 4 mm) collected after the end of 10 freeze-thaw cycles.

Figure 63 S.E.I.S. fine particles (< 4 mm) collected after the end of 10 freeze-thaw cycles.

4.1.11 Volume Stability-Drying Shrinkage

Results of average drying shrinkage measurements for all four fraction (N.E.S., N.E.I.S., S.E.S. and S.E.I.S.) prisms together with the values obtain from the control samples are given in **Table 31**.

Table 31 Average drying shrinkage of prisms versus time.

Time (days)	Average drying shrinkage (% of prism length)				
	Control	N.E.S.	N.E.I.S.	S.E.S.	S.E.I.S.
0	0	0	0	0	0
3	0.042	0.043	0.048	0.044	0.046
7	0.064	0.059	0.066	0.060	0.057
14	0.065	0.064	0.071	0.069	0.067

Based on the above results it is obvious that all four mineral fractions and control prisms comply with the maximum limit of 0.075% set by [13].

4.1.12 Alkali-Silica Reactivity

Criteria for the evaluation of results obtained by using the [33] test method have not yet been agreed by RILEM. However, trials performed by RILEM on aggregates of well-known performance from different parts of the world, indicate no potential alkali reactivity for values less than 0.1% [55]. Results for all tested mineral fractions (including control samples) are shown in **Figure 64**. Based on these results, it was obvious that the percentage expansion of all tested mineral fractions was well below 0.1% at 14 days. Consequently, the potential of alkali reactivity for all mineral fractions was judged to be very low. However, since the testing was performed at 40 °C instead of at 80 °C, as stipulated in the standard, the method might not have been aggressive enough to trigger ASR reactions during the short testing period. Thus, these results must be interpreted with care.

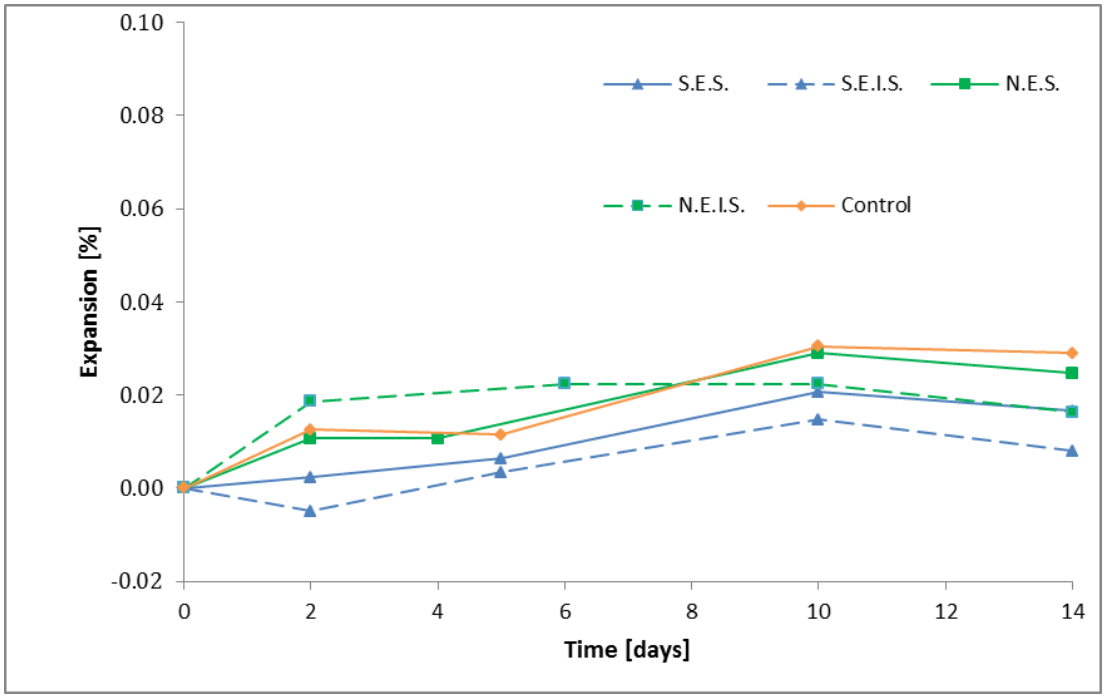

Figure 64 Expansion of mortar prisms versus time in ASR test.

4.1.13 Grading

The results from the sieving of N.E.S. mineral size-fractions 8/16, 2/8 and 0/2 are presented in **Figure 65**, **Figure 66**, **Figure 67** and **Figure 67** and **Table 32**, **Table 33** and **Table 34**, respectively. The results from the sieving of S.E.S. mineral size-fractions 8/16, 2/8 and 0/2 are presented in **Figure 68**, **Figure 69** and **Figure 70**, and **Table 35**, **Table 36** and **Table 37**, respectively.

The particle size distribution seems to be good in most cases. For the 8/16 fraction, 23 wt% of the N.E.S. particles and 12 wt% of the S.E.S. particles are < 8 mm. No grains are > 16 mm in the N.E.S. 8/16 fraction, while 3 wt% are > 16 mm in the S.E.S. 8/16 fraction.

For the 2/8 fraction, 3 wt% of the N.E.S. particles and 4 wt% of the S.E.S. particles are < 2 mm. No grains are > 8 mm in the N.E.S. 8/16 fraction, while 1 wt% are > 16 mm in the S.E.S. 8/16 fraction.

In the 0/2 fraction, 4 wt% of the N.E.S. particles and 5 wt% of the S.E.S. particles are < 0.063 mm. In the N.E.S. 0/2 fraction, 10 wt% of the particles are > 2 mm, while 9 wt% of the particles in the S.E.S. 0/2 fraction are > 2 mm.

Table 32 Particle-size distribution of N.E.S. mineral-fraction 8/16 mm.

Aperture size [mm]	Retained on sieve				Cumulative passing		
	mass (g) A	mass (g) B	mass% A	mass% B	mass% A	mass% B	mass% Average
20	0.0	0.0	0.0	0.0	100	100	100
16	0.0	5.7	0.0	0.4	100	100	100
12.5	400.7	347.6	28.2	24.8	72	75	73
11.2	186.9	230.9	13.2	16.5	59	58	59
10	206.7	214.7	14.6	15.3	44	43	44
8	312.9	274.5	22.0	19.6	22	24	23
6.3	174.3	178.0	12.3	12.7	10	11	10
5.6	26.9	28.7	1.9	2.0	8	9	8
5	10.6	10.3	0.7	0.7	7	8	8
4	12.3	14.7	0.9	1.0	6	7	7
2	20.4	23.6	1.4	1.7	5	5	5
1	12.5	13.6	0.9	1.0	4	4	4
0.5	8.0	10.1	0.6	0.7	3	4	4
0.25	9.5	10.5	0.7	0.7	3	3	3
0.125	7.6	8.7	0.5	0.6	2	2	2
0.063	9.6	9.7	0.7	0.7	2	5	3.1
<0,063	21.6	21.6	1.5	1.5			
Sum (g)	1420.5	1402.9					
Total dry mass (g)	1420.4	1403.6					
Loss (g)	-0.1	0.7					

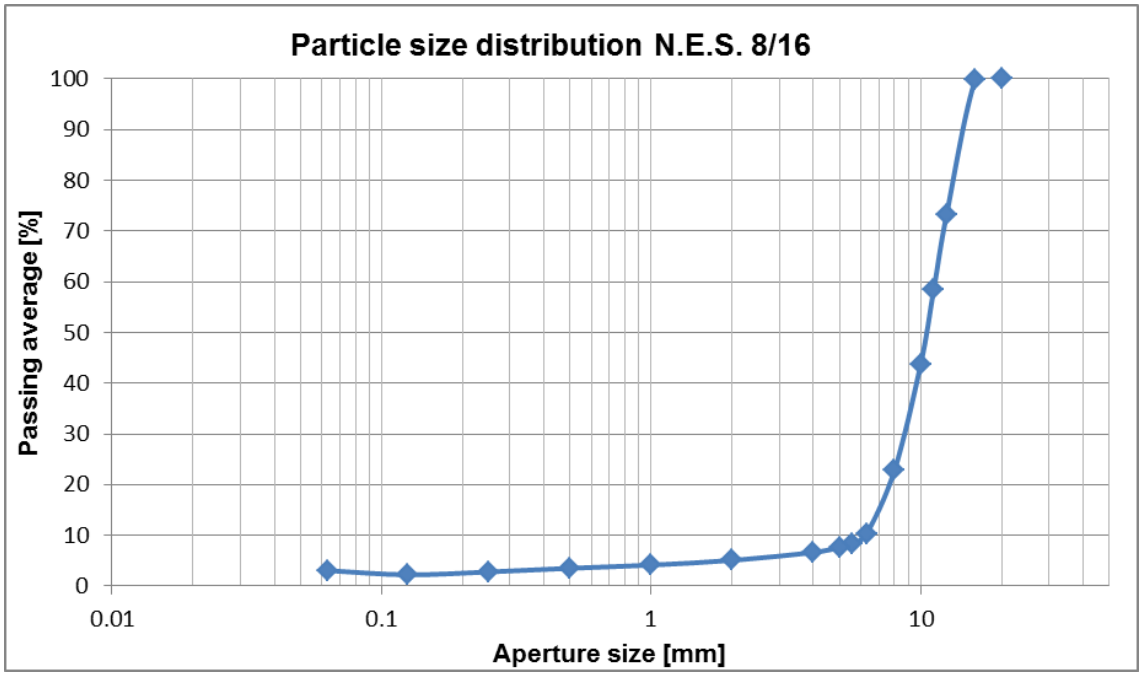

Figure 65 Particle size distribution of N.E.S. mineral-fraction 8/16.

Table 33 Particle-size distribution of N.E.S. mineral-fraction 2/8 mm.

Aperture size [mm]	Retained on sieve				Cumulative passing		
	mass (g) A	mass (g) B	mass% A	mass% B	mass% A	mass% B	mass% Average
12.5	0.0	0.0	0.0	0.0	100	100	100
11.2	0.0	0.0	0.0	0.0	100	100	100
10	0.0	0.0	0.0	0.0	100	100	100
8	0.9	1.6	0.2	0.3	100	100	100
6.3	39.4	32.1	6.9	5.5	93	94	94
5.6	49.8	43.0	8.7	7.4	84	87	86
5	52.9	61.4	9.3	10.5	75	76	76
4	122.7	126.7	21.5	21.7	53	55	54
2	285.5	301.1	50.1	51.5	3	3	3
1	8.8	9.7	1.5	1.7	2	2	2
0.5	1.6	1.4	0.3	0.2	1	1	1
0.25	2.7	1.6	0.5	0.3	1	1	1
0.125	1.0	1.1	0.2	0.2	1	1	1
0.063	0.9	0.8	0.2	0.1	1	1	1
<0,063	5.5	4.3	1.0	0.7			
Sum (g)	571.7	584.8					
Total dry mass (g)	569.7	584.8					
Loss (g)	-2.0	0.0					

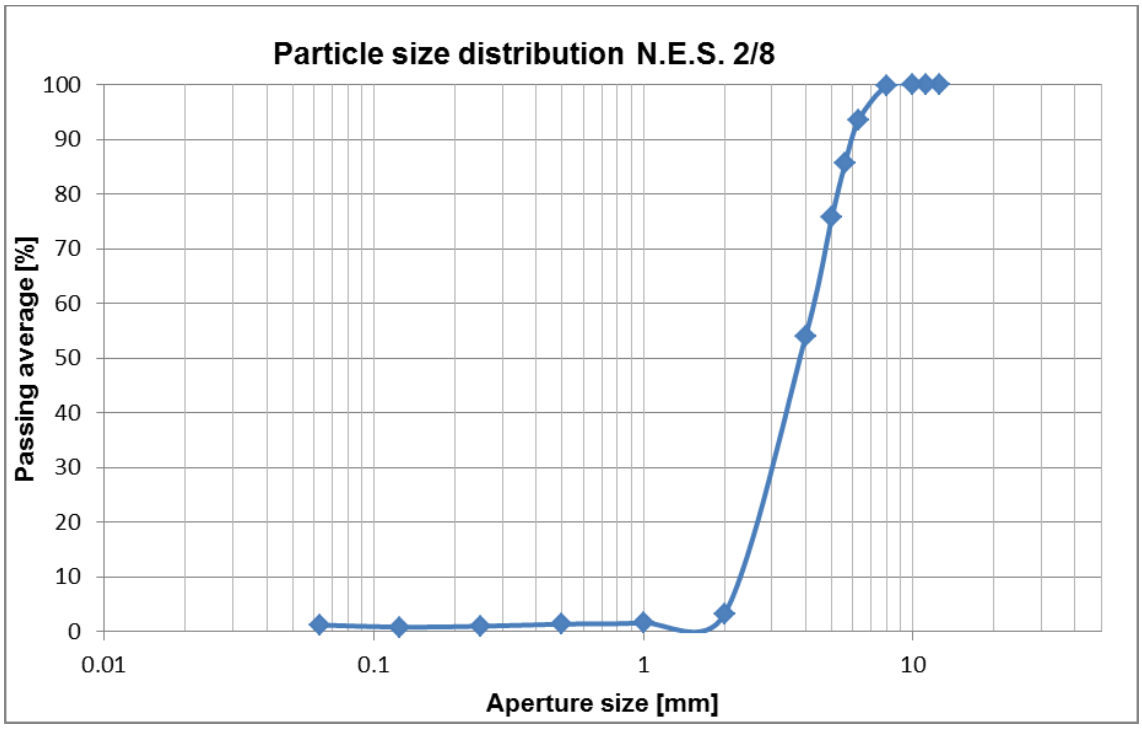

Figure 66 Particle size distribution of N.E.S. mineral-fraction 2/8

Table 34 Particle-size distribution of N.E.S. mineral-fraction 0/2 mm.

Aperture size [mm]	Retained on sieve				Cumulative passing		
	mass (g) A	mass (g) B	mass% A	mass% B	mass% A	mass% B	mass% Average
8	0.0	0.0	0.0	0.0	100	100	100
5.6	0.0	0.0	0.0	0.0	100	100	100
4	0.3	0.0	0.1	0.0	100	100	100
2	24.4	25.5	10.0	10.6	90	89	90
1	59.6	59.4	24.4	24.8	65	65	65
0.5	52.9	52.6	21.7	21.9	44	43	43
0.25	50.8	47.3	20.8	19.7	23	23	23
0.125	35.2	34.3	14.4	14.3	9	9	9
0.063	11.8	11.3	4.8	4.7	4	4	4
<0,063	7.6	7.2	3.1	3.0			
Sum (g)	242.6	237.6					
Total dry mass (g)	244.3	239.8					
Loss (g)	1.7	2.2					

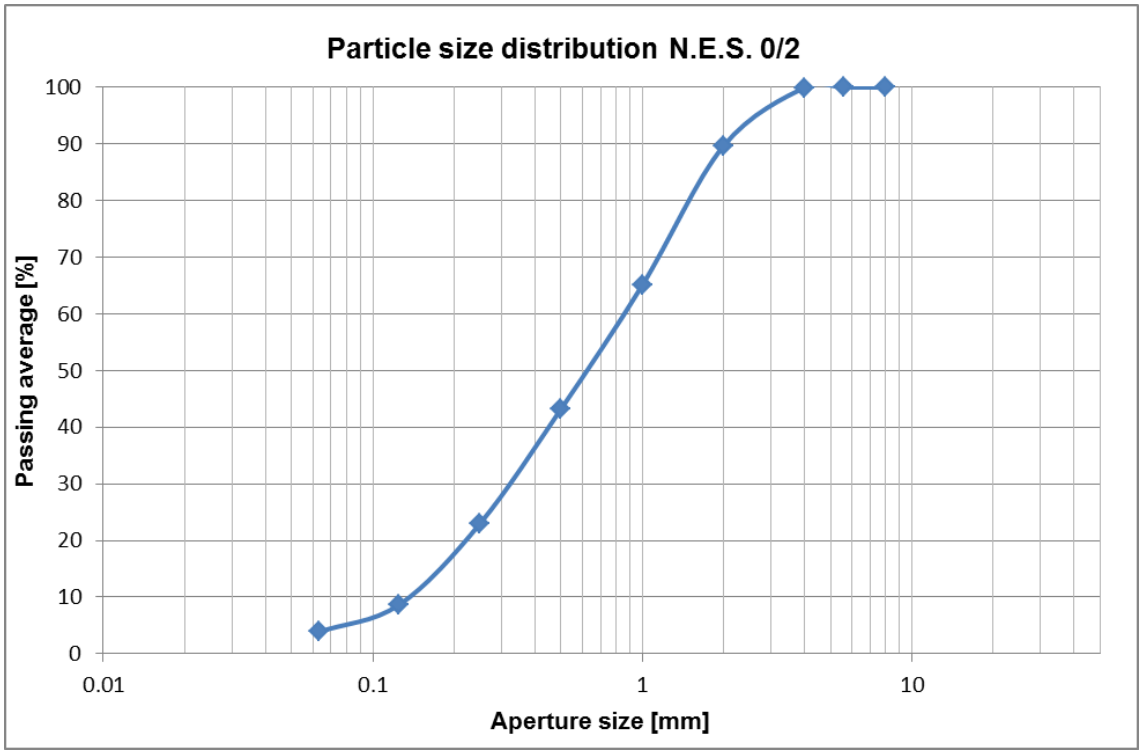

Figure 67 Particle-size distribution of N.E.S. mineral-fraction 0/2 mm

Table 35 Particle-size distribution of S.E.S. mineral-fraction 8/16 mm.

Aperture size [mm]	Retained on sieve				Cumulative passing		
	mass (g) A	mass (g) B	mass% A	mass% B	mass% A	mass% B	mass% Average
20	0.0	0.0	0.0	0.0	100	100	100
16	28.4	53.6	1.9	3.4	98	97	97
12.5	488.7	496.3	32.6	31.7	65	65	65
11.2	250.2	279.8	16.7	17.9	49	47	48
10	243.1	257.8	16.2	16.5	33	30	31
8	295.6	294.5	19.7	18.8	13	12	12
6.3	110.8	101.4	7.4	6.5	5	5	5
5.6	9.1	12.0	0.6	0.8	5	4	5
5	3.0	4.7	0.2	0.3	5	4	4
4	4.7	4.8	0.3	0.3	4	4	4
2	9.3	10.1	0.6	0.6	4	3	3
1	7.5	8.2	0.5	0.5	3	3	3
0.5	9.3	8.4	0.6	0.5	2	2	2
0.25	10.5	8.5	0.7	0.5	2	2	2
0.125	6.9	6.3	0.5	0.4	1	1	1
0.063	5.2	5.5	0.3	0.4	1	3	1.9
<0,063	14.0	13.1	0.9	0.8			
Sum (g)	1496.3	1565.0					
Total dry mass (g)	1497.1	1564.1					
Loss (g)	0.8	-0.9					

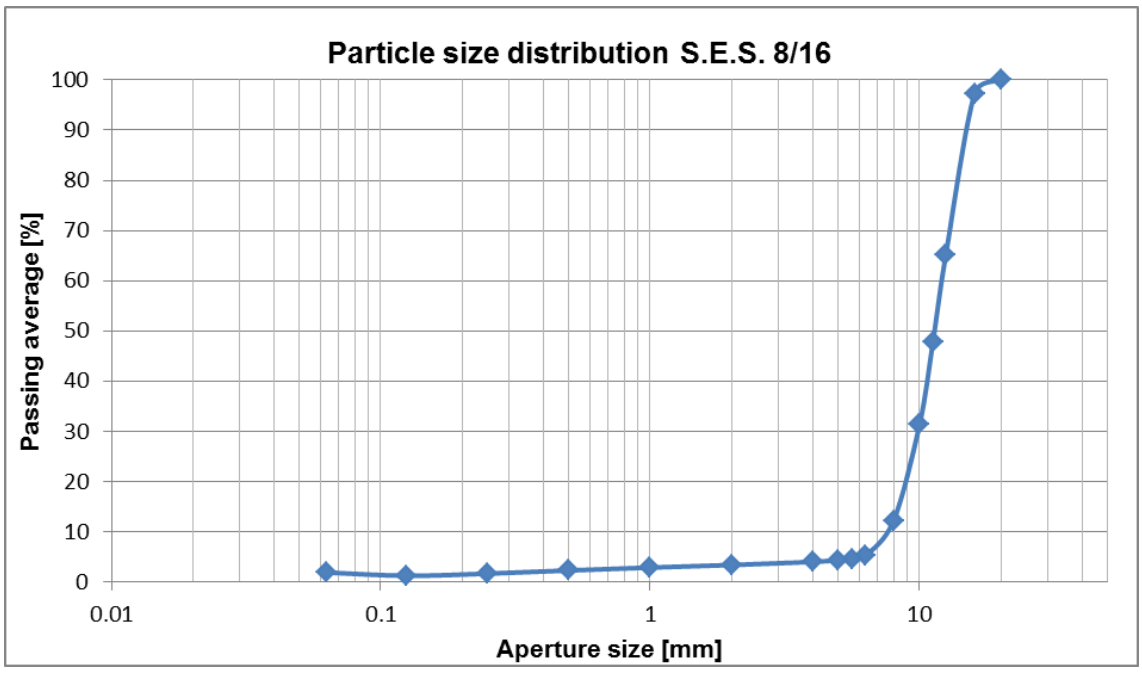

Figure 68 Particle-size distribution of S.E.S. mineral-fraction 8/16 mm.

Table 36 Particle-size distribution of S.E.S. mineral-fraction 2/8 mm.

Aperture size [mm]	Retained on sieve				Cumulative passing		
	mass (g) A	mass (g) B	mass% A	mass% B	mass% A	mass% B	mass% Average
12.5	0.0	1.6	0.0	0.3	100	100	100
11.2	0.0	0.0	0.0	0.0	100	100	100
10	1.1	0.0	0.2	0.0	100	100	100
8	3.2	0.6	0.5	0.1	99	100	99
6.3	54.9	54.5	8.7	9.8	91	90	90
5.6	80.3	66.1	12.8	11.9	78	78	78
5	91.3	90.5	14.5	16.3	63	62	62
4	168.2	147.2	26.7	26.5	37	35	36
2	205.6	175.3	32.7	31.6	4	3	4
1	7.0	6.0	1.1	1.1	3	2	3
0.5	3.0	2.8	0.5	0.5	2	2	2
0.25	3.4	2.3	0.5	0.4	2	1	2
0.125	1.8	1.4	0.3	0.3	1	1	1
0.063	1.7	1.0	0.3	0.2	2	2	2
<0.063	8.1	4.9	1.3	0.9			
Sum (g)	629.6	554.2					
Total dry mass (g)	629.1	554.8					
Loss (g)	-0.5	0.6					

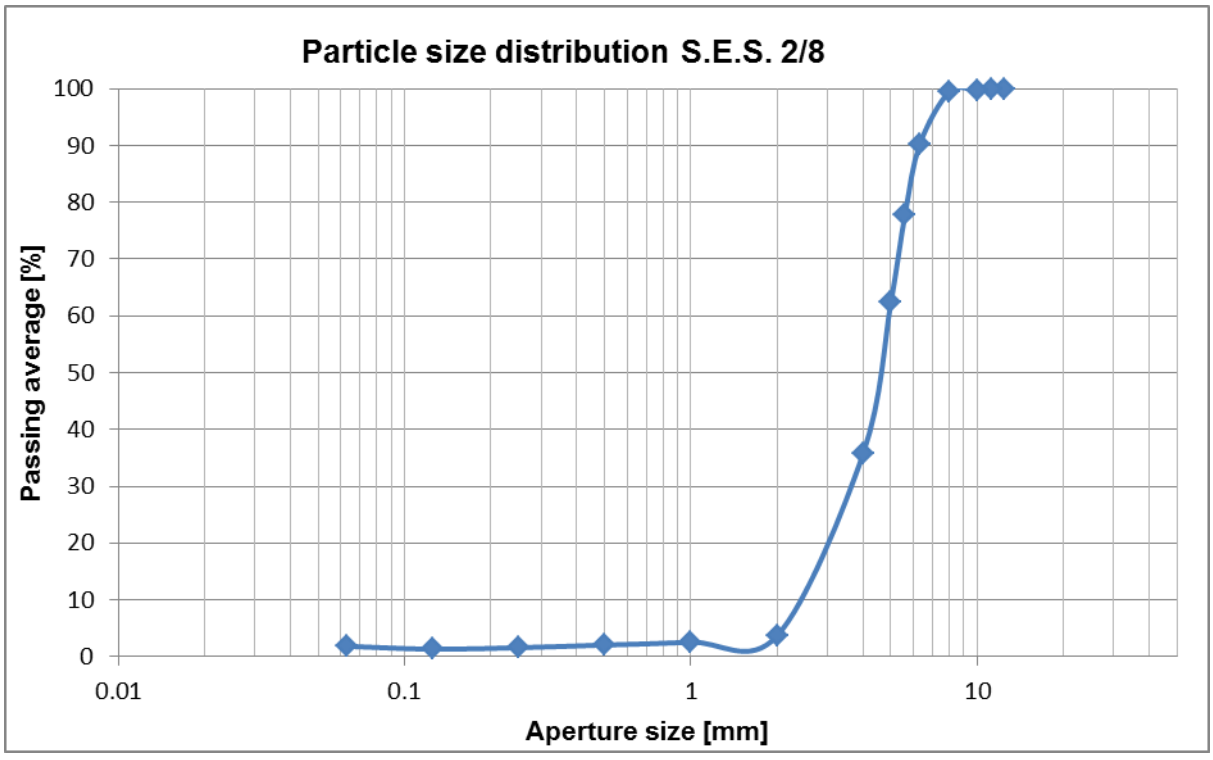

Figure 69 Particle-size distribution of S.E.S. mineral-fraction 2/8 mm.

Table 37 Particle-size distribution of S.E.S. mineral-fraction 0/2 mm.

Aperture size [mm]	Retained on sieve				Cumulative passing		
	mass (g) A	mass (g) B	mass% A	mass% B	mass% A	mass% B	mass% Average
8	0.0	0.0	0.0	0.0	100	100	100
5.6	0.1	0.0	0.0	0.0	100	100	100
4	0.1	0.4	0.0	0.2	100	100	100
2	21.6	23.0	8.9	8.9	91	91	91
1	49.8	54.2	20.6	21.0	70	70	70
0.5	64.1	68.4	26.5	26.5	44	43	44
0.25	57.0	60.5	23.5	23.4	20	20	20
0.125	29.9	31.7	12.3	12.3	8	8	8
0.063	8.0	8.6	3.3	3.3	5	4	5
<0,063	11.2	10.9	4.6	4.2			
Sum (g)	241.8	257.7					
Total dry mass (g)	242.3	258.2					
Loss (g)	0.5	0.5					

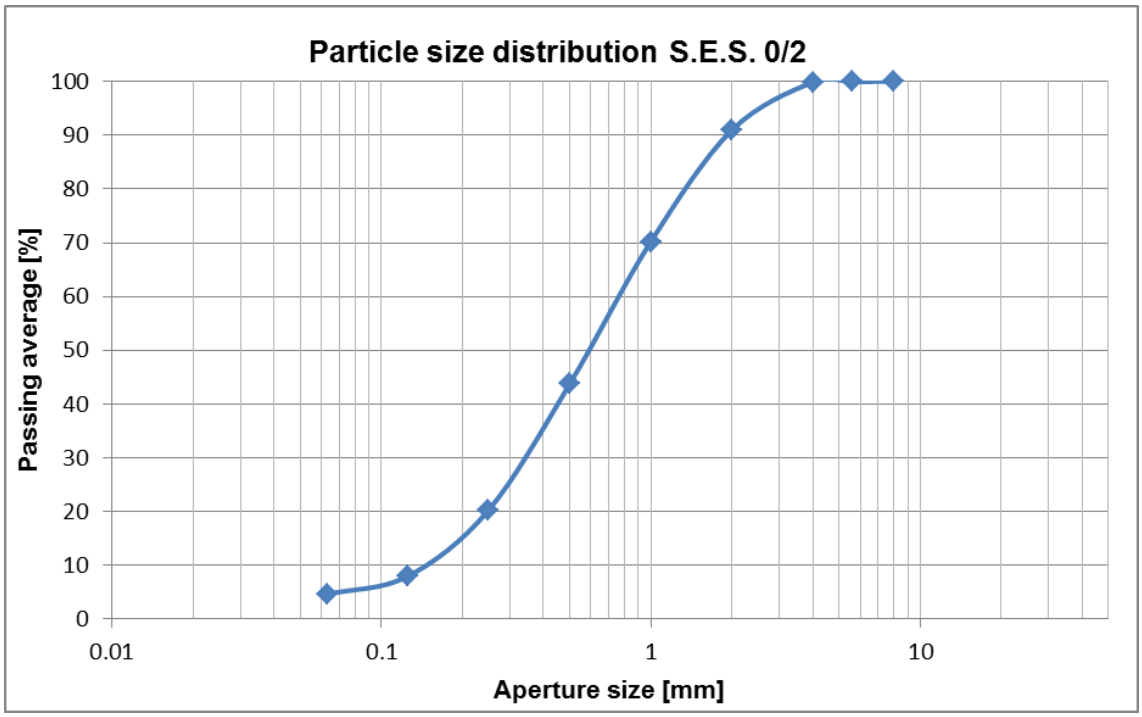

Figure 70 Particle-size distribution of S.E.S. mineral-fraction 0/2 mm.

4.1.14 Flakiness Index

The results of flakiness index are presented in **Table 38**. The Flakiness index for all tested fractions is well below the limit of FI 50, stated in **Table 4**.

Table 38 Results on flakiness index.

Property	Unit	Northern Europe		Southern Europe	
		2/8 mm	8/16 mm	2/8 mm	8/16 mm
Flakiness index		19	9	17	8

4.1.15 Flow coefficient of Fine Aggregates

The results on Flow coefficient of Fine aggregates are presented in **Table 39**. Since no reference sand was tested, the results are only comparable between the samples and not with other materials. Accordingly, the results show that the S.E.S. sand has lower flow coefficient compared with the N.E.S. sand, and thus grain-shape and/or more well-distributed particles that probably will give a better mortar rheology.

Table 39 Results on flow coefficient on fine aggregates.

Property	Unit	Northern Europe	Southern Europe
		0/2 mm	0/2 mm
Flow coefficient of Fine Aggregates	s	34	29

4.1.16 Mechanical properties (Resistance to Fragmentation and Resistance to Wear)

The results on resistance to fragmentation and resistance to wear are presented in **Table 40**. Both fractions satisfy the requirement in **Table 4**, stating that LA should be ≤ 50.

Table 40 Results on resistance to fragmentation and wear.

Property	Unit	Northern Europe	Southern Europe
		8/16 mm	8/16 mm
Resistance to Fragmentation, LA		33	41
Resistance to Wear, M_{DE}		25	36

4.1.17 Particle Density and Water Absorption

The results from measurements on particle densities and water absorption, using the standard procedures (i.e. 110 °C drying and 24 h water saturation), are presented as Test #1 in **Table 41**. In Test #2, one sample from each aggregate fraction was halved to two subsamples, on which the same procedure as used for Test #1 were conducted (**Table 41**). The only difference was that one of the subsamples was dried to constant mass at 40 °C instead of 110 °C. The purpose was to test a) the laboratory internal variation, and b) the difference achieved when drying recycled aggregate

containing temperature sensitive particles. Drying at lower temperature proved to yield a bit lower WA_{24} but similar density values, compared with the tests conducted using higher temperature. The largest variation between different measurements is on the 0/2 fraction. However, this fraction is tested according to Clause 9 in [39], with a methodology originally developed for virgin sand. From commission work experience, this method seems a bit uncertain already when working with crushed 0/2 rock particles, and thus might be unsuitable when the particles are not completely rounded.

Table 41 Mineral fraction particle densities and 24 h water absorption.

Property	Unit	Northern Europe			Southern Europe		
		0/2 mm	2/8 mm	8/16 mm	0/2 mm	2/8 mm	8/16 mm
Test #1, drying at 110 °C							
Water absorption, WA_{24}	%	1.4	3.3	3.0	4.0	8.1	7.7
Apparent density, ρ_a	kg/m³	2650	2690	2510	2640	2680	2530
Particle density on an oven dried basis, ρ_{od}	kg/m³	2550	2470	2340	2390	2200	2120
Particle density on a saturated and surface-dried basis, ρ_{ssd}	kg/m³	2590	2560	2410	2480	2380	2280
Test #2, drying at 110 °C							
Water absorption, WA_{24}	%	1.7	3.5	3.1	4.4	8.1	6.7
Apparent density, ρ_a	kg/m³	2690	2690	2650	2650	2540	2520
Particle density on an oven dried basis, ρ_{od}	kg/m³	2570	2460	2450	2370	2100	2150
Particle density on a saturated and surface-dried basis, ρ_{ssd}	kg/m³	2620	2540	2520	2470	2270	2300
Test #2, drying at 40 °C							
Water absorption, WA_{24}	%	2.0	2.9	2.8	4.1	7.4	6.4
Apparent density, ρ_a	kg/m³	2700	2650	2610	2620	2510	2460
Particle density on an oven dried basis, ρ_{od}	kg/m³	2560	2460	2430	2370	2120	2130
Particle density on a saturated and surface-dried basis, ρ_{ssd}	kg/m³	2610	2530	2500	2460	2270	2260

The coarse fractions were also tested for long-time water absorption and results are presented in **Table 42**. The purpose of this test was twofold: to see how much of the saturation that takes place on short term (hour to hours) and to reveal how much more saturation that takes place after the initial 24 hours. For N.E.S. material, the WA_{24} was reached after already 1 h and was more or less the total absorption also after 14 days. For S.E.S. material, the WA_{24} was also here reached after just 1 h, but the material continued to soak water and increased its WA after 7 days, with not much more happening the second week.

Table 42 Mineral fraction particle densities and long-time water absorption.

Property	Unit	Northern Europe			Southern Europe		
		0/2 mm	2/8 mm	8/16 mm	0/2 mm	2/8 mm	8/16 mm
Test #3, drying at 110 °C – Water absorption (WA_x)							
1 h	%	n/a	3.7	3.6	n/a	8.7	7.4
5 h	%	n/a	3.9	3.5	n/a	8.7	7.3
24 h	%	n/a	3.7	3.5	n/a	8.9	7.6
7 days	%	n/a	3.7	3.5	n/a	9.5	7.8
14 days	%	n/a	3.6	3.5	n/a	9.3	7.9
Test #3, drying at 110 °C – Apparent density (ρ_a)							
1 h	kg/m³	n/a	2680	2660	n/a	2500	2540
5 h	kg/m³	n/a	2690	2660	n/a	2520	2530
24 h	kg/m³	n/a	2690	2660	n/a	2560	2540
7 days	kg/m³	n/a	2700	2670	n/a	2620	2590
14 days	kg/m³	n/a	2700	2670	n/a	2620	2600

Mineral fraction water absorption and densities were also measured by other laboratories (ACCIONA, CETMA and QUB). Their results are summarized in **Table 43**, together with the CBI results from Test #2. QUB also tested water absorption and density on improved mineral fractions (i.e. hand-sorted N.E.S. and S.E.S. 8/16 fractions) from both Northern and Southern Europe; these results are also included in **Table 43**. These results show a relatively large spread, particularly when it comes to water absorption on the fine fraction (0/2 mm). Possible reasons might be large material heterogeneity within and/or between batches (i.e. big-bags), operator related, laboratory unique steps/deviations from the method, difficulties to maintain the aggregates saturated while surface drying and the drying procedures in the end of the test (i.e. reaching a constant mass properly). The reason(s) for these deviations will be investigated in Task 4.3 (along with investigation of variability between different CDW batches) and reported in D4.3, which is specifically related to the effect of the CDW-derived materials variability on technological properties of developed products.

Table 43 Compilation of results on density and water absorption obtained from several laboratories.

Property	Unit	ACC	CBI		CETMA	QUB	QUB Improved
	Drying temperature (°C)	110	40	110	110	40	40
Northern Europe Sorted CDW (N.E.S.) – 8/16							
WA_{24}	%	2.3	2.8	3.1	3.7	2.4	1.8
ρ_a	kg/m³		2610	2650	2690	2630	2770
ρ_{rd}	kg/m³		2430	2450	2440	2480	2630
ρ_{ssd}	kg/m³	2650	2500	2520	2530	2540	2680
Northern Europe Sorted CDW (N.E.S.) – 2/8							
WA_{24}	%	4.5	2.9	3.5	3.5	2.8	2.2
ρ_a	kg/m³		2650	2690	2750	2410	2710
ρ_{rd}	kg/m³		2460	2460	2510	2250	2560
ρ_{ssd}	kg/m³	2590	2530	2540	2590	2320	2620
Northern Europe Sorted CDW (N.E.S.) – 0/2							
WA_{24}	%	4.1	2.0	1.7	7.9	3	
ρ_a	kg/m³		2700	2690	2525		
ρ_{rd}	kg/m³		2560	2570	2110		
ρ_{ssd}	kg/m³	2430	2610	2620	2270		
Southern Europe Sorted CDW (S.E.S.) – 8/16							
WA_{24}	%		6.4	6.7	1.9	5.2	2.0
ρ_a	kg/m³		2460	2520	2560	2470	2730
ρ_{rd}	kg/m³		2130	2150	2440	2180	2590
ρ_{ssd}	kg/m³		2260	2300	2480	2300	2640
Southern Europe Sorted CDW (S.E.S.) – 2/8							
WA_{24}	%		7.4	8.1	1.7	6.0	3.2
ρ_a	kg/m³		2510	2540	2380	2590	2690
ρ_{rd}	kg/m³		2120	2100	2290	2240	2470
ρ_{ssd}	kg/m³		2270	2270	2330	2370	2550
Southern Europe Sorted CDW (S.E.S.) – 0/2							
WA_{24}	%		4.1	4.4	6.5	7	
ρ_a	kg/m³		2620	2650	2480		
ρ_{rd}	kg/m³		2370	2370	2140		
ρ_{ssd}	kg/m³		2460	2470	2280		

4.2 Fine materials

The results from the chemical and physical characterization of the CDW fine mineral fraction (< 0.063 mm) are summarized and commented below.

4.2.1 Liquid Limit

The penetration depth was tested on pastes prepared with increasing amount of water (higher moisture contents) as to plot the penetration depth with moisture content, as shown in **Figure 71**. From **Figure 71** the liquid limit was estimated to be 66%.

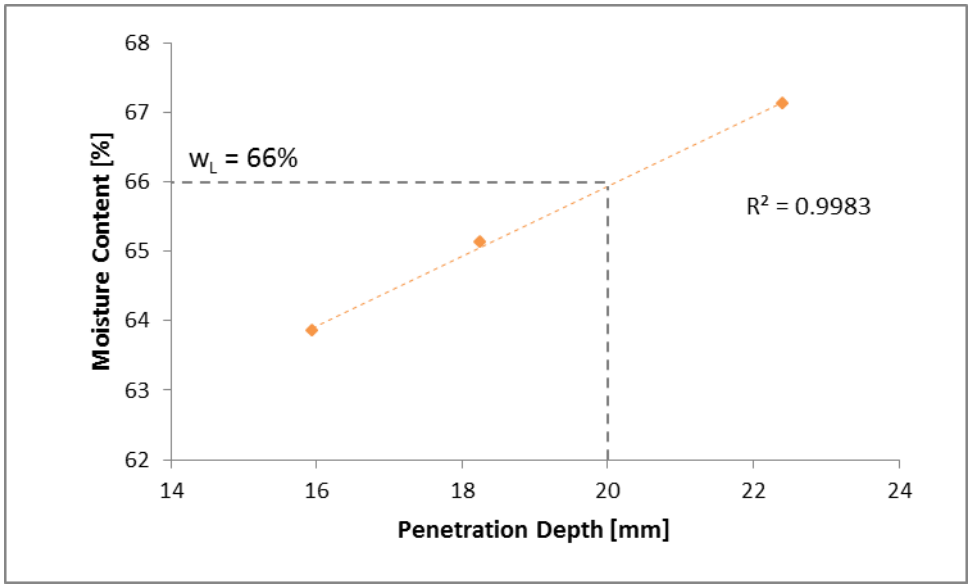

Figure 71 Penetration depth of cone penetrometer as a function of paste moisture content.

4.2.2 Plastic Limit (w_p)

The plastic limit (w_p) value was found to be 39%, based on the results of **Table 44**.

Table 44 Determination of the plastic limit.

	Sample 1	Sample 2
Mass of empty container (g)	3.332	3.338
Mass of empty container + wet soil (g)	5.154	5.231
Mass of empty container + dry soil (g)	4.645	4.703
Plastic Limit (%)	39	39

4.2.3 Plasticity

The Plasticity Index (I_P) was determined as follows:

$$I_p = w_L - w_P = 66\% - 39\% = 27\%$$

Figure 72 shows the plasticity chart (adopted from BS 5930:2015 [56]) used to compare the plasticity of a soil by plotting the plasticity index against the liquid limit. The A line divides the graph into such a way that soils who fall below the line are classified as silts, whereas soils who fall above the line are classified as clays. In addition, the graph is divided into 5 categories of plasticity (low, intermediate, high, very high and extremely high). According to the plasticity chart, the fine material under investigation, marked by the red x, appears to be silt like in consistency with high plasticity. However, it should be noted that different clay types, composition, pH value and the presence of contaminants can greatly influence the Atterberg limits of clay soils [57] and [58]. In addition, the presence of organic matter can increase the liquid and plastic limit values of clay [59] and [60]. High

amounts of organic material can also affect the plasticity index. Malkawi et al. [60] observed a reduction in plasticity index when the organic content of the soil exceed 5%. As such, clays rich in organic matter tend to lie below the A line.

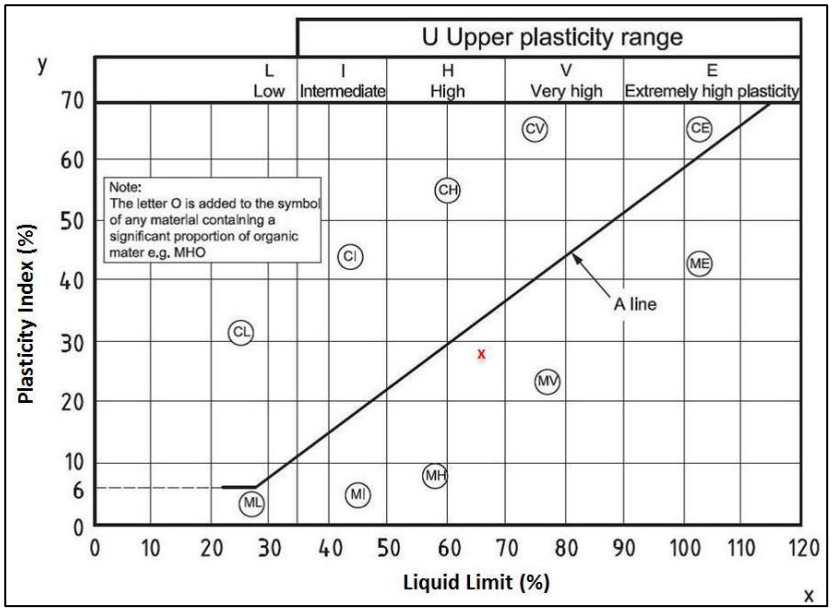

Figure 72 Plasticity chart adopted from BS 5930:2015 [56].

It should be noted that the fine material contains significant amounts of organics, as shown by the results of TGA presented below. The presence of organics is likely to increase the liquid and plastic limit of the silt, but reduce its plasticity index placing it below the A line.

4.2.4 XRF Analysis

XRF analysis (**Table 45**) of the uncalcined fine material revealed that it is rich in SiO_2, CaO, SO_3 and Al_2O_3. The fine material also contains, in minor amounts, Fe_2O_3, MgO, K_2O, and Na_2O.

Table 45 XRF analysis of the fine material.

Oxide	Amount (wt%)
CaO	14.3
SiO_2	43.2
Al_2O_3	9.7
Fe_2O_3	3.6
MgO	1.8
SO_3	7.9
Na_2O	0.5
K_2O	2.0
LOI	17.5
Total	100.4

4.2.5 XRD Analysis

Figure 73 shows an XRD spectrum of the uncalcined fine material from which several crystalline phases can be identified. The more prominent include quartz (Si), calcite (Ca) and gypsum (G). Muscovite (M) and feldspar (F) were also identified, along with several clay minerals, including clay minerals belonging to the smectite (S) and kaolin (K) group, plus illite (I) overlapping with muscovite.

Quantifying the major phases only, the fine material contained relatively low amounts of quartz (31.7%) and calcite (12.7%) compared to the mineral fractions of Subtask 4.2.1. The fine material was also found to contain 18.3% of gypsum (gypsum plasterboard), probably from the washing and separation of the aggregates. The remaining 37.3% constitutes the minor phases identified (smectite, muscovite and kaolin) plus any amorphous phases as shown in **Table 46**. The higher SiO_2 content measured by XRF is due to the presence of silicon in the clays.

Upon calcining the fine material at 700 °C, XRD analysis showed that calcium carbonate had decomposed (**Figure 74**). Similarly, gypsum had dehydrated to produce its anhydrous analogue, anhydrite ($CaSO_4$). The broad peaks of smectite and kaolinite minerals, seen at ~6 2θ and ~12.5 2θ respectively in **Figure 73**, have disappeared, suggesting their dehydroxylation. Illite, however, was still present after calcination. It has been previously suggested that illite requires temperatures in excess of 700 °C for its decomposition [41] and [61].

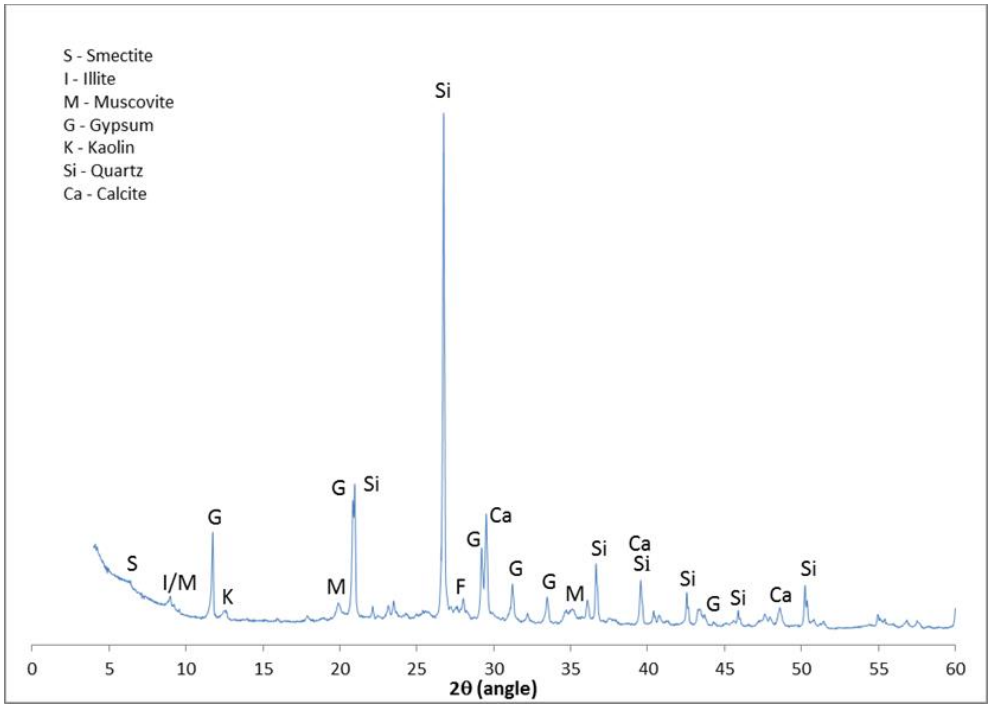

Figure 73 XRD analysis of uncalcined fine material oven dried at 40 °C.

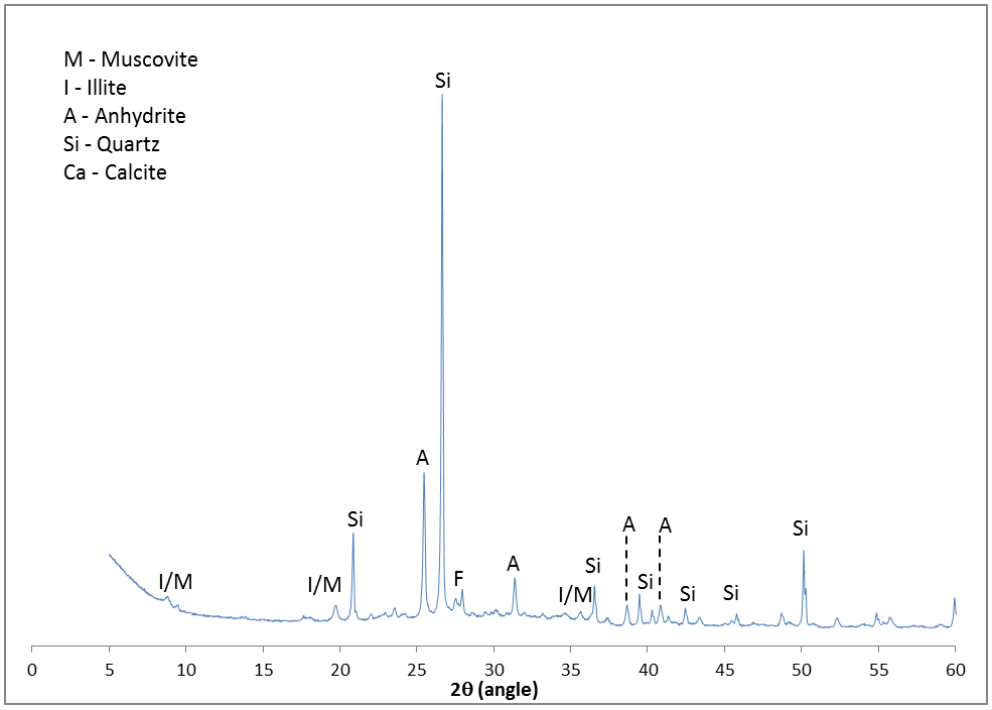

Figure 74 XRD analysis of fine material calcined at 700 °C.

Table 46 Quantification of major phases identified by XRD

Phase	Amount (weight %)
Quartz (SiO_2)	31.7
Calcite ($CaCO_3$)	12.7
Gypsum ($CaSO_4 \cdot 2H2O$)	18.3
Remaining	37.3

4.2.6 FTIR Spectroscopy

The obtained FTIR results measured on the uncalcined and calcined fine material are shown in **Figure 75**. The uncalcined fine material is characterised by having 9 major distinct bands.

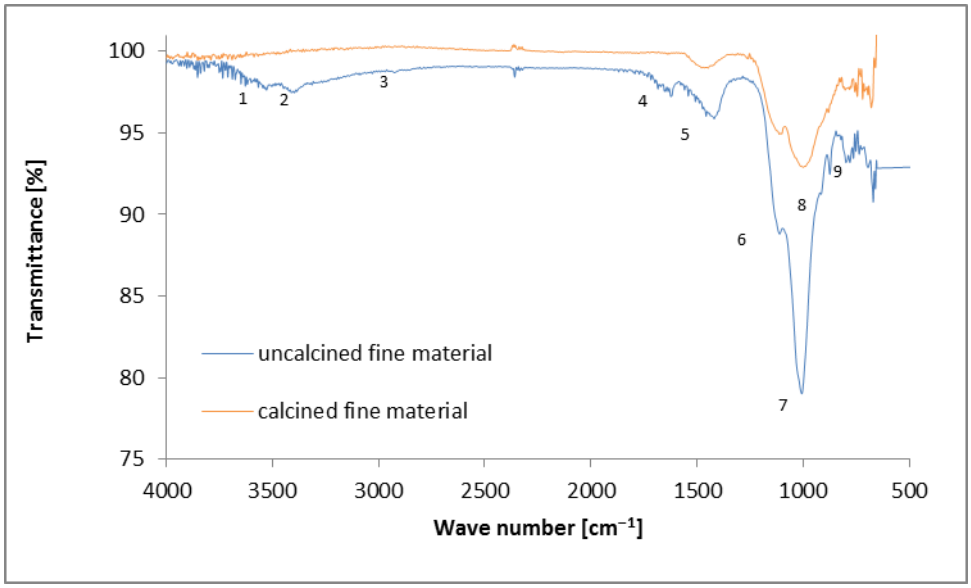

Figure 75 FTIR spectra of uncalcined and calcined fine material.

From higher to lower wave numbers, a first diffuse band was observed from 3500 to 2300 cm^{-1} and corresponds to the stretching vibrations of OH bonds. Two bands, 1 and 2, centred at 3527 cm^{-1} and 3395 cm^{-1} possibly relate to the stretching vibration of OH in kaolinite and illite [41], although the band at 3395 cm^{-1} can also be due to the stretching of OH bonds seen in aliphatic polyols [62]. A very shallow band (3), seen at 2893 cm^{-1}, corresponds to symmetric vibrations of CH groups found in aliphatics [62]. The presence of water was again confirmed in band 4 (at 1619 cm^{-1}), where the band represents the bending vibration of OH bonds. Carbonates were also confirmed in the sample with a band centred at 1417 due to the stretching of CO_3^{2-} bonds.

Bands 6 and 7 both relate to asymmetric stretching of aluminosilicate bonds (Si-O-Si or Si-O-Al). Band 8, a diffuse band observed as a shoulder on band 7, is due to the bending vibration of Al-OH bonds. A final major band, band 9 centred at 871 cm^{-1}, is due to the bending or deformation of Fe-OH bonds ([63] and [64]). The presence of iron could possibly suggest the presence of nontronite, an iron rich member of the smectite group, previously observed by XRD (**Figure 73**). Furthermore, XRF analysis (**Table 45**) showed that the fine material contained 3.6 % Fe_2O_3. All the major bands identified are summarized in **Table 47**.

Table 47 FTIR bands of the uncalcined fine material spectrum.

Band number	Wave number (cm^{-1})	Species
0	3500-2300	Stretching vibrations of OH
1	3527	Stretching vibrations of OH in fine material
2	3395	Stretching vibrations of OH in fine material Stretching vibrations of OH in aliphatics
3	2893	Vibrations of CH groups in aliphatics

Band number	Wave number (cm^{-1})	Species
4	1619	Bending vibrations of H-O-H
5	1417	Stretching vibrations of COO-
6	1107	Stretching vibration of Si-O-Si
7	1000	Stretching vibration of Si-O-Al
8	910	Bending vibration of Al-OH
9	871	Vibration of Fe-OH

Upon calcining the fine material, bands 1 – 4 disappeared as water was driven of the sample. The carbonate band (band 5) shifted from 1417 to 1447 cm^{-1}. This band remained even after calcination, as thermal analysis showed carbonates decomposing at temperatures beyond 700 °C, the calcining temperature of the fine material. However, calcite was no longer observed by XRD after calcination. This discrepancy is unclear. All Si-O bonds persisted, although bands 8 and 9 were greatly diminished.

4.2.7 DTA-TGA

Figure 76 shows the fine material undergoing thermal decomposition. The mass loss is plotted with its derivative, with the latter showing several endotherms pinpointing the decomposition of several compounds. The gaseous compounds associated with thermal decomposition are shown in **Figure 77**.

The mass loss can be divided into 4 regions. The first region corresponds to minimal mass loss up to 100 °C. This slow mass loss was followed by a faster mass drop from 100 to 150 °C. Thereafter, the mass loss was gradual up to temperatures of 600 °C. The rate of mass loss accelerates one last time from 600 to 900 °C before stabilizing until the end of the test. At low temperatures (<200 °C), two endotherms can be observed. The first, at 78 °C, was due to the evaporation of any adsorbed water remaining. The second endotherm is due to the thermal decomposition of gypsum, previously observed by means of XRD (**Figure 73**). The mass loss, 3.3 g/100 g of fine material, is associated with the loss of water (**Figure 75**), which equates to 15.6 g of gypsum (against 18.3 g measured by XRD). The two subsequent endotherms, seen at 290 and 430 °C, were most likely due to the decomposition of organic matter present in the soil, possibly aliphatic and aromatic structures respectively, with carbon dioxide being the main gas released [65], [66], [67] and [68]. Beyond 600 °C, two endotherms were observed and due to any carbonate present in the sample.

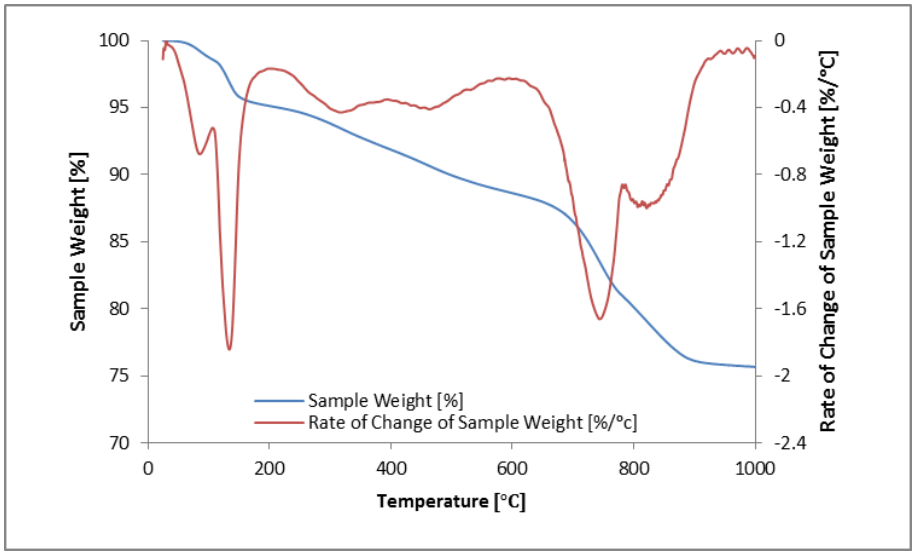

Figure 76 Sample weight (%) and rate of change of sample weight (%/°C) versus temperature (°C).

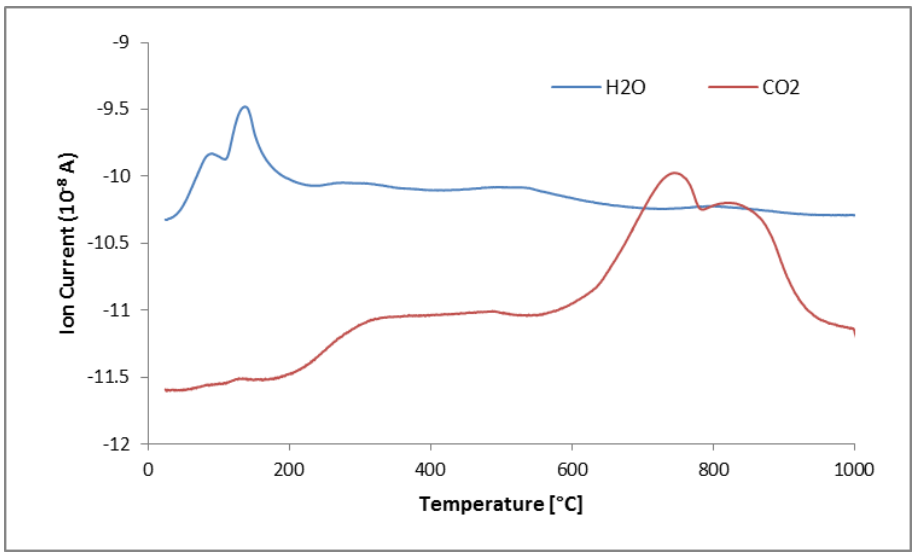

Figure 77 Ion current of H_2O and CO_2.

Thermal analysis did not suggest any dehydroxylation of clays during the heat treatment. However, XRD analyses suggested only trace amounts of the illite, kaolinite and montmorillonite, and any dehydroxylation from the clays would have been minimal.

4.2.8 Soluble components (humus, fulvo acid, sulphates, chlorides & alkalis)

As can be seen in **Figure 51**, fine material contained more humus compared to the mineral fractions of Northern and Southern Europe (0/2 mm, 2/8 mm & 8/16 mm). However, the test result was still negative compared to the colour of the standard solution.

Like the mineral fractions of Northern and Southern Europe (0/2 mm, 2/8 mm & 8/16 mm), the fine material showed little or no fulvo acid (**Figure 52**).
The water-soluble sulphate content was determined using both methods detailed in EN 1744-1. When mixing 500 g of the fine material in 1000 g of water for 24 hours, the fine material was found to have leached 0.274 g/100g of fine material. However, when 25 g is mixed in 1000 g of water at 60°C, 3.126 g of SO_3 leached for every 100 g of fine material (**Table 48**).

Table 48 Amount of water soluble SO_3.

SO_3 extraction method	$\%SO_3$
2:1 water:solids at 20°C	0.274
40:1 water:solids at 60°C	3.126

It is unclear which method was most suitable for the fine material but the amount leached does not correspond to the amount of SO_3 determined by XRF (7.9%) or correspond to the amount of gypsum determined by XRD (18.3). In fact, 7.9 g/100 g of fine material equates to 17 g of gypsum for every 100 g of fine material. As such, much of the SO_3 present in the fine material is bound as gypsum. However, gypsum is poorly soluble (2-2.5 g/l at 25 °C and 60 °C) and exhibits retrograde solubility [69]. The likely cause is due to the changes in the water/solids ratio.

Due to the lack of studies, it is not known if this reservoir of gypsum in the fine material will cause expansion in geopolymer concretes. Excess sulphates in OPC lead to expansion, as is the case with delayed ettringite. However, it is not known if ettringite will form readily in geopolymer based concretes as geopolymers are typically calcium deficient compared to OPC. Bakharev [70] did observe the formation of ettringite in fly ash based geopolymers activated with sodium silicate, exposed to external sulphate attack. It should be noted, however, that external sulphate attack differs from internal sulphate; in the latter case, there is an exchange of ions between the specimen and the aggressive solution which does not exist in the case of internal sulphate attack.

The water-soluble chloride content was determined using the potentiometric method only. The chloride content of the fine materials was found to be 0.192 g/100g of fine material (C = 0.192 %). The fine fraction contained much greater amounts of chlorides compared to the mineral fractions. If this material is intended to be used as a precursor to make geopolymer concrete, it is unclear if the fine material contains excessive amounts of chlorides. For OPC concrete, [2] specifies that the chloride content of a concrete should not exceed 0.2 % by mass of the cement. However, [2] may not be suitable for geopolymer concretes. Previous research has shown that fly ash based geopolymers can effectively passivate steel [71] [72]. Tennakoon et al. [73] found steel reinforcement imbedded in a geopolymer concrete artificially contaminated with 2 % chloride by weight of binder showed greater resistance to chloride corrosion compared to steel reinforcement imbedded in OPC concrete equally contaminated.

The amounts of water-soluble alkalis (K and Na) are showed in **Table 49.** It was found that the fine material leached only 2.27 mg and 2.39 mg, respectively, per 100 g of fine material. The amounts remain minimal and should have no effect on a resultant geopolymer prepared the fine material. El-

Didamony [74] did notice, however, increased strength in geopolymers prepared with seawater compared to the same geopolymers prepared with tap water due to the presence of the alkalis aiding hydration.

Table 49 Amount of water-soluble alkalis present in the fine material.

Alkali	amount of soluble alkali (mg/kg)	mg/100g of fine material
K	227	22.7
Na	239	23.9

4.2.9 Activity Index

Table 50 shows the particle size distribution of the fine material after mechanical sieving. It can be seen that the fine material is made up of 76% of particles smaller than 0.063 mm in size.

Table 50 Particle size distribution of the fine material from mechanical sieving.

Sieve	Cumulative passing [g]	Cumulative passing [%]
> 3.35 mm	499.6	100.0
> 2 mm	499.1	99.9
> 1 mm	498.6	99.8
> 0.6 mm	497.8	99.6
> 0.425 mm	495.6	99.2
> 0.3 mm	488.5	97.8
> 0.212 mm	474.5	95.0
> 0.15 mm	455.1	91.1
> 0.063 mm	382.0	76.5
< 0.0063 mm	0	0.0

Figure 78 shows the size distribution of the particles <0.063 mm present in the fine material. It is obvious that this fraction is made up predominantly of silt size particles. The data from **Table 50** has been combined to create the full size distribution of the fine material, also presented in **Figure 78**. It can be observed that only 8.9% of the fine material is made up of clay size particles. This is in agreement with the plasticity chart (**Figure 72**).

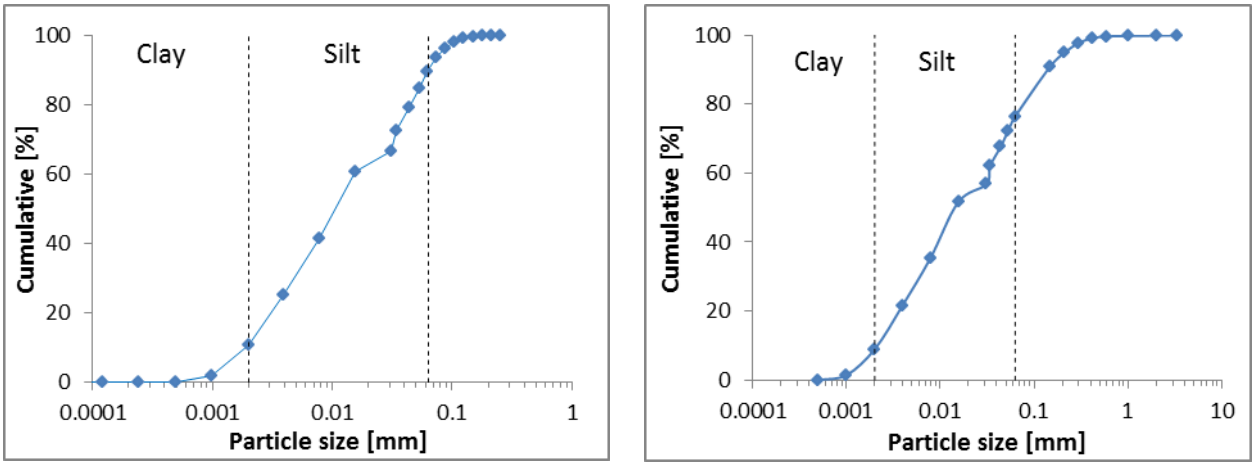

Figure 78 Particle size distribution of the particles < 0.063 mm determined by laser diffractometer (left). Cumulative particle size distribution of the fine material (right).

As it is the particle sizes < 0.425 mm that are used for determining the liquid and plastic limit, the clay content is normalised for the %passing of that fraction. As such, the clay content is

$$\left(\frac{8.9\%}{99.2\%}\right)(100\%) = 9.05\%$$

The activity index is therefore estimated at:

$$\mathrm{A} = \frac{\mathrm{I_p}}{\%\ \text{Clay particles}} = \frac{27\%}{9.05\%} = 2.98$$

The fine material is therefore considered to be highly active. In comparison, kaolinite has an activity index of 0.4, organic alluvial clays have an activity ranging from 1.2 to 1.7 and bentonite, 7 [75].

4.2.10 Reactivity/Isothermal calorimetry

The heat released during hydration of uncalcined fine material is shown in **Figure 79**.

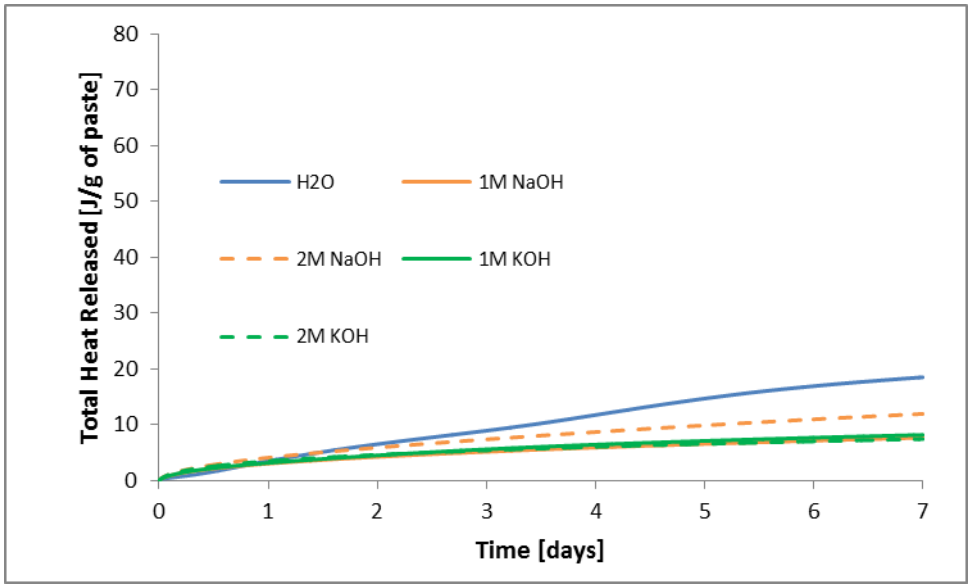

Figure 79 Heat release during hydration of uncalcined fine material versus time.

Upon wetting the fine material, a minimal amount of heat was recorded in all samples after 7 days of hydration. The paste prepared with deionized water evolved the most heat by the end of the testing period – 18 J/g of paste. The addition of NaOH or KOH did not promote hydration of the fine material, and rather seemed to reduce reactivity. None of the paste had set by the end of the 7 days testing period. The heat released during hydration of calcined fine material is shown in **Figure 80**.

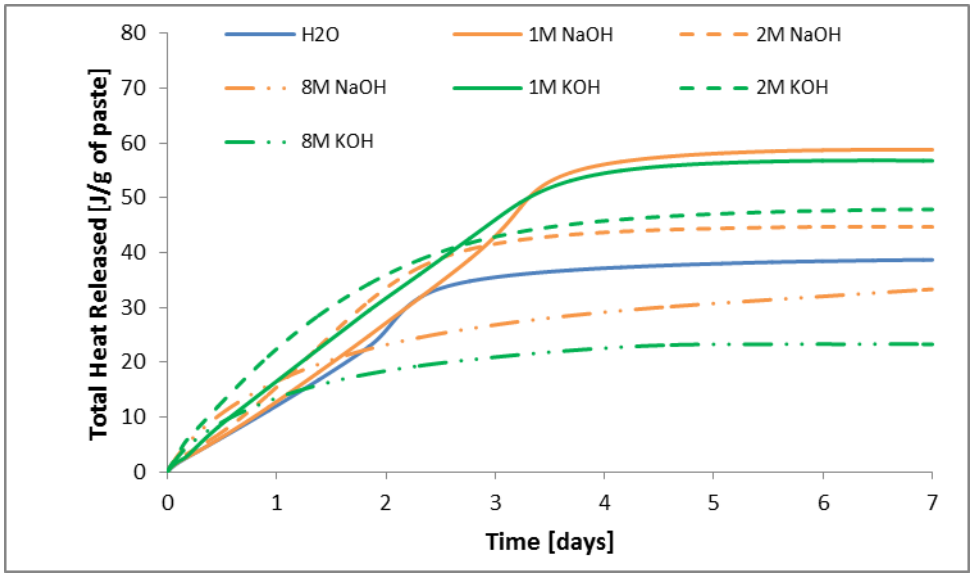

Figure 80 Heat release during hydration of calcined fine material versus time.

Upon calcination of the fine material, reactivity was markedly improved. All systems investigated showed moderate signs of reactivity in the first 2 to 3 days after which all systems plateaued. By the

end of the testing period, the pastes activated with 1 M NaOH or KOH showed the greatest amount of reactivity, with 56 and 58 J/g of paste released for the KOH and NaOH activated fine materials, respectively. Further increasing the concentration of the activating solution to 2 M or 8 M actually reduced reactivity. In fact, the pastes prepared with 8 M NaOH or KOH were the least reactive. The paste prepared with deionized water was shown to be the least reactive. Unlike their non-activated counterparts, all calcined fine materials had shown some setting by the end of the testing period as shown in **Figure 81**.

Figure 81 Visual observation of the uncalcined (bottom) and calcined (top) fine material.

4.3 Lightweight materials

The results from the characterization tests of the CDW lightweight/LW fractions (wood and plastic/WP, rigid plastic/RP and wood/W) are summarized and commented below.

4.3.1 Grain size

The results from the sieving of S.E.S and N.E.S. **WP fine fractions** are presented in **Table 32** and **Figure 82** and in **Table 52** and **Figure 83** and respectively. In both cases the granules are almost below 4 mm, the distribution is quite similar up to 1 mm but with a higher concentration of particles below 2 mm for WP from S.E.S (70% of passing material against 23% of N.E.S.).

Table 51 Grading size distribution of Wood and Plastic fine fractions (S.E.S.) according to UNI EN 933-1.

WP | S.E.S.				
Aperture size [mm]	**Retained mass [g]**	**Retained percentage [%]**	**Cumulative passing [%]**	**Passing material [%]**
mm	g	%	%	%
125	0,0	0%	0%	100%
63	0,0	0%	0%	100%
31,5	0,0	0%	0%	100%
20	0,0	0%	0%	100%
16	0,0	0%	0%	100%
10	0,0	0%	0%	100%
8	0,0	0%	0%	100%
6,3	0,0	0%	0%	100%
4	0,0	0%	0%	100%
2	25,5	30%	30%	70%
1	54,5	64%	94%	6%
0,500	3,5	4%	98%	2%
0,250	0,5	1%	98%	2%
0,125	0,5	1%	99%	1%
0,063	0,5	1%	99%	1%
< 0,063 (g)	0,5			
Sum (g)	85,5			
Total dry mass (g)	87,5			
Loss (g)	2,0			

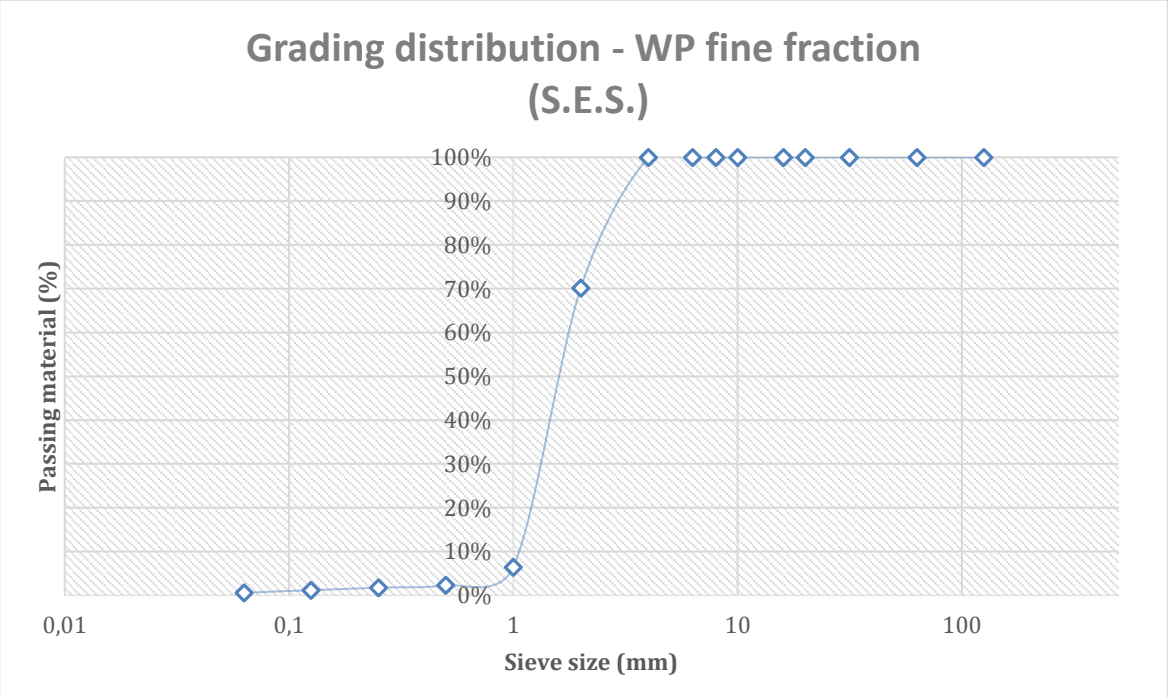

Figure 82 Grading size distribution of Wood and Plastic fine fractions (S.E.S.) according to UNI EN 933-1.

Table 52 Grading size distribution of Wood and Plastic fine fractions (N.E.S.) according to UNI EN 933-1.

WP | N.E.S.				
Aperture size [mm]	**Retained mass [g]**	**Retained percentage [%]**	**Cumulative passing [%]**	**Passing material [%]**
mm	g	%	%	%
125	0,0	0%	0%	100%
63	0,0	0%	0%	100%
31,5	0,0	0%	0%	100%
20	0,0	0%	0%	100%
16	0,0	0%	0%	100%
10	0,0	0%	0%	100%
8	0,0	0%	0%	100%
6,3	0,0	0%	0%	100%
4	5,5	5%	5%	95%
2	85	73%	77%	23%
1	24	21%	98%	2%
0,500	1,5	1%	99%	1%
0,250	0,5	0%	100%	0%
0,125	0,5	0%	100%	0%
0,063	0,0	0%	100%	0%
< 0,063 (g)	0,0			
Sum (g)	117,0			
Total dry mass (g)	121,5			
Loss (g)	4,5			

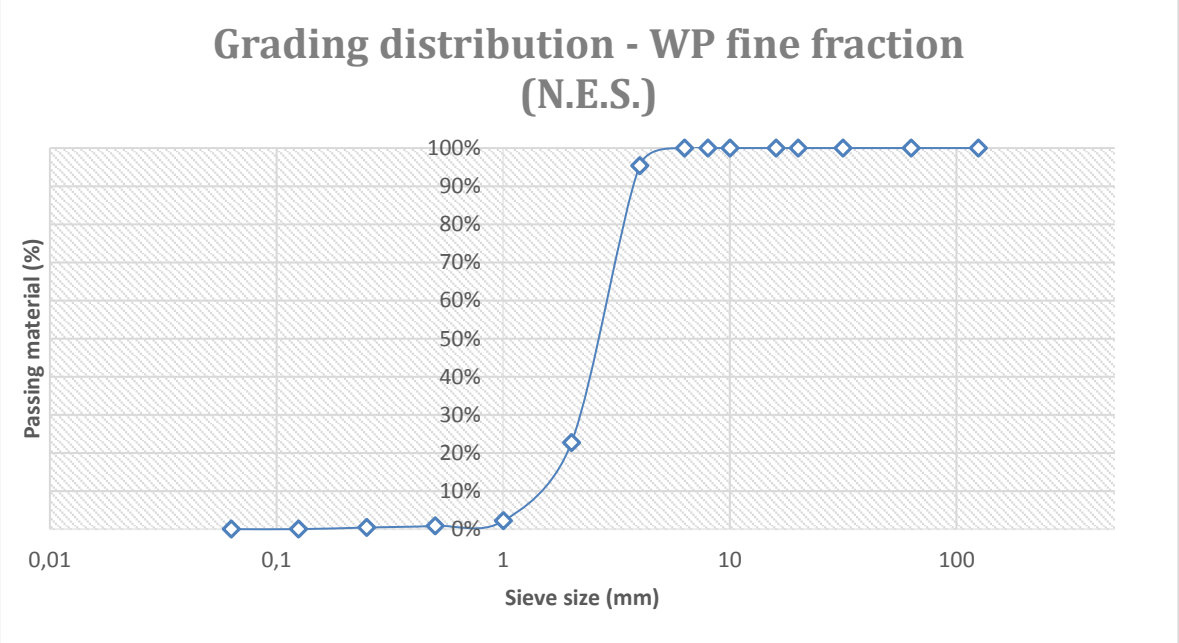

Figure 83 Grading size distribution of Wood and Plastic fine fractions (N.E.S.) according to UNI EN 933-1.

WP is only available in one size, directly supplied by CDE, with maximum diameter below 4 mm. This material represents a typical by-product of CDW treatment process, it consists of floating lightweight parts produced during washing steps required for materials cleanings. The potential of such material, which currently does not have any specific application, as fine fraction for LW mortars/concretes will be assessed.

The results from the sieving of S.E.S and N.E.S. **RP fine fractions** are presented in **Table 53** and **Figure 84**, and **Table 54** and **Figure 85** respectively. In both cases, the granules are below 6.3 mm, with most of the granules below 4 mm (82% and 97% for S.E.S. and N.E.S., respectively). Overall, the size distribution is slightly different when comparing the two materials, this is possibly due to the grinding process that cannot allow a precise size control.

Table 53 Grading size distribution of Rigid Plastic fine fractions (S.E.S.) according to UNI EN 933-1.

RP | S.E.S.				
Aperture size [mm]	**Retained mass [g]**	**Retained percentage [%]**	**Cumulative passing [%]**	**Passing material [%]**
mm	g	%	%	%
125	0	0%	0%	100%
63	0	0%	0%	100%
31,5	0	0%	0%	100%
20	0	0%	0%	100%
16	0	0%	0%	100%
10	0	0%	0%	100%
8	0	0%	0%	100%
6,3	0	0%	0%	100%
4	46	18%	18%	82%
2	166	67%	85%	15%
1	24	10%	95%	5%
0,500	7	3%	97%	3%
0,250	3,5	1%	99%	1%
0,125	1,5	1%	99%	1%
0,063	1	0%	100%	0%
< 0,063 (g)	0,5			
Sum (g)	249,5			
Total dry mass (g)	252,0			
Loss (g)	2.5			

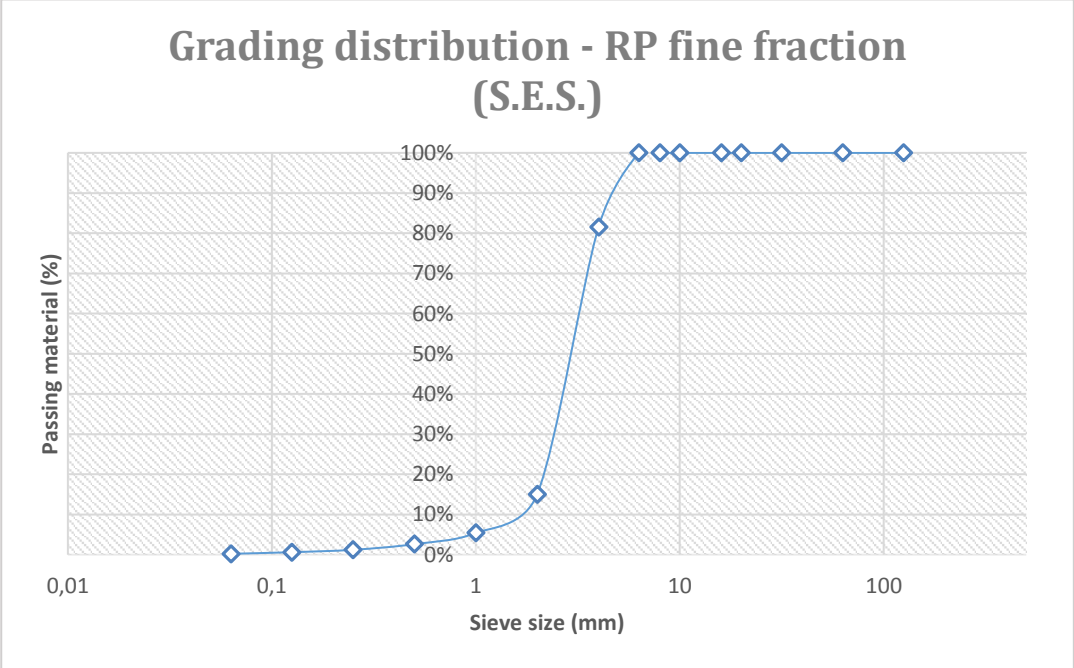

Figure 84 Grading size distribution of Rigid Plastic fine fractions (S.E.S) according to UNI EN 933-1.

Table 54 Grading size distribution of Rigid Plastic fine fractions (N.E.S.) according to UNI EN 933-1.

RP | N.E.S.				
Aperture size [mm]	**Retained mass [g]**	**Retained percentage [%]**	**Cumulative passing [%]**	**Passing material [%]**
mm	g	%	%	%
125	0,0	0%	0%	100%
63	0,0	0%	0%	100%
31,5	0,0	0%	0%	100%
20	0,0	0%	0%	100%
16	0,0	0%	0%	100%
10	0,0	0%	0%	100%
8	0,0	0%	0%	100%
6,3	0,0	0%	0%	100%
4	6,0	3%	3%	97%
2	97,5	49%	52%	48%
1	23,5	12%	64%	36%
0,500	23,0	12%	76%	24%
0,250	23,5	12%	87%	13%
0,125	19,0	10%	97%	3%
0,063	5,0	3%	99%	1%
< 0,063 (g)	1,0			
Sum (g)	198,5			
Total dry mass (g)	200,0			
Loss (g)	1,5			

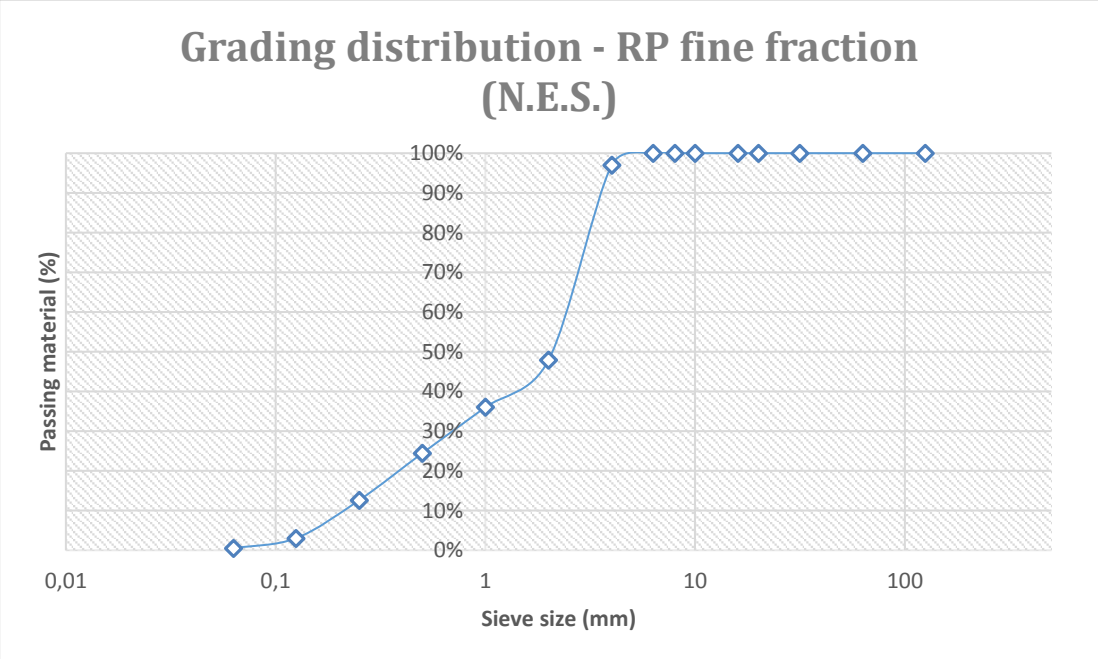

Figure 85 Grading size distribution of Rigid Plastic fine fractions (N.E.S.) according to UNI EN 933-1.

RP is provided by CDE in large scraps, which need a further mechanical treatment to allow the size reduction. The process consists in crushing and grinding operations, then the plastic scraps can be sieved in the desired size. Three different size classes can be considered (fine, medium and coarse fractions) depending on the intended application. The suitability of fine and medium fractions as aggregates for LW mortars/concretes will be assessed, while medium and coarse fractions can be considered for LW panels development.

In **Figure 86** and **Figure 87** size and length distribution of S.E.S. and N.E.S. **W fractions** are presented.

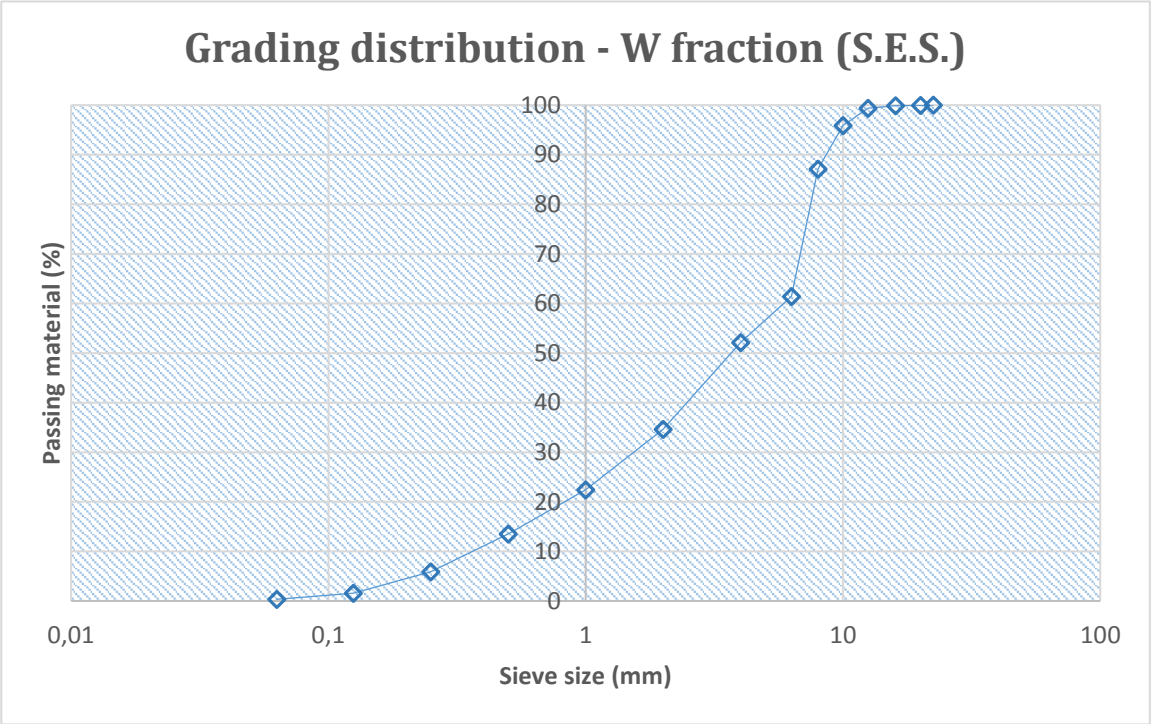

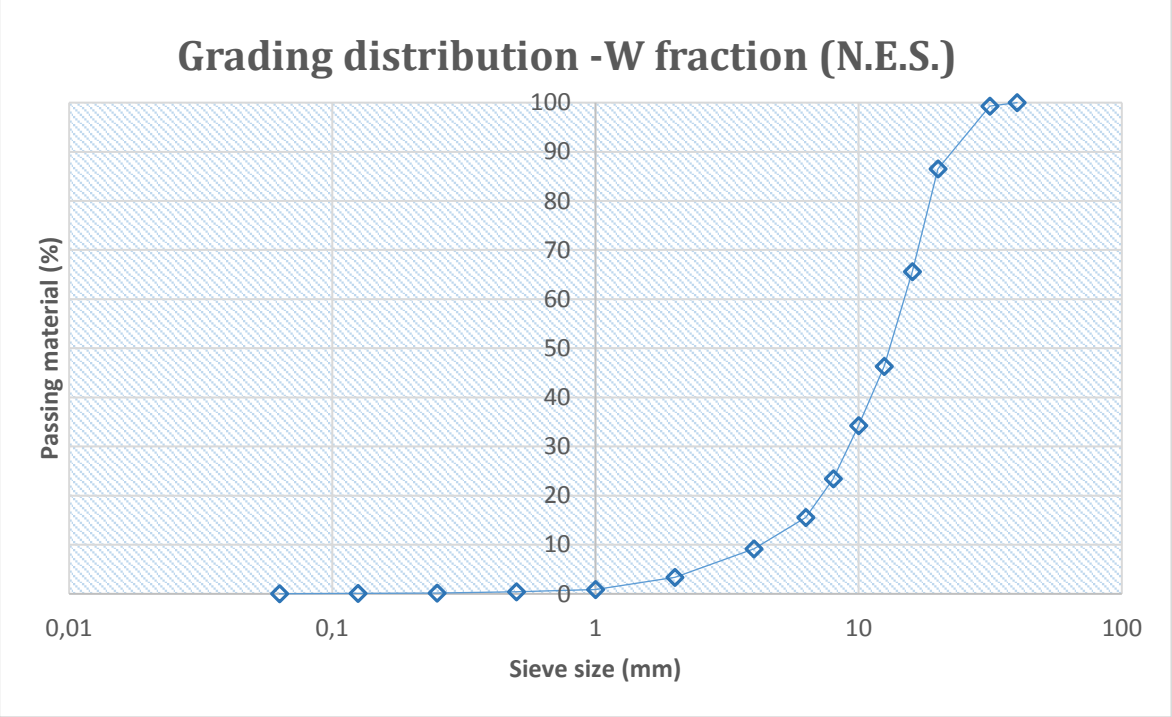

Figure 86 Grading size distribution of W (S.E.S. and N.E.S.) according to UNI EN 933-1.

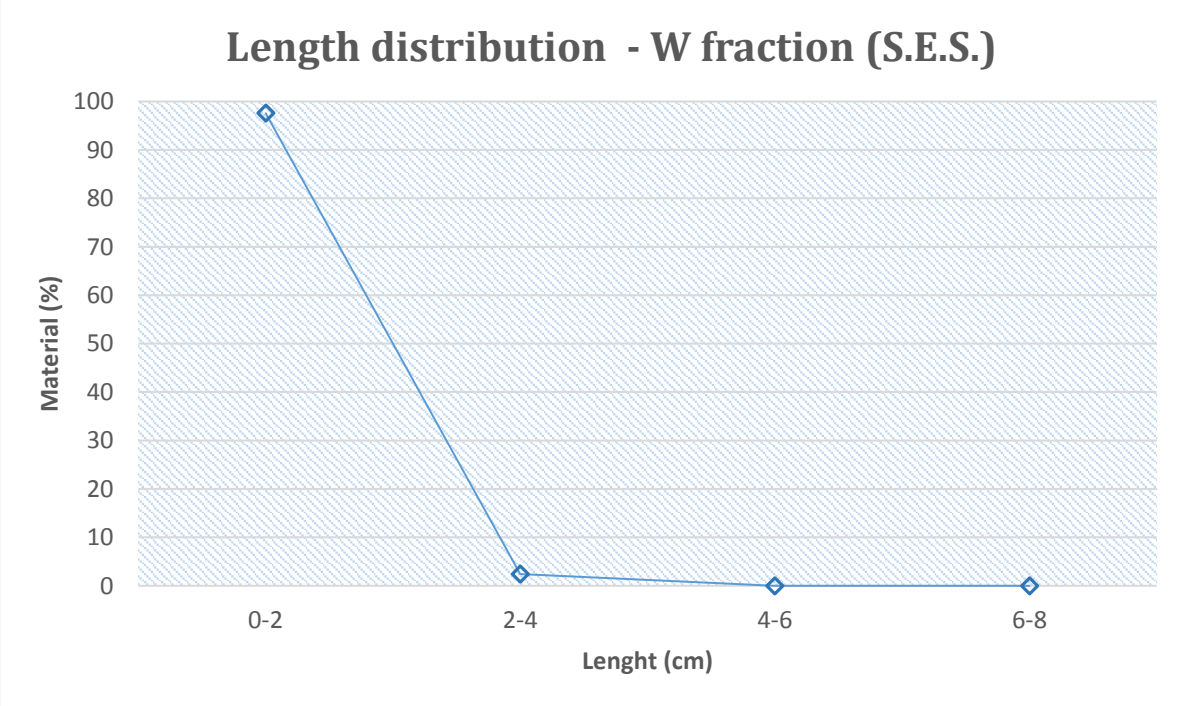

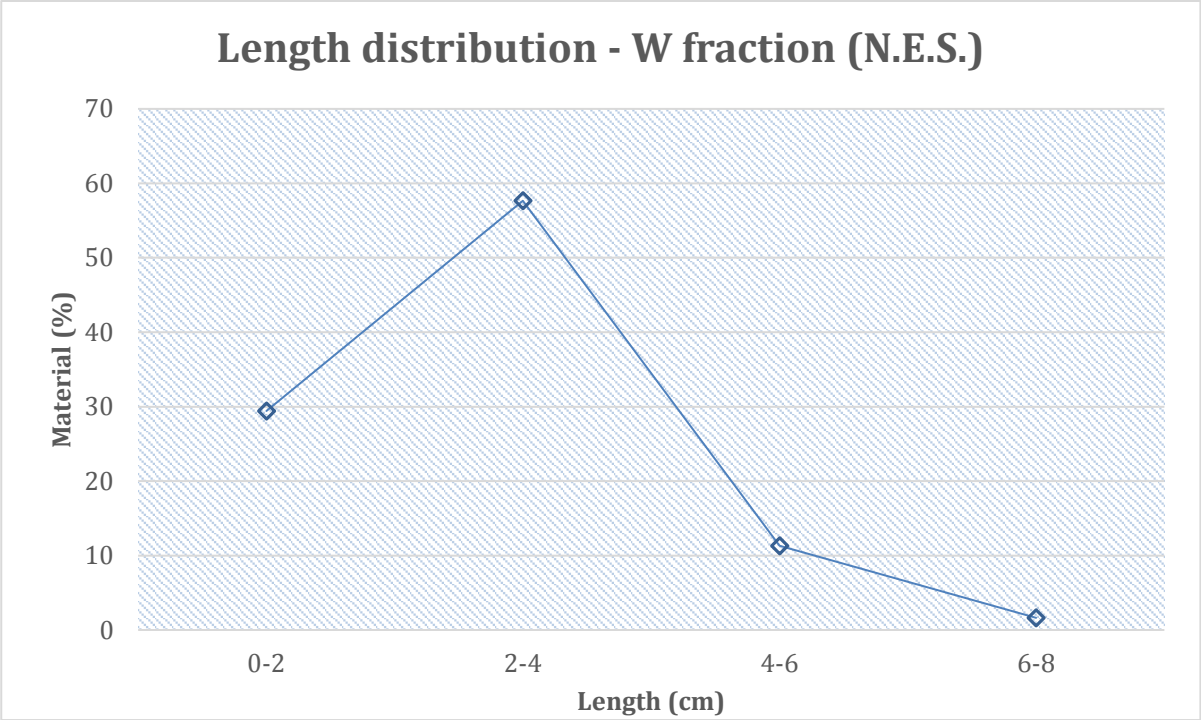

Figure 87 Length distribution of W fractions (S.E.S. and N.E.S.).

S.E.S. wood, grinded in CETMA, is for the 90 % smaller than 10 mm. The N.E.S. fraction is instead characterized by a higher fraction of particles bigger than 10 mm. Such result is confirmed also by the manual length sorting (**Figure 88**). The S.E.S. wood fraction, grinded in CETMA, is almost completely in the length range between 0 and 2 cm; while the N.E.S. fraction is in the range between 2 and 4 cm for 60% by weight.

Figure 88 Length distribution result of W, from S-EU and N-EU.

4.3.2 Density, Water Absorption and Moisture content

In **Table 55**, densities and water absorption measurements, for S.E.S. and N.E.S. source, are reported.

Table 55 Results of CDW lightweight fractions: density and water absorption.

Property	Unit	Southern Europe		Northern Europe	
		0/4 mm	4/10 mm	0/4 mm	4/10 mm
Mixed Wood and Plastic (WP) intended as LW aggregate for concretes					
Loose bulk density, ρ_b	kg/m³	165.76	/	209.39	/
Apparent density, ρ_a	kg/m³	571.43	/	398.41	/
Particle density on an oven dried basis, ρ_{rd}	kg/m³	354.53	/	231.48	/
Particle density on a saturated and surface-dried basis, ρ_{ssd}	kg/m³	734.10	/	650.46	/
Water absorption @24h, WA_{24h}	%	107.10	/	98.41	/
Mixed Rigid Plastic (RP) intended as LW aggregate for concretes and component material for LW panels					
Loose bulk density, ρ_b	kg/m³	487.42	n.a. [4]	440.15	391.48
Apparent density, ρ_a	kg/m³	1141.09	1080.31	1223.12	995.49
Particle density on an oven dried basis, ρ_{rd}	kg/m³	1054.92	1029.63	858.49	932.35
Particle density on a saturated and surface-dried basis, ρ_{ssd}	kg/m³	1130.43	1076.54	1156.60	995.77
Water absorption @ 24h, WA_{24h}	%	7.16	4.56	9.85	6.80

As expected, for both sources (S.E.S. and N.E.S.), WP resulted in lower density and higher water uptake if compared to RP. By way of example, WP 0-4 mm in saturated with dried surface condition[5] has an average density of approximately 692 kg/m³ against 1144 kg/m³ measured for RP 0-4 mm. Both materials, according to EN 206-1 and UNI EN 13055-1 (even if these standards are specific for mineral aggregates), have the physical requirements to be considered lightweight aggregates. Moreover, WP 0-4 mm resulted in higher water uptake after 24 hours (around 103% as average on both sources) if compared with RP 0-4 mm (around 9% as average on both sources). These different performances are clearly related to the different composition of the materials under investigation; WP is mainly based on wood and expanded polystyrene having high tendency to absorb water, on the other hand, RP mainly includes hydrophobic materials that reduce the overall water uptake.

However, it should be observed that the standards followed for WP and RP testing are set for conventional materials and might be not properly suitable for recycled materials, with heterogeneous composition, such as RE[4] LW fractions. In addition, such tests are mainly based on manual operations (e.g. air removal, operations to make the aggregate saturated with the dried surface) and, therefore, dependent on the operator. The heterogeneous nature of the materials under investigation may also results in a certain variability of the measured properties However, based on previous experiences on recycled LW materials, a

[4] RP 4-10 mm fraction was not enough for testing (5 l for aggregates < 16 mm according to UNI EN 1097-3).
[5] Density evaluated in this condition (ρ_{ssd}) is the reference density to use for the mix design of concretes.

general approach to follow consists in the direct check of specific properties required for the design of mortars/concretes (e.g. ρ_{ssd}, WA_{24h}) when these materials will be produced.

Figure 89 Equipment used for testing Wood and Plastic and Rigid Plastic materials.

In **Table 56**, densities and moisture content measurements on W fractions, for S-EU and N-EU source, are reported.

Table 56 Results of CDW lightweight W fractions: density and moisture content.

Property	Unit	Southern Europe	Northern Europe
Wood (W)			
Density, ρ_u	kg/m³	243.07	145.79
Anhydrous material density, ρ_a	Kg/m³	139.28	140.89
Moisture content, u	%	61.23	8.84

The evaluation of density for the W fraction is extremely dependent from the way of filling the volume to be measured. For this reason, the operator carried out the measurement using always the same procedure: filling a 1 l volume container; hit gently five times the container on the desk; refill the container untill the 1 l volume; hit gently five times the container on the desk; adjust the quantity till the volume of 1 l. In the table are reported the calculated average values of density and moisture content on five different samples for each source. Density values are referred to the calculated moisture content. The high difference in terms of density

is dependent on the difference in moisture content of the two W fractions, as confirmed from the density of anhydrous materials.

4.3.3 Considerations on variability of physical properties of LW fractions

With regard to the variability of physical properties of different LW materials batches, based on the scraps of WP, RP and W received and tested, it can be reasonable assumed that the typical quality and average composition of the materials under investigation are at least comparable, regardless of the source (S-EU or N-EU). Of course, there is an intrinsic heterogeneity of each LW material (wood/plastic relative percentage in WP fractions, different typologies of plastics included in RP fractions, different nature of W fractions) which may induce a certain variability of the measured properties.

4.4 Timber materials

The results from the procurement and characterization of CDW timber are summarized and commented below.

4.4.1 In situ strength assessment

Most methods for in situ strength assessment have initially been developed for tree examination. All procedures are combined with high utilisation of technology and interpretation by the examiner. As wood is an inhomogeneous material, the results can differ significantly according to the surveyed areas. All non- or semi- destructive in situ test methods aim to determine certain physical characteristics as bending strength, density and modulus of elasticity, which correlate with the strength of the surveyed element. To make a statement on the strength of tested timber elements, the results need to be interpreted by an experienced person. In situ strength assessment can be an effective method within the scope of assessing historical buildings or to detect local defects in timber elements. Due to the absence of standards, the high costs, and the poor reproducibility, in situ strength grading is not applicable for the intended purpose of grading timber for reuse in bigger scale.

4.4.2 Visual on-site inspection

Visual inspection (**Figure 90**) helps to maximize the reuse of timber. By estimating the quantities of reusable timber, demolition strategies and recommendations for on-site separation can be made. The inspection needs to be performed by an experienced person with special knowledge on timber construction, wood species and possible defects.

Figure 90 On-site Inspection of a roof structure.

The following steps have to be taken during a visual inspection:

- Identification of wood species
- Wood moisture content
- Cross sections and estimated amount of timber
- Areas with decay due to wood destroying fungi
- Areas with decay due to wood destroying insects
- Indications of chemical contamination
- Impurities as paint, coatings, glue.

4.4.3 Assessment on chemical contamination

Chemical contamination is the most decisive sorting criteria for post-consumer wood. To receive secure raw material for further processing, sampling and analyses on chemical contamination needs to be made, unless other information can prove that no harmful contamination exists.

Sampling needs to be carried out in compliance with the requirements of the laboratory performing the analysis. Amount of samples and areas tested; need to be chosen according to possible findings of the visual inspections. Usually composite samples are taken to determine possible contamination in certain areas of the building e.g. roof and floor beams.

The development of new techniques to determine contamination in waste wood materials has big potential to help increasing the cascade use of wood. Detection techniques can be distinguished in stationary and in situ techniques [76].

Stationary processes:

- Near Infrared Spectroscopy (NIR), Fourier-Transform-Infrared-Spectroscopy (FTIR) and optical methods to detect impurities as paint, plastics or glue.
- Ion Mobility Spectrometry (IMS). Method to detect chemical contamination by liberation of gases.
- X-Ray Fluorescence Analysis (XRF). The wavelengths of X-rays emitted upon excitation by primary beam, are characteristic of specific elements and can be used to interpret and detect chemical contamination. For a brief description of XRF, please refer to Total/bulk chemistry of the material – using XRF.

In situ assessment

A promising development for in situ assessment is a handhold device that works with X-Ray Fluorescence Analysis (XRF) to determine chemical contamination [76]. In situ devices that fulfil all needs for assessing timber are not market ready yet. Future development in this area will enhance the reuse of timber from demolition sites.

Limits of contamination

No EU wide directives for waste wood classifications exist. Some countries have directives on waste wood that define limits on chemical contamination. The limit values are not consistent as shown in the following **Table 57**.

Table 57 Limits of chemicals in recycled wood used for wood based panels.

			Germany	United Kingdom	Italy	Belgium (Flanders)	Austria
	max. concentration in untreated wood	**European Panel Federation** (not obligatory)	**Altholzverordnung** (waste wood directive)	**PAS 111:2012** specification for the requirements and test methods for processing waste wood	**Standard per la certificazione dei prodotti realizzati con materiali da riciclo** (Standard for the certification of products made from recycled materials)	**VLAREM II** Vlaams Reglement betreffende de Milieuvergunning	**Recyclingholzverordnung** (recyclingwood directive)
Elements/ Compounds		**upper limits mg/kg recycled wood**					**80% percentile**
Arsenic (As)	< 1,0	25	2	25	2	2	1,8
Cadmium (Cd)	< 0,8	50	2	50	2	x	1,2
Chromium (Cr)	< 5,0	25	30	25	25	30	15
Copper (Cu)	< 10,0	40	20	40	20	20	x
Lead (Pb)	< 10	90	30	90	30	90	15
Mercury (Hg)	< 0,2	25	0,4	25	0,4	x	0,075
Fluorine (F)	< 100	100	100	100	100	30	20
Chlorine (Cl)	< 100	1000	600	1000	600	600	300
Pentachlorphenol (PCP)		5	3	5	3	3	3
chlorinated diphenyls (PCB)		x	5	x	x	x	x
Creosote (Benzoapyrene)		0,5	x	0,5	0,5	0,5	x

Sources: Column 1 [77], Column 2 [78], Column 3 [79], Column 4 [80], Column 7 [81]

The extreme variation of limit values shows, that EU wide standardization of waste wood directives, could help to break down constraints in the wood processing industry.

4.4.4 On-site separation

To increase the quality in waste wood streams, on site separation is an effective tool. The on site assessment should result in recommendations for sorting categories for all parts of the building. Sorting criteria have been developed by the following national directives:

- Germany, AltholzV
- Austria, RecyclingholzV
- Belgium Flemish Regulation on Waste Prevention and Management
- Netherlands The National Waste Plan (LAP)
- United Kingdom BSI PAS 111 Specifications for the requirements and test methods for processing waste wood.

The categories range from grade A to D respectively I to IV
Grade A or I is natural wood, only mechanically processed.
Grade D or IV is hazardous waste, contaminated with preservatives that require licensed disposal.

Grade B or II wood has the targeted quality to be recycled or reprocessed in cascade use. Some directives, as the German waste wood directive [79] include quality assumptions according to the origin of the material. Following the directive, structural timber, recovered from dismantled buildings is supposed to be categorised in category IV (hazardous waste). The directive gives the opportunity to not follow the presumptions, if tests have been made to verify the grade of impurities. The on-site assessment including tests on wood preservatives could be a way to upgrade the classification of wood from demolition sites.

Beside the categorisation due to possible or actual contamination with wood preservatives, chemicals or other coatings, sorting can take the possible future reprocessing steps into account, see **Table 58**.

Table 58 Possible sorting categories according to future reprocessing steps.

Intended reprocessing	raw material	solid timber	panel board resource	thermal use	complete reuse	hazardous waste
Associated waste wood categories	A (I)	B (II)	A/B (I/II)	C (III)	A (I) - C (III)	D (IV)
Impurities	Minor inpurities: Metal fixings, Minor amounts of paint	Coating Paint Glue No organic halogen compounds No wood preservatives Testing might be necessary to determine amount of chemical contamination	Coating Paint Glue No organic halogen compounds No wood preservatives Testing might be necessary to determine level of chemical contamination	Coating Paint Glue Organic halogen compounds No wood preservatives Testing might be necessary to exclude wood preservatives	Coating Paint Glue Testing might be necessary according to the intended reuse	Coating Paint Glue Organic halogen compounds Wood preservatives no Pentachlorphenol (PCP)
Possible building components	Packaging Untreated interior elements	Rafters Ceiling beams Glue laminated beams Cross laminated elements Columns Studs	Battens Flooring Wood based panels cladding Doors Windows	All kind of timber elements	Windows Doors Flooring Timber frame elements Glue laminated elements	All kind of timber elements, with focus on roof construction and exterior application
Cross sections	no requirements	Practical for structual timber: min. 6x10cm Practical for lamellaes for glue laminated timber: min. 3x6cm	no requirements	nor requirements	according to intended reuse	no requirements

The share of timber constructions in the European building sector is increasing and chemical contamination of timber elements is decreasing due to new standards and public awareness. The increased demand of timber, and less contaminated elements in today's buildings, may possibly increase the complete reuse of elements like prefabricated facade or timber frame elements, ceiling elements and cross laminated timber elements in the future.

Looking at the future, it is possible that contamination as the most decisive parameter of today for sorting and reusing timber, will be replaced by simplicity of easy disassembly and size of the elements. Therefore today's planning process of new timber structures needs to take the possibly disassembly and reuse into account.

4.4.5 Reprocessing and strength grading

Especially the presence of metal impurities is a challenge for the processing procedure. Screws nails and other metal parts need to be detected and removed carefully, to avoid damage to woodworking machines. Technical solutions for detecting metal impurities range from handhold devices to industrial tunnel metal detectors used in sawmills.

Reprocessing can be distinguished into different categories according to the final use:

- complete reuse of elements, columns, beams with minimal processing
- reprocessing into standardized cross sections of solid timber
- reprocessing into lamellas for the production of glue laminated timber

To integrate salvaged timber into existing material streams, strength grading is necessary. Since the 1950´s, different research projects and studies addressed the strength assessment of aged timber. A summary of results by different investigations is given in [82]. Investigating aged timber, different factors have to be taken into account. The state of conservation, dismantling damages, and previous load condition can have an influence on the load capacity of the timber. In conclusion, the review [82] states the following results see **Table 59**.

In summary, it can be stated that the influence of aging can be neglected if the state of conservation and other impurities are surveyed carefully.

To apply grading rules according to [49] and national grading standards, salvaged timber needs to be cleaned and cut or planed into its final cross section. The use of standardized cross sections can be helpful to avoid storage costs and increase the market acceptance for salvaged timber.
Further processing into lamellas for glued laminated timber gives the advantage that defects can be cut out and shorter pieces can be finger jointed into an endless lamella that will be cut into the length needed, see **Figure 91**.

Table 59 Mechanical properties of aged timber – summary of comparative study.

Mechanical properties	Database	Conclusion	Difficulties
Modulus of elasticity	largely investigated	remains unchanged	affected by state of conservation, load history and damages
Modulus of rupture	largely investigated	remains unchanged	affected by state of conservation, load history and damages
Tensile and compressive strength	fewer studies, results differ	assumed to remain unchanged, no clear results	affected by density
Shear strength	few studies, different results	assumed to remain unchanged, no clear results	results affected by bolt holes, splits and cracks
Impact bending strength	most studies that tested impact bending strength have same results	affected by aging	different testing methods

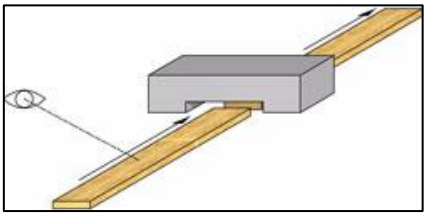

Strength grading

The planed dried boards are strength-graded either visually or mechanically.

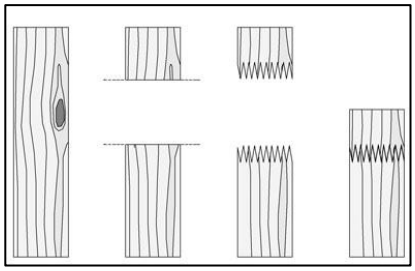

Cutting off knots and other wood defects

Board sections with wood-defects having significant influence on the strength or the outward appearance such as knots, resin- or bark-pockets and are cut out off the boards dependent on the strength class and the surface-class.

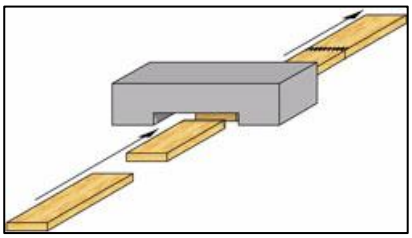

Gluing endless lamella
The boards are jointed together lengthwise to a theoretically infinite lamella using finger joints.

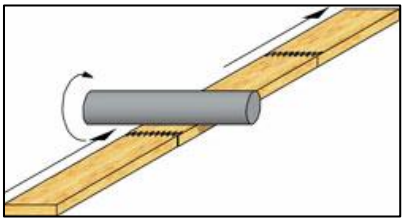

Planning finger jointed lamella
After the glue within the finger joints has hardened, the lamellas are planned to a thicknesses of up to 45mm.

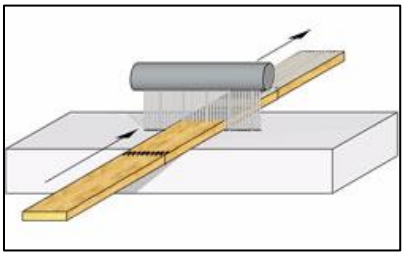

Applying the glue
The glue is applied on the broader edge of the lamella.

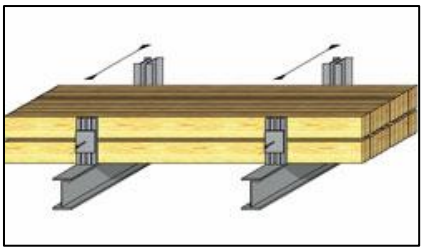

Size press
At least three lamellas are stacked and pressed in an either straight or curved press.

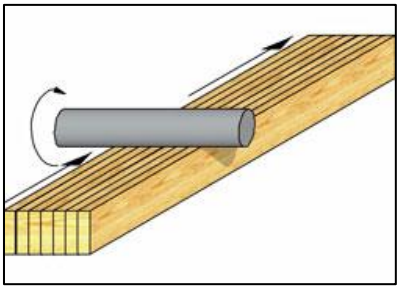

Planer
After the glue lines are hardened the raw glulam is usually planed and chamfered.

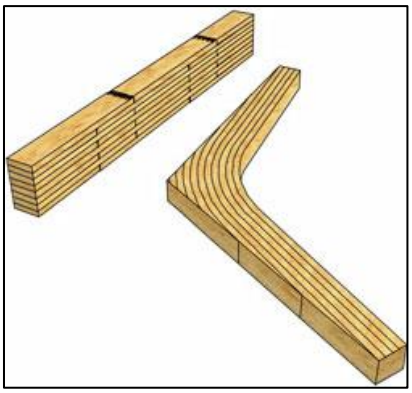

Factory assembly and further detailing

In most cases, the glulam members are cut to their final size and joints are fixed in the plant. If necessary, the members are given temporary coating against the influence of direct weathering during construction and the members are wrapped with packing material.

Figure 91 Production process of glue laminated timber. © Glued Laminated Timber Research Association [83].

The harmonized standard [49] defines the outline for national grading rules, which define sorting classes that can be associated with strength classes listed in [84] (C-classes for softwood and D-classes for hardwood). Uniform strength classes help to simplify the timber market and are commonly used performing structural calculations for timber structures.
The categories used in sorting norms are based on strength, stiffness and density. Depending on the used grading rules and way of grading, different approaches exist to evaluate the required parameters.

Visual strength grading is a widely used method and has a long historic Background. Visual grading rules are defined by national standards but have to follow the harmonized standard EN 14081-1, which defines basic principles. The basic parameters that need to be addressed in national grading rules according to Annex A [47], are:

- Limitations for strength-reducing characteristics:
  - Knots
  - Slope of grain
  - Density and rate of growth
  - Fissures
- Limitations for geometrical characteristics:
  - Wane
  - Warp
- Limitations for biological characteristics:
  - Fungal and insect damage
  - Soft rot
  - Insect attack
- Other characteristics:
  - Reaction wood

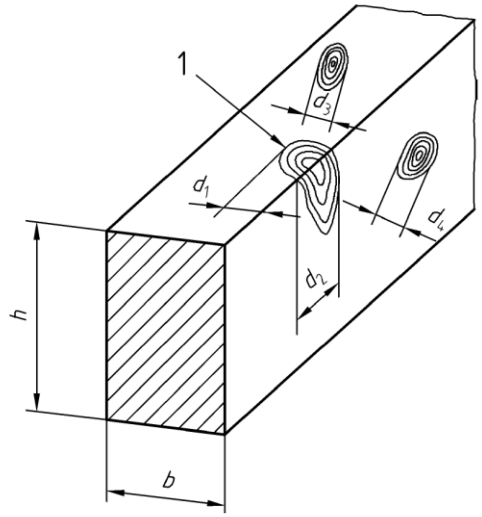

$$A = \max.\left(\frac{d_1}{b};\frac{d_2}{h};\frac{d_3}{b};\frac{d_4}{h}\right) \qquad (1)$$

Figure 92 Example from national grading rule DIN 4074: Measurement of knots and knot content in square shaped timber.

Today, visual strength grading can be assisted by machines, which can lead to a better yield in higher strength classes.

Beside visual strength grading, machine strength grading is a more and more powerful tool used to determine the strength of timber. Traditionally grading machines work by bending the timber and assessing the stiffness. Today machine grading also includes technologies as flexural resonant frequency, x-ray measurements and ultrasonic wave speed.
Additional criteria for grading lamellas for glued laminated timber are defined in [49].

Example of reprocessing

Following the described procedure for reprocessing used timber, exemplary reprocessing, has been performed to test feasibility, see **Figure 93**

On-site inspection: the roof structure inspected was partly rebuilt after fire damage. Beams from different building periods have been chosen for exemplary reprocessing. The chosen rafters are marked red. Prior dismantling, the structure was tested negative for chemical contamination.

Timber beams ready for reprocessing, cleaned of nails and cut in half for logistic reasons. Amount 0,08m³ salvaged timber.

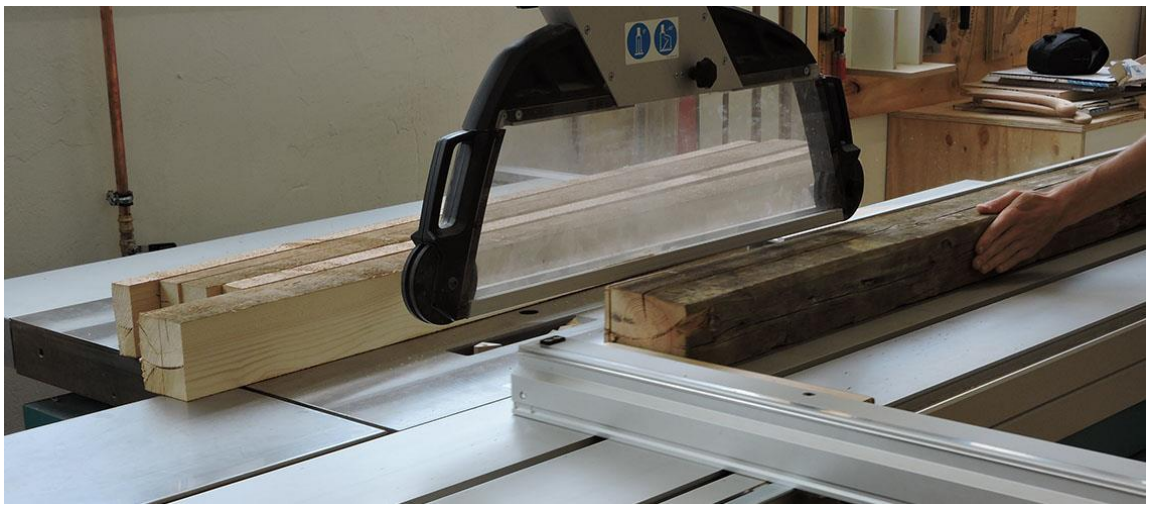

Small scale reprocessing.

Cut and planed lamellas ready for strength grading. The marked areas need to be cut out, due to impurities.

Reprocessed lamellas, one lamella has been rejected due to cracks, some impurities have been cut out.

0.05m³ finished lamellas for glue laminated timber.
Approximately amount referring to raw material:

- 60% finished Lamellas
- 30% solid cut offs
- 10% saw dusk and wood chips

Professionalizing the procedure can reveal opportunities to increase the yield of finished lamellas.

Figure 93 Exemplary reprocessing of salvaged timbers.

5. CONCLUSION AND RECOMMENDATIONS

This report focuses on geometrical, chemical and physical characterization of different sorted CDW fractions, delivered by CDE from recycling centres in Southern and Northern Europe and summarizes the properties of mineral fraction, fine fraction, LW fraction and timber fraction. The main results obtained together with recommendations are listed below, split into each fraction typology.

Mineral fraction – chemical and mineralogical properties

- The constituent composition of N.E.S. and S.E.S. coarse (8/16 mm) fractions complies with the limits set by [2] and [13], for use in structural concrete.
- All tested sorted and improved sorted mineral fractions contain very low levels of water soluble chlorides, perhaps as a result of the wet process of sorting CDW in recycling plants which use equipment developed by CDE). Consequently, they comply with the requirements set by [2] for use in structural concrete.
- All tested sorted and improved sorted mineral fractions, with the exception of S.E.S. (0/2 mm), contain low levels of water soluble sulphates. Consequently, they comply with the requirements set by [3] for use in structural concrete.
- All tested sorted and improved sorted mineral fractions contain very low levels of organic matter (humus and fulvo acid). Consequently, they comply with the requirements set by [2] and [13] for use in structural concrete.
- Any water soluble components present in sorted mineral fractions do not affect the setting time of cement pastes.
- Petrography, XRD, TGA and XRF results indicate that all mineral fractions are rich in $CaCO_3$ and hence may be more susceptible to the disruptive action of repeated freeze-thaw cycles.
- As expected, all tested coarse (8/16 mm) mineral fractions are more susceptible to freeze-thaw damage compared to controlled samples (N. Ireland virgin basalt). However, S.E.S. and S.E.I.S. suffer much higher mass loss compared to N.E.S. and N.E.I.S. samples.
- Drying shrinkage of concrete prisms with N.E.S., N.E.I.S., S.E.S. or S.E.I.S. is similar to control samples with virgin aggregate and complies with the requirements set by [13].
- All tested fine mineral fractions (N.E.S., N.E.I.S., S.E.S. and S.E.I.S.) show no signs of alkali-aggregate reaction based on [33] test method.
- The particle size distribution of all fractions were fully satisfying, with the exception of the N.E.S. 8/16 fraction that contained little too much particles < 8 mm (23 %).
- The Flakiness index for all tested fractions was well below the limit of FI_{50}.
- There are no limits when it comes to Flow coefficient of the two sands. However, the results showed that the S.E.S. sand has lower flow coefficient compared with the N.E.S. sand, and thus probably will give a little better concrete rheology (by that not saying that the N.E.S. sand will not give a good concrete rheology).
- When it comes to resistance to fragmentation, both tested 8/16 fractions (N.E.S. and S.E.S.) passed the LA ≤ 50 requirement.

- Water saturation and density tests were performed on all the different size-fractions from both CDW sources: N.E.S. and S.E.S. Different temperatures were used for drying, several laboratories performed the tests, and a special long-time saturation test was adopted. The results of the different laboratories differed somewhat, but was mostly within the same rough figures. Some major deviations were identified, e.g. for the 0/2 fraction from N.E.S. The reason for this deviation will be investigated in the further work. When it comes to long-time saturation, the N.E.S. material reached the WA_{24} already after 1 h and did not absorb much more even after 14 days. For the S.E.S. material, the WA_{24} was reached after just 1 h, but the material continued to soak water and increased its WA up to 7 days.
- The above results confirm that all mineral fractions with the exception of S.E.S. 0/2 mm (due to relatively high water soluble sulphate content) can be used in the production of new OPC or geopolymer concrete.

Fine fraction – physical and chemical properties

- The fine material was characterised as silt with high plasticity.
- TGA results suggest presence of organic material, which increase both the liquid and plastic limits, but typically reduce the plasticity index. The high organic content was gleaned when determining the presence of humus.
- XRD results show that uncalcined fine material contained predominantly quartz (32%), calcite (13%) and gypsum (18%). The remaining phases included illite, muscovite, feldspar, kaolinite, smectite plus any XRD amorphous phases present. XRD results of the calcined fine material showed that calcite had decomposed and that gypsum had converted to anhydrite. In addition, the absence of kaolinite and smectite peaks suggests their dehydroxilation.
- Isothermal calorimetry results indicate that uncalcined fine material was of low reactivity (hydration reaction leading to setting) when mixed either with water or water plus hydroxide activating solutions. When calcined, however, the fine material was far more reactive and exhibited setting behaviour.
- FTIR of the uncalcined fine material showed the presence of clay materials, with the vibration of OH and Si-O-Si(Al), and carbonates. Upon calcination, all clays had shown dehydroxylation with the exception of illite. Carbonate bands were still present, which were not detected by XRD.
- The fine material contained no or little fulvo acid.
- Low water soluble alkali contents were measured.
- The fine material was rich in SO_3 (7.9% by XRF), in the form of gypsum. As such, compared to the mineral fraction, much more had leached during water solubility tests – depending on approach adopted, the fine material contained 0.274 wt% and 3.126 wt% soluble SO_3.
- The silt and clay fraction contained 0.192 wt% soluble chloride. This is significantly higher than what was observed for the mineral fraction. EN 206 does not specify a chloride content limit for geopolymer based concretes and as such, it is unclear if this will cause increased corrosion of any imbedded steel, if this material is to be used as a precursor for geopolymer concrete.

- If to be used as a precursor for geopolymer concrete, either on its own or blended with PFA/GGBS, further testing is required to assess strength gain and the effect of higher chloride and sulphate contents.

LW fraction – physical properties

- Based on physical characterizations performed on mixed wood and plastic scraps (by-products of the CDW processing plant without a specific application), it can be concluded that this has the potential to be used as received as LW aggregate for concrete.
- Mixed plastic and wood fractions (separated before the mineral CDW fractions processing) required a further mechanical process for size reduction in order to comply with the characterization protocols. Based on physical characterizations performed on mixed plastic and wood scraps, it can be concluded that these have the potential to be used as LW aggregate for concrete and/or insulating panels.
- For all the LW materials investigated it can be reasonable assumed that the typical quality and average composition are comparable, regardless of the source (S-EU or N-EU). Of course, there is an intrinsic heterogeneity of each LW material (wood/plastic relative percentage in WP fractions, different typologies of plastics included in RP fractions, different nature of W fractions) which may induce a certain variability of the technical properties.

Timber fraction – physical properties

- Timber elements from dismantled buildings can be reused as structural components. Possible defects, decay and contamination have to be assessed carefully to receive a safe building material.
- In situ testing methods to assess chemical contamination of timber structures prior to dismantling would help to separate material streams at an early stage and result in a higher reuse fraction of timber from CDW.
- The standardization of limit values of contamination could help to break down constraints in the reuse of timber elements.
- The investigated reprocessing of salvaged timbers into lamellas for glued laminated timber is a good opportunity to cut out impurities and defects. The technical opportunity to create endless lamellas increases the amount of timber being reused. By reprocessing, the strength class of the end product can be upgraded compared to the entry material.

REFERENCES

[1] *EN 1097-2:2010. Tests for mechanical and physical properties of aggregates - Part 2: Methods for the determination of resistance to fragmentation. 2010.*

[2] *EN 206-1:2013+A1:2016. Concrete. Specification, performance, production and conformity. British Standards Institution, London, UK, 2016.*

[3] *EN 12620:2002+A1:2008. Aggregates for concrete. British Standards Institution, London, UK, 2008.*

[4] *EN 932-2:1999. Tests for general properties of aggregates. Methods for reducing laboratory samples. 1999.*

[5] *DIN 4266-100:2002. Aggregates for concrete and mortar. Recycled aggregates. Deutsches Institute Fur Normung, 2002.*

[6] *DAfStb Guideline: Concrete with recycled aggregates. German Committee for Reinforced Concrete (DAfStb), 1998.*

[7] *LNEC E471. Guide for the use of recycled coarse aggregates in hydraulic binders. National Laboratory for Civil Engineering, Lisbon, Portugal, 2006.*

[8] *CUR Report 5. Masonry rubble granulates as aggregate material for concrete. Centre for Civil Engineering Research and Codes (CUR), Gouda, Netherlands, 1994.*

[9] *ARMASUISSE Instruction technique (tV) 70085. Utilisation de materiaux de construction mineraux secondaires dans la construction d'abris. ARMASUISSE, Berne, Switzerland, 2006.*

[10] *COPRO PTV 406. Granulats de debris de demolition et de construction recycles. Impartial Certification Body in the Construction Sector (COPRO), Brussels, Belgium, 2012.*

[11] *EHE-08. Code on structural concrete. Comisión Permanente del Hormigón (CPH), Madrid, Spain, 2008.*

[12] *RILEM TC 121-DRG. Specifications for concrete with recycled aggregates. Materials and Structures (1994) 27:173.*

[13] *BS 8500-2:2015+A1:2016. Concrete. Complementary British Standard to BS EN 206. Specification for constituent materials and concrete. British Standards Institution, London, UK, 2016.*

[14] *RE4 project 2016. D2.1 - CDW specifications and material requirements for prefabricated structures,* 2016.

[15] *EN 932-3:1997. Tests for general properties of aggregates. Procedure and terminology for simplified petrographic description. British Standards Institution, London, UK, 1997.*

[16] *EN 933-11:2009. Tests for geometrical properties of aggregates. Classification test for the constituents of coarse recycled aggregate. British Standards Institution, London, UK, 2009.*

[17] *C.L. Page and K.W.J. Treadaway. Aspects of the electrochemistry of steel in concrete. Nature 297 (1982) 109-115.*

[18] *EN 1744-1:2009+A1:2012. Tests for chemical properties of aggregates. Chemical analysis. British Standards Institution, London, UK, 2012.*

[19] *A.M. Neville, Properties of Concrete, 5th ed., Pearson Education Limited, Harlow, Essex, UK, 2011.*

[20] *N.J. Crammond. The thaumasite form of sulfate attack in the UK. Cement and Concrete Composites 25 (2003) 809-818.*

[21] *F. Bektas, K. Wang and J. Ren. Carbon aggregate in concrete (Report No MN/RC 2015-14). Minnesota Department of Transportation, St Paul Minnesota, USA, 2015.*

[22] *https://serc.carleton.edu/research_education/geochemsheets/techniques/XRD.html.*

[23] *P.C. Hewlett, Lea's Chemistry of cement and concrete, fourth ed., Elsevier Ltd, 2003.*

[24] *L. Forsen, The chemistry of retarders and accelerators, in: Proceedings, Symposium on the chemistry of cements, Stockholm 1938, pp. 298-394.*

[25] *K.E. Claire and P.T. Sherwood, The effect of organic matter on the setting of soil-cement mixtures. Journal of Applied Chemistry, 4 (1954) 625-630.*

[26] *EN 1744-6:2006. Tests for chemical properties of aggregates. Determination of the influence of recycled aggregate extract on the initial setting time of cement, British Standards Institution, London, UK, 2006.*

[27] *EN 196-3:2016. Methods of testing cement. Determination of setting times and soundness, British Standards Institution, London, UK, 2016.*

[28] *https://www.thermofisher.com/uk/en/home/industrial/spectroscopy-elemental-isotope-analysis/spectroscopy-elemental-isotope-analysis-learning-center/elemental-analysis-information/xrf-technology.html.*

[29] *EN 1367-1:2007. Tests for thermal and weathering properties of aggregates. Determination of resistance to freezing and thawing, British Standards Institution, London, UK, 2007.*

[30] *EN 1367-2:2009. Tests for thermal and weathering properties of aggregates. Magnesium sulfate test, British Standards Institution, London, UK, 2009.*

[31] *R.V. Silva, J. de Brito and R.K. Dhir. Prediction of the shrinkage behaviour of recycled aggregate concrete: A review. Construction and Building Materials 77 (2015) 327-339.*

[32] *EN 1367-4:2008. Tests for thermal and weathering properties of aggregates. Determination of drying shrinkage. British Standards Institution, London, UK, 2008.*

[33] *RILEM TC 106-2: Detection of potential alkali-reactivity of aggregates-The ultra-accelerated mortar-bar test. Materials and Structures (2000) 33 pp 283-293.*

[34] *ASTM C227-10. Standard test method for potential alkali reactivity of cement-aggregate combinations (mortar-bar method). Americal Society for Testing and Materials, West Conshohocken, PA, USA, 2010.*

[35] *EN 933-1:2012. Tests for geometrical properties of aggregates - Part 1: Determination of particle size distribution - Sieving method,* 2012.

[36] *EN 933-3:2012. Tests for geometrical properties of aggregates - Part 3: Determination of particle shape - Flakiness index. 2012.*

[37] *EN 933-6:2014. Tests for geometrical properties of aggregates - Part 6: Assessment of surface characteristics - Flow coefficient of aggregates. 2014.*

[38] *EN 1097-1:2011. Tests for mechanical and physical properties of aggregates - Part 1: Determination of the resistance to wear (micro-Deval). 2011.*

[39] *EN 1097-6:2013. Tests for mechanical and physical properties of aggregates - Part 6: Determination of particle density and water absorption. 2013.*

[40] *C. Lampris, R. Lupo and C.R. Cheeseman. Geopolymerisation of silt generated from construction and demolition waste washing plants. Waste Management 29 (2009) 368-373.*

[41] *S. Laouti, S. Baklouti and B. Samet. Acid based geopolymerization kinetics: Effect of clay particle size. Applied Clay Science 132-133 (2016) 571-578.*

[42] *R. Fernandez Lopez. PhD Thesis-Calcined clay soils as a potential replacement for cement in developing countries. Ecole Polytechnique Federale de Lausanne, Switzerland, 2009.*

[43] *BS 1377-2:1990. Methods of test for soils for civil engineering purposes. Classifcation tests. British Standards Institution, London, UK, 1990.*

[44] *https://www.thermofisher.com/uk/en/home/industrial/spectroscopy-elemental-isotope-analysis/spectroscopy-elemental-isotope-analysis-learning-center/molecular-spectroscopy-information/ftir-information/ftir-basics.html..*

[45] *CEN/TR 16632:2014. Isothermal conduction calorimetry (ICC) for the determination of heat of hydration of cement. State of the art report and recommendations. Brtish Standards Institution, London, UK, 2014.*

[46] *Bartůňková E, Kukliková A (2011/2012) Non-destructive tests of timber. Faculty of civil engineering, University Brunn.*

[47] *EN 14081-1:2016. Timber structures, strength graded structural timber with rectangular cross section. European Committee for Standardization, Brussels.*

[48] *EN 14081-2:2010+A1:2012. Strength graded structural timber with rectangular cross section - machine grading. European Committee for Standardization, Brussels.*

[49] *EN 14080:2013. Timber structures, glued laminated timber and glued solid timber - Requirements. European Committee for Standardization, Brussels.*

[50] *BS 812-104:1994. Testing aggregates. Method for qualitative and quantitative petrographic examination of aggregates. British Standards Institution, London, UK, 1994.*

[51] *BS 7943:1999. Guide to the interpretation of petrographical examinations for alkali-silica reactivity. British Standards Institution, London, UK, 1999.*

[52] *M.C. Limbachiya, E. Marrocchino and A. koulouris. Chemical-mineralogical characterisation of coarse recycled concrete aggregate. Waste Management 27 (2007) 201-208.*

[53] *S.C. Angulo, C. Ulsen, V.M. John, H. Kahn and M.A. Cincotto. Chemical-mineralogical characterisation of C&D waste recycled aggregates from Sao Paolo, Brazil. Waste Management, 29 (2009) 721-730.*

[54] *C. Medina, W. Zhu, T. Howind, M. Frias and M.I. Sanchez de Rojas. Effect of the constituents of construction and demolition waste on the properties of recycled concretes. Construction and Building Materials 79 (2015) 22-33.*

[55] *RILEM Recommended Test Method AAR-0: Detection of alkali-reactivity potential in concrete. Outline guide to the use of RILEM methods in the assessment of aggregates for potential alkali-reactivity. Materials and Structures 36 (2003) 472-479.*

[56] *BS 5930:2015. Code of practice for ground investigations. British Standards Institution, London, UK, 2015.*

[57] *M.J. Dumbleton and G. West. Some factors affecting the relation between the clay minerals in soils and their plasticity. Clay Minerals 6 (1966) 179-193.*

[58] *E. Polidori. Relationship between the Atterberg limits and clay content. Soils and Foundations 47:5 (2007) 887-896.*

[59] *J.A. Bain. A plasticity chart an an aid to the identification and assessment of industrial clays. Clay Minerals 9 (1971) 1-17.*

[60] *A.I.H. Malkawi, A.S. Alawneh and O.T. Abu-Safaqah. Effects of organic matter on the physical and the physicochemical properties of an illitic soil. Applied Clay Science 14 (1999) 257-278.*

[61] *C. He, E. Makovicky and B. Osbaeck. Pozzolanic reactions of six principal clay minerals: Activation, reactivity assessments and technological effects. Cement and Concrete Research 25:8 (1995) 1691-1702.*

[62] *A. Naidja et al. Fourier transform infrared, uv-visible, and x-ray diffraction analyses of organic matter in hmin, humic acid and fulvic acid fractions in soil exposed to elevated CO2 and N fertilization. Applied Spectroscopy 56:3 (2002) 318-324.*

[63] *J.W. Stucki and C.B. Roth. Interpretation of infrared spectra of oxidized and reduced nontronite. Clays and Clay Minerals (1976) 293-296.*

[64] *P. Djomgoue and D. Njopwouo. FT-IR spectroscopy applied for surface clays charactrerisation. Journal of Surface Engineered Materials and Advanced Technology 3 (2013) 275-282.*

[65] *P. Melis and P. Castaldi. Thermal analysis for the evaluation of the organic matter evolution during municipal solid waste aerobic composting process. Thermochimica Acta 413 (2004) 209-214.*

[66] *M. Otero, L.F. Calvo, B. Estrada, A.I. Garcia and A. Moran. Thermogravitry as a technique for establishing the stabilization progress of sludge from wastewater treatment plants. Thermochimica Acta 389 (2002) 121-132.*

[67] *W. Geyer, F.A.H. Hemidi, L. Bruggemann and G. Hanschmann. Investigation of soil humic substances from different environments using TG-FTIR and multivariate data analysis. Thermochimica Acta 361 (2000) 139-146.*

[68] *J. Peuravuori, N. Passo and K. Pihlaja. Kinetic study of the thermal degradation of lake aquatic humic matter by thermogravimetric analysis. Thermochimica Acta 325:2 (1999) 181-193.*

[69] *E.P. Partridge and A.H. White. The solubility of calcium sulfate from 0 to 200. Journal of the American Chemical Society 51:2 (1929) 360-370.*

[70] *T. Bakharev. Geopolymer materials in sodium and magnesium sulfate solutions. Cement and Concrete Research, 35:6 (2005) 1233-1246.*

[71] *D.M. Bastidas, A. Fernandez-Jimenez, A. Palomo and J.A. Gonzalez. A study on the passive state stability of steel embedded in activated fly ash mortars. Corrosion Science 50:4 (2008) 1058-1065.*

[72] *J.M. Miranda, A. Fernandez-Jimenez, J.A. Gonzalez and A. Palomo. Corrosion resistance in activated fly ash mortars. Cement and Concrete Research 35(6) 2005 1210-1217.*

[73] *C. Tennakoon, A. Shayan, J.G. Sanjayan and A. Xu. Chloride ingress and steel corrosion in geopolymer concrete based on long term tests. Materials and Design 116 (2017) 287-299.*

[74] *H. El-Didamony, A.A. Amer and H.A. Ela-ziz. Properties and durability of alkali-activated slag pastes immersed in sea water. Ceramics International 38 (2012) 3773-3780.*

[75] *G. Barnes (2016). Soil Mechanics-Principles and Practice 4th edition. Palgrave, London.*

[76] *Meinlschmidt P, Berthold D, Briesenmeister R. 2013: Neue Wege der Sortierung und Wiederverwertung von Altholz, in Recycling und Rohstoffe: Kapitel 6. TK-Verlag, Neuruppin.*

[77] *Lambertz G, Welling J. 2010: Die chemische Zusammensetzung von naturbelassenem Holz. Johann Henrich von Thünen Institut.*

[78] *EPF, European Panel Federation, 2002, Industry Standard for delivery conditions of recycled wood, europanels.org.*

[79] *Altholzverordnung - AltholzV vom 15 August 2002 (BGBI. I S. 3302), die durch Artikel 6 der Verordnung vom 2. Dezember 2016 (BGBI. I S. 2770) geändert worden ist.*

[80] *PAS 111:2012, Specification for the requirements and test methods for processing waste wood.*

[81] *Recyclingholzverordnung - RecyclingholzV vom 15. Mai 2012 (BGBI II Nr. 160/2012.*

[82] *Cavalli A, Cibechhini D, Togni M, Sousa HS. 2016: A review on the mechanical properties of aged wood and salvaged timber.*

[83] *http://www.glued-laminated-timber.com/glued-laminated-timber/production.*

[84] *EN 1912:2012 (2013) Structural timber - Strength classes - Assignment of visual grades and species. European Committee for Standardization, Brussels.*

[85] *EN 13055-1. Lightweight aggregates. Lightweight aggregates for concrete, mortar and grout.*

[86] *EN 1097-3:1998. Tests for mechanical and physical properties of aggregates - Part 3: Determination of loose bulk density and voids. 1999.*

DISCLAIMER

The sole responsibility of this publication lies with the author. The European Union is not responsible for any use that may be made of the information contained therein.